



Cindy de Oliveira

Fotodegradação do sulfametoxazol presente em ambientes aquáticos usando radiação solar simulada

Photodegradation of sulfamethoxazole in aquatic environments using simulated solar radiation



Cindy de Oliveira

Fotodegradação do sulfametoxazol presente em ambientes aquáticos usando radiação solar simulada

Photodegradation of sulfamethoxazole in aquatic environments using simulated solar radiation

Tese apresentada à Universidade de Aveiro para cumprimento dos requisitos necessários à obtenção do grau de Mestre em Química, realizada sob a orientação científica da Doutora Diana Luísa Duarte de Lima, Estagiária de Pós-Doutoramento do Departamento de Química da Universidade de Aveiro e Professora Adjunta do Departamento de Ciências Complementares da Escola Superior de Tecnologia da Saúde de Coimbra, do Doutor Valdemar Inocêncio Esteves, Professor Auxiliar do Departamento de Química da Universidade de Aveiro e da Doutora Carla Patrícia Gonçalves Silva, Bolseira de Investigação do Departamento de Química da Universidade de Aveiro.

Aos meus pais e ao meu irmão, sempre.

o júri

presidente

Prof. Doutor Artur Manuel Soares da Silva

professor catedrático do Departamento de Química da Universidade de Aveiro

Doutora Marta Otero Cabero

investigadora principal do Departamento de Ambiente e Ordenamento da Universidade de Aveiro

Doutora Diana Luísa Duarte de Lima

estagiária de pós-doutoramento do Departamento de Química da Universidade de Aveiro e professora adjunta do Departamento de Ciências Complementares da Escola Superior de Tecnologia da Saúde de Coimbra

agradecimentos

Porque chegamos mais longe se caminarmos acompanhados, agradeço bastante a quem de forma mais ou menos direta me acompanhou e apoiou no desenvolvimento desta tese.

À minha orientadora, Doutora Diana Lima, pelos muitos e importantes conhecimentos transmitidos, inteira disponibilidade e dedicação, confiança depositada em mim, oportunidades dadas e, principalmente, pela amizade e motivação que surgiram nos momentos mais cruciais. Estou muito grata por tudo!

Ao Professor Doutor Valdemar Esteves e à Doutora Patrícia Silva, co-orientadores deste trabalho, por todo o apoio, disponibilidade, pela importante transmissão de conhecimentos, motivação e confiança dada! Principalmente, por me incentivarem a fazer e a querer sempre mais!

Às meninas do laboratório por todos os ensinamentos transmitidos, conhecimentos partilhados e ajuda prestada. Principalmente, à Vitória pela amizade, companhia, apoio e ajuda.

À Doutora Vânia Calisto, à Doutora Nádia Osório, à Doutora Joana Barata, à Doutora Anabela Pereira e à Dra. Teresa Caldeira por toda a disponibilidade demonstrada em colaborar, assim como pela transmissão de conhecimentos.

A todos que fizeram e/ou fazem parte da minha vida, pois todos são essenciais para a construção daquilo que eu sou.

Aqueles que são realmente família, nomeadamente à minha avó por todo o apoio dado e interesse demonstrado, por sonhar com a realização deste objetivo tanto ou mais do que eu, embora sem entender muito bem do que se trata.

Aos meus amigos, que são família, que me acompanham desde sempre e que sabem bem quem são, um grande obrigada, sem vocês não seria a mesma coisa! A motivação dada, o interesse pelo trabalho em desenvolvimento e a partilha de momentos felizes e menos felizes foi essencial! Mais uma vez obrigada por existirem na minha vida!

Ao Casimiro por tudo! Pelo apoio, motivação e ajuda dada, paciência e interesse demonstrado, por nunca me deixar desanimar, por acreditar mais do que eu nas minhas capacidades e, principalmente, pelo amor dado sempre!

Aos meus pais, por tudo hoje e sempre! Pelos sacrifícios feitos em prol dos meus sonhos, pela constante dedicação e esforço, pelo apoio incondicional, pelo grande exemplo que são e por nunca me deixarem desistir de mim. Espero um dia poder retribuir todos os sacrifícios feitos e que estejamos novamente todos juntos. Devo um agradecimento especial ao meu irmão, pela fonte de inspiração que é, pela boa energia transmitida, pela tentativa e interesse em compreender o trabalho realizado e, principalmente, pelas ausências nunca cobradas. Estarei aqui para o que der e vier.

palavras-chave

Sulfametoxazol, fotodegradação, atividade antibacteriana, rendimento quântico.

resumo

A ocorrência de fármacos, nomeadamente antibióticos, no meio ambiente é um tema de elevada preocupação devido ao seu impacto ambiental, uma vez que as estações de tratamento de águas residuais não são totalmente eficientes na sua remoção. No que diz respeito aos antibióticos, usados no tratamento e prevenção de infeções, estes representam um problema para o meio ambiente e para os seres vivos em geral, devido ao desenvolvimento da resistência bacteriana. O antibiótico sulfametoxazol (SMX) pertence ao grupo das sulfonamidas, um dos grupos de antibióticos mais utilizados, sendo encontrado com regularidade não só em efluentes provenientes de estações de tratamento de água residuais, como no ambiente aquático. Assim, a fotodegradação surge como um processo alternativo para a remoção deste tipo de contaminantes do meio aquático. O recurso a fotossensibilizadores, naturais ou sintéticos, poderá ser uma forma de aumentar a eficiência da fotodegradação e, consequentemente, a taxa de fotodegradação. No entanto, neste trabalho, as substâncias húmicas, consideradas fotossensibilizadores naturais, não se mostraram eficientes no aumento da taxa de fotodegradação do SMX. O composto em estudo foi fotodegradado em água ultrapura, sob radiação solar simulada, muito rapidamente, tendo-se obtido um tempo de meia vida de 0,86 horas. Contudo, em amostras ambientais de diferentes origens, a taxa de fotodegradação do SMX mostrou ser muito mais lenta quando comparada com a observada em água ultrapura e na presença das substâncias húmicas, com tempos de vida a variar entre as 5,30 e as 7,54 horas. Tendo em conta a conversão destes tempos de meia vida para tempos de meia vida em condições ambientais, obtiveram-se valores que variaram entre 1.4 e 1.98 dias soalheiros de verão. Desta forma, foi importante estudar a influência de algumas das propriedades das matrizes aquosas para perceber quais os principais fatores responsáveis pela persistência do SMX no ambiente aquático. Dessa forma, concluiu-se que o pH, a salinidade e o carbono orgânico dissolvido influenciam de forma acentuada a fotodegradação do SMX. Com o objetivo de aplicar a fotodegradação às estações de tratamento de águas residuais, nomeadamente, como tratamento terciário, testou-se um método de fotodegradação em modo contínuo em que os tempos de irradiação diminuíram acentuadamente relativamente ao método em descontínuo. Por fim, foi avaliada a atividade antibacteriana do SMX em água ultrapura e em três amostras ambientais, antes e durante a fotodegradação, tendo-se concluído que a fotodegradação é eficiente para combater a problemática da resistência bacteriana, uma vez que a atividade bacteriana aumentou com a fotodegradação total do SMX. A única exceção foi a amostra da estação de tratamento de águas residuais para a qual não foi possível retirar conclusões, uma vez que esta, só por si, inibe muito o crescimento das bactérias *Vibrio fischeri*.

keywords

Sulfamethoxazole, photodegradation, antibacterial activity, quantum yield.

abstract

The occurrence of pharmaceuticals, namely antibiotics, in the environment is a subject of high concern due to their environmental impact, since the sewage treatment plants (STPs) are not completely efficient in their removal. In relation to antibiotics, used in the treatment and prevention of infections, they represent a problem for the environment and for living organisms in general, because of the imminent development of bacterial resistance. The antibiotic sulfamethoxazole (SMX) belongs to the group of sulfonamides, one of the most commonly used antibiotics, and is regularly found, not only in effluents from STPs, but also in the aquatic environment. Thus, photodegradation appears as an alternative process for the removal of this type of contaminants from the aquatic environment. The use of natural and synthetic photosensitizers may be a way of increasing the efficiency of photodegradation and, consequently, the rate of photodegradation. However, in this work, the humic substances (HS), considered natural photosensitizers, were not efficient in increasing the SMX photodegradation rate. The compound under study was photodegraded very fast in ultrapure water under simulated solar radiation, presenting a half-life time of 0.86 hours. However, in environmental water samples from different origins, the SMX photodegradation rate was shown to be much slower than that observed in ultrapure water or under the presence of HS, with half-life times that varied between 5.30 and 7.54 hours. **With** the conversion of these half-life times to half-life times under environmental conditions, values ranging from 1.4 to 1.98 sunny summer days were obtained. Thus, it was important to study the influence of some of the properties of the water matrices on the SMX photodegradation to understand the main factors responsible for the persistence of SMX in the aquatic environment. It was concluded that pH, salinity and dissolved organic carbon strongly influence the photodegradation of SMX. In order to apply the photodegradation in STPs, namely as a tertiary treatment, a method of photodegradation was tested in a continuous flow mode in which the irradiation times decreased sharply in relation to the batch method. Finally, the antibacterial activity of SMX in ultrapure water and in three environmental water samples was evaluated before and during photodegradation. It was concluded that the photodegradation is an efficient method to combat the problem of bacterial resistance, since the bacterial activity increased with the total photodegradation of the SMX. The exception was the STP sample, in which it was not possible to obtain conclusions, because the sample itself inhibited the growth of the *Vibrio fischeri* bacteria.

Abbreviations

AOPs – Advanced Oxidation Processes

CAM – Clarithromycin

DNA – DesoxyriboNucleic Acid

DOC – Dissolved Organic Carbon

DOM – Dissolved Organic Matter

E1 – Estrone

E2 – 17 β -Estradiol

EE2 – 17 α -ethinylestradiol

E3 – Estriol

ERY – Erythromycin

EU – European Union

FA – Fulvic Acid

FAO – Food and Agriculture Organization of the United Nations

HA – Humic Acid

HPLC-FLD – High-Performance Liquid Chromatography with Fluorescence Detection

HS – Humic Substances

IUPAC – International Union of Pure and Applied Chemistry

LCM – Lincomycin

Lin – Linearity

LOD – Limit of Detection

N-Ac-SMX – N4-acetylsulfamethoxazole

NED – Netherlands

NOR – Norfloxacin

NSAID – Non-Steroidal Anti-Inflammatory Drug

OD – Optical density

OFL – Ofloxacin

OM – Organic Matter

OTC – Oxytetracycline

RNA – RiboNucleic Acid

ROX – Roxithromycin

RSD – Relative Standard Deviation

SD – Sulfadiazine

SMX – Sulfamethoxazole/Sulfametoxazol

SSD – Sunny Summer Days

STP – Sewage Treatment Plant

STPF – Sewage Treatment Plant effluent after secondary treatment

TMP – Trimethoprim

TOC – Total Organic Carbon

USA – United States of America

UV – Ultraviolet

UV-Vis – Ultraviolet-Visible

XAD-4 – registered trademark (matrix: styrene divinylbenzene)

XAD-8 – registered trademark (matrix: poly(methylmethacrylate))

Symbols

a – Intersection with the y-axis

A_m – Absorbance value of the mixture (SMX + HS) at 290 nm

A_{SMX} – Absorbance value of SMX at 290 nm

b – Slope of the calibration curve

C – Concentration of SMX at a given irradiation time

C_0 – Concentration of the SMX protected to light

ε – Molar absorptivity of the SMX at the wavelength λ_i

$HO_2\cdot$ – Hydroperoxyl radical

${}^3HS^*$ – Humic substances in the triplet excited state

$\left(\frac{I_a}{I_0}\right)_m$ – Fraction of light absorbed by the mixture (SMX + HS) at 290 nm

$\left(\frac{I_a}{I_0}\right)_{SMX}$ – Fraction of light absorbed by SMX alone (in ultrapure water) at 290 nm

$\left(\frac{I_a}{I_0}\right)_{SMX/m}$ – Fraction of light that was absorbed by SMX in the presence of HS at 290 nm

$I_{\lambda_i}^{abs}$ – Rate of light absorption at the wavelength λ_i

$I_{\lambda_i}^0$ – Lamp emission intensity at the wavelength λ_i

K_{calc} – Calculated first-order rate constant for degradation of SMX in presence of HS acting only as inner filter

K_{meas} – Pseudo first order degradation rate constant measured

K_{ow} – Octanol/water partition coefficient

k_i – Pseudo first-order degradation rate constant at wavelength λ_i

l – Path length inside the photoreactor

LOD_x – Value of LOD in the x-axis

LOD_y – Value of LOD in the y-axis

n – Number of standard solutions that were used for calibration

$^1\text{O}_2$ – Singlet oxygen

$\text{O}_2^{\cdot-}$ – Superoxide anion

$\cdot\text{OH}$ – Hydroxyl radical

pK_a – Acid dissociation constant

R^2 – Determination coefficient

$rate\ \lambda_i$ – Photodegradation rate of SMX induced by the absorption of radiation with wavelength λ_i .

RSD_b – Relative standard deviation of slope

$S_{y/x}$ – Statistical parameter that estimates the random errors in the y axis

t – Time

t_r – Retention time

$t_{1/2}$ – Half-life time

t_1 – About 50 % of SMX photodegradation

t_2 – After more than 95 % of SMX photodegradation

t_3 – No SMX was detected

y_i – Experimental values of y obtained for each calibration standard

\hat{y}_i – Calculated y-values by using the calibration curve equation, corresponding to the individual x-values of standards

ϕ – Quantum yield

ϕ_{ave} – Average quantum yield

$\Delta\lambda$ – Wavelength interval of acquisition of the spectral irradiance of the lamp

Index

Abbreviations	i
Symbols	iii
1. Introduction	3
1.1. Pharmaceuticals in the environment	3
1.1.1. Occurrence of antibiotics in the aquatic environment.....	8
1.1.1.1. Bacterial resistance	15
1.1.1.2. Sulfamethoxazole	16
1.1.1.2.1. Structure and physico-chemical properties.....	16
1.2. Removal processes for pharmaceuticals in STPs	17
1.2.1. Physical processes	18
1.2.2. Biological processes	18
1.2.3. Oxidation processes.....	19
1.2.3.1. Photodegradation of SMX	21
1.2.3.2. Importance of photosensitizers.....	23
1.2.3.2.1. Humic substances	23
1.3. Objectives of the dissertation	25
2. Materials and Methods.....	27
2.1. Chemicals.....	29
2.2. Instrumentation.....	29
2.3. Humic substances	32
2.4. Environmental water samples	32
2.5. Photodegradation experiments	34
2.5.1. Solutions of SMX.....	34
2.5.2. Photodegradation of SMX in batch mode	35
2.5.3. Photodegradation of SMX in continuous flow mode	39
2.5.4. Antibacterial activity	41
3. Results and Discussion.....	43

3.1. Calibration curve.....	45
3.2. Photodegradation of SMX in batch mode.....	47
3.2.1. Direct photodegradation kinetics of SMX.....	47
3.2.2. Photodegradation of SMX in the environmental water samples.....	48
3.2.2.1. Characterization of environmental water samples	48
3.2.2.2. Photodegradation kinetics of SMX.....	52
3.2.3. Effect of HS on SMX photodegradation	55
3.2.3.1. Characterization of HS	55
3.2.3.2. Photodegradation kinetics of SMX.....	57
3.2.4. Effect of pH on SMX photodegradation	62
3.2.4.1. Importance of pH.....	62
3.2.4.2. Photodegradation kinetics of SMX.....	66
3.2.4.2.1. In ultrapure water	66
3.2.4.2.2. In estuarine water	67
3.2.5. Effect of sea salts on SMX photodegradation	69
3.2.5.1. Evaluation of inorganic salts on SMX photodegradation	69
3.2.5.2. Photodegradation kinetics of SMX.....	73
3.3. Photodegradation of SMX in continuous flow mode	75
3.3.1. Photodegradation kinetics of SMX in ultrapure water and environmental water samples	75
3.4. Antibacterial activity	78
4. Conclusions	83
5. Future Work.....	89
6. References	93
7. Annex	103

Index of figures

Figure 1- Routes of pharmaceuticals introduction into the environment (adapted from Silva (2014)).	8
Figure 2- SMX chemical structure (a) and general chemical structure of sulfonamides (b).	16
Figure 3- Direct and indirect photolysis occurring in the aquatic environment.	20
Figure 4- Degradation path of SMX by direct photolysis in distilled water (from Trovó et al. (2009)).	22
Figure 5- Location of the sampling points.	34
Figure 6- Scheme of SMX photodegradation in continuous flow mode.	40
Figure 7- Kinetics of SMX photodegradation in ultrapure water - direct photodegradation (x) and control during the photodegradation experiment (▲).	47
Figure 8- UV-Vis spectra of the environmental water samples analysed.	49
Figure 9- UV-Vis spectra of SMX [10 mg/L] and SMX [100 µg/L] in ultrapure water.	50
Figure 10- Kinetics of SMX photodegradation in ultrapure water and in environmental water samples. Shown error bars are standard deviations (n = 3) (note that, for most of the experimental points error bars are too small to be visible in the figure).	52
Figure 11- UV-Vis spectra of SMX in ultrapure water and in the three fractions of HS.	56
Figure 12- Kinetics of SMX photodegradation in absence and presence of three fractions of HS. Shown error bars are standard deviations (n=3) (note that, for most the experimental points, error bars are too small to be visible in the figure).	58
Figure 13- Variation of the chemical structure of SMX with pH.	63
Figure 14- Speciation diagrams of SMX (adapted from Dias et al., (2014)).	63
Figure 15- UV-Vis spectra of SMX [10 mg/L] in ultrapure water at different pH values.	64
Figure 16- SMX photodegradation rate (%) in presence and absence of different HS fractions together with phosphate buffer (0.001 M) at pH 5.00 and 7.30 after 1 hour of irradiation. Shown error bars are standard deviations (n=3).	65
Figure 17- Kinetics of SMX photodegradation in ultrapure water with natural pH and with phosphate buffer at pH 5.00 and 7.30. Error bars in the graph are standard deviations (n=3) (note that, for most of the experimental points error bars are too small to be visible in the figure).	66
Figure 18- Kinetics of SMX photodegradation in estuarine water at pH 6.30 and 7.33. In the graph are also represented error bars with standard deviations (n=3) (note that, for most of the experimental points error bars are too small to be visible in the figure).	68

Figure 19- SMX photodegradation rate in ultrapure water in presence and absence of calcium, magnesium, sodium chloride and red sea salts with phosphate buffer at pH 7.30 and in estuarine water at pH 7.33 after 5 hours of irradiation. Shown error bars are standard deviations (n=3).	70
Figure 20- 3D fluorescence spectrum (contour map) of SMX 100 µg/L in ultrapure water at pH 7.30 with phosphate buffer (0.001M) in absence of salts (a) and in presence of 785 mg/L magnesium (b), 261 mg/L calcium (c), 21 g/L sodium chloride (d) and 21 g/L Red Sea Salts (e).....	71
Figure 21- UV-Vis spectra of SMX 10 mg/L in ultrapure water at pH 7.30 with phosphate buffer (0.001 M) in absence of salts and in presence of 785 mg/L magnesium, 261 mg/L calcium, 21 ‰ sodium chloride and 21 ‰ Red Sea Salts.	72
Figure 22- Kinetics of SMX photodegradation and curves of pseudo first-order decay fitted to the data by nonlinear regression when present in ultrapure water, in ultrapure water with sea salts and in a NaCl solution buffered with phosphate buffer at pH 7.30 and in estuarine water at pH=7.33. Shown error bars are standard deviations (n=3) (note that, for most of the experimental points error bars are too small to be visible in the figure).	73
Figure 23- Kinetics of SMX photodegradation in continuous flow mode and curves of pseudo first-order decay fitted to the data by nonlinear regression when present in ultrapure water and in environmental samples.	76
Figure 24- Comparison between SSD obtained in batch mode and continuous flow mode in ultrapure water and in environmental water samples in the same conditions.....	78
Figure 25- Correlation between luminescence at wavelength 420 nm and bacterial growth at wavelength 600 nm.....	78
Figure 26- Percentage of viable cells <i>Vibrio fischeri</i> in A - ultrapure water (matrix) without SMX and without irradiation; B - control without irradiation (50 mg/L of SMX); C – control covered with aluminum at t ₃ of irradiation (50 mg/L of SMX); D - control without irradiation (100 mg/L of SMX); E - sample at t ₁ (50 mg/L of SMX); F - sample at t ₂ (SMX concentration < 5 mg/L); G - sample at t ₃ (no SMX detected). Statistical hypothesis test: *- p value = 0.05; **- p value = 0.01; ***- p value = 0.001.....	79
Figure 27- Percentage of viable cells <i>Vibrio fischeri</i> in A – Poço da Cruz (matrix) without SMX and without irradiation; B - control without irradiation (50 mg/L of SMX); C - control covered with aluminum at t ₃ of irradiation (50 mg/L of SMX); D - control without irradiation (100 mg/L of SMX); E - sample at t ₁ (50 mg/L of SMX); F - sample at t ₂ (SMX concentration < 5 mg/L); G - sample at t ₃ (no SMX detected). Statistical hypothesis test: **- p value = 0.01; ***- p value = 0.001.....	80

Figure 28- Percentage of viable cells *Vibrio fischeri* in A – Fonte Nova (matrix) without SMX and without irradiation; B - control without irradiation (50 mg/L of SMX); C - control covered with aluminum at t_3 of irradiation (50 mg/L of SMX); D - control without irradiation (100 mg/L of SMX); E - sample at t_1 (50 mg/L of SMX); F - sample at t_2 (SMX concentration < 5 mg/L); G - sample at t_3 (no SMX detected). Statistical hypothesis test: * - p value = 0.05.....81

Figure 29- Percentage of viable cells *Vibrio fischeri* in A – STPF (matrix) without SMX and without irradiation; B - control without irradiation (50 mg/L of SMX); C – control covered with aluminum at t_3 of irradiation (50 mg/L of SMX); D - control without irradiation (100 mg/L of SMX); E - sample at t_1 (50 mg/L of SMX); F - sample at t_2 (SMX concentration < 5 mg/L); G - sample at t_3 (no SMX detected).....82

Index of tables

Table 1- Concentrations of pharmaceuticals detected in the aquatic environment (adapted from Bila et al. (2003)). NSAID* - Non-Steroidal Anti-Inflammatory Drug.	4
Table 2- Important classes of antibiotic compounds (adapted from Kümmerer et al. (2009)).	9
Table 3- Important antibiotics in human and animal medicine (adapted from Kemper et al. (2008))......	11
Table 4- Concentration of SMX in aquatic environment.	14
Table 5- Physicochemical properties of SMX (adapted from Boreen et al., (2004), Sulfamethoxazole-Toxicology Data Network and Yalkowsky et al., (2010)).	17
Table 6- Salinity, conductivity, pH and DOC values of the samples tested and respective standard errors.	49
Table 7- Concentration range used, calibration curve equation, R^2 and LOD obtained in determination of calcium, magnesium, sodium, potassium and iron by atomic absorption.	51
Table 8- Concentration of calcium, magnesium, sodium, potassium and iron determined in environmental samples and respective standard errors.	51
Table 9- Data on apparent first-order rate constants, k_{meas} (h^{-1}), R^2 , $t_{1/2}$ (h), and $t_{1/2}$ (SSD) obtained in ultrapure water and in environmental water samples and respective standard errors.	53
Table 10- Elemental analysis of HS fractions selected to study the effect of DOM on SMX photodegradation. Results are corrected for humidity at 60°C and ashes at 750 °C (adapted from Esteves et al. (1995))......	55
Table 11- K_{meas} (h^{-1}), R^2 , $t_{1/2}$ (h), $t_{1/2}$ (SSD), K_{cal} (h^{-1}) and contribution of three different HS isolates to degradation obtained and respective standard errors.	61
Table 12- K_{meas} (h^{-1}), R^2 , $t_{1/2}$ (h), $t_{1/2}$ (SSD) and ϕ_{ave} obtained for SMX in ultrapure water at different pH values and respective standard errors.	67
Table 13- K_{meas} (h^{-1}), R^2 , $t_{1/2}$ (h) and $t_{1/2}$ (SSD) obtained for estuarine water at different pH values and respective standard errors.	68
Table 14- K_{meas} (h^{-1}), R^2 , $t_{1/2}$ (h), $t_{1/2}$ (SSD) and ϕ_{ave} obtained for ultrapure water, 21 ‰ sea salts, 21 ‰ NaCl buffered with phosphate buffer (0.001 M) at pH 7.30 and Fonte Nova sample at pH 7.33.....	74
Table 15- Photodegradation of SMX in flow mode - K_{meas} (h^{-1}), R^2 , $t_{1/2}$ (h) and $t_{1/2}$ (SSD) obtained in ultrapure water and in environmental water samples and respective standard errors.	77

1. Introduction

1.1. Pharmaceuticals in the environment

Demographic growth and industrial expansion brought, as a consequence, air, soil and water resources pollution worldwide. This situation is worrying, being necessary to reverse or leastways minimize this process (Melo et al., 2009).

The question related with water quality has been widely discussed, because this is a natural resource essential to many human activities, for example, public and industrial supply, agricultural irrigation, electric power production, leisure and recreation activities, as well as to the preservation of aquatic life. Given this context, treatment of waste water has been gaining more and more importance (Melo et al., 2009).

The presence of pharmaceuticals in aquatic environments was verified for the first time in the 70's. Since that, many studies have been performed and residual pharmaceuticals have been detected in different parts of the world (Bastos, 2012), (Katsumata et al., 2014), (Melo et al., 2009). These compounds and their metabolites have been found in municipal sewage, because the conventional STPs do not have adequate processes for their removal from the aqueous matrix and also because they are used in high amounts worldwide (Bastos, 2012), (Katsumata et al., 2014). Therefore, it is important and imperative for the scientific community to conduct investigations to solve this problem.

More recently, investigation on pharmaceuticals monitoring in the aquatic environment has been performed in different countries such as Germany, Brazil, Canada, United States of America (USA), Netherlands (NED), England, Sweden and Italy. These compounds were found in STPs, surface water, ground water and potable water in concentrations ranging from $\mu\text{g/L}$ to ng/L (table 1) (Bila and Dezotti, 2003), (Kümmerer, 2001). So, the development of sufficiently sensitive analytical methods for the determination (identification and quantification) of these compounds in aquatic environments is important (Bastos, 2012), (Bila and Dezotti, 2003), (Melo et al., 2009).

Table 1- Concentrations of pharmaceuticals detected in the aquatic environment (adapted from Bila et al. (2003)). NSAID* - Non-Steroidal Anti-Inflammatory Drug.

Drug	Drug Class	Concentration (ng/L)	Aquatic Matrix
Acetylsalicylic acid	NSAID*	220	Effluent of STP in Germany
Diclofenac	NSAID*	200-370	Effluent of STP in Sweden
		150	Surface Water in Germany
		<1-12	Surface Water in Sweden
Ibuprofen	NSAID*	87	Surface Water in Canada
		370	Effluent of STP in Germany
		1000-3300	Domestic sewage in Sweden
Indomectacine	NSAID*	950	Domestic sewage in Brazil
		270	Effluent of STP in Germany
		170	Surface Water in Germany
Ketoprofen	NSAID*	200	Effluent of STP in Germany
Ciprofloxacin	Antibiotic	20	Surface Water in USA
Chlorotetracycline	Antibiotic	420	Surface Water in USA
Erythromycin	Antibiotic	100	Surface Water in USA
		150	Surface Water in Germany
		2500	Effluent of STP in Germany
Lincomycin	Antibiotic	60	Surface Water in USA
Norfloxacin	Antibiotic	120	Surface Water in USA
Oxytetracycline	Antibiotic	340	Surface Water in USA

Penicillin	Antibiotic	1.8-5.9	Surface Water in Germany
Roxitrocin	Antibiotic	50	Surface Water in USA
		560	Surface Water in Germany
		680-1000	Effluent of STP in Germany
Sulfamethoxazole	Antibiotic	30	Surface Water in Germany
		30-85	Surface Water in Germany
		6-150	Surface Water in USA
		300-1500	Effluent of STP in Germany
		400	Effluent of STP in Germany
		410	Ground Water in Germany
Tetracycline	Antibiotic	110	Surface Water in USA
Trimethoprim	Antibiotic	13-150	Surface Water in USA
		150	Surface Water in Germany
		320-660	Effluent of STP in Germany
		2500	Effluent of STP in Germany
Tylosin	Antibiotic	40	Surface Water in USA
Vancomycin	Antibiotic	700-3800	Surface Water in Germany
17α- Ethinylestradiol	Hormone	9	Effluent of STP in Canada
		0.2-7.0	Effluent of STP in England
		450	Surface Water in Germany
		73	Surface Water in USA
		<0.5-10	Domestic sewage in Italy and NED

17β-Estradiol	Hormone	21	Domestic sewage in Brazil
		<0.5-17	Domestic sewage in Italy and NED
		2.7-48	Effluent of STP in England
		9-160	Surface Water in USA
Estrone	Hormone	20-50	Surface Water in Brazil
		27	Surface Water in USA
		40	Domestic Sewage in Brazil
		<0.5-38	Domestic sewage in Italy and NED
		9	Effluent of STP in Germany
		<0.5-54	Effluent of STP in Italy and NED
Estriol	Hormone	19	Surface Water in USA
		2-4	Effluent of STP in England
		0.43-18	Effluent of STP in Italy
		1.2-3.1	Surface Water in England
		24-188	Domestic sewage in Italy
Progesterone	Hormone	110	Surface Water in USA
Testosterone	Hormone	116	Surface Water in USA

In table 1, the concentrations for different pharmaceuticals detected in the environment are presented and it is possible to verify that there are different concentration values depending not only on the type of water, but also on the sampling site. Also, other factors play a role on the concentrations found: studies show that the typical concentration values of the pharmaceuticals found in aquatic environments are related to their consumption pattern by the population, the rate of removal in the STP, the type of effluent that arrives to the STP and by seasonality (Bastos, 2012), (Melo et al., 2009).

In some locations in the world, the raw sewage is released directly into surface water, because they have a deficit in sanitation infrastructures (Melo et al., 2009). When there are sanitation infrastructures, these compounds pass through a STP, where they are subjected to conventional treatment processes, but are not totally eliminated, being found in significant amounts in STP effluents and surface water.

Conventional processes are based on adsorption to solid component of sludge and on biological degradation of the contaminants which are not efficient in completely remove this type of compounds, since they can have biocide action or complex chemical structures not amenable to biodegradation (Castiglioni et al., 2006), (Kümmerer, 2001), (Melo et al., 2009). Consequently, many pharmaceuticals enter the aquatic environment (persisting in the environment) and eventually reach drinking water (Bila and Dezotti, 2003), (Melo et al., 2009).

The veterinary use, including in aquaculture, as growth promoters and in the prevention and treatment of diseases, also counts for the discharge of pharmaceuticals and their metabolites into the environment through (waste) water or by water run-off from fields after application of manure. Pharmaceuticals can therefore enter the ground water system through the soil after the application of liquid manure or sewage sludge as fertilizers (Bila and Dezotti, 2003), (Kümmerer, 2001), (Melo et al., 2009). However, the waste water from pharmaceuticals' companies and hospitals and the improper disposal of pharmaceuticals should also be considered as significant contributors to the presence of these compounds in the environment (Bila and Dezotti, 2003), (Melo et al., 2009). In figure 1, possible routes for the introduction of pharmaceuticals in the aquatic environment are schematized (Bastos, 2012), (Bila and Dezotti, 2003).

From all the stated above, it is clear that the water contamination by pharmaceuticals deserve special attention, since the real risks to human health and to the aquatic environment are not yet fully known and because there is no established legal limits for environmental concentrations (Bastos, 2012), (Melo et al., 2009). Antibiotics, hormones, analgesics, anti-inflammatories are examples of different pharmaceuticals detected in waste water. However, some groups need special attention, mainly antibiotics, because of their pronounced toxicity and their potential of fostering bacterial resistance (Bila and Dezotti, 2003), (Kümmerer, 2001).

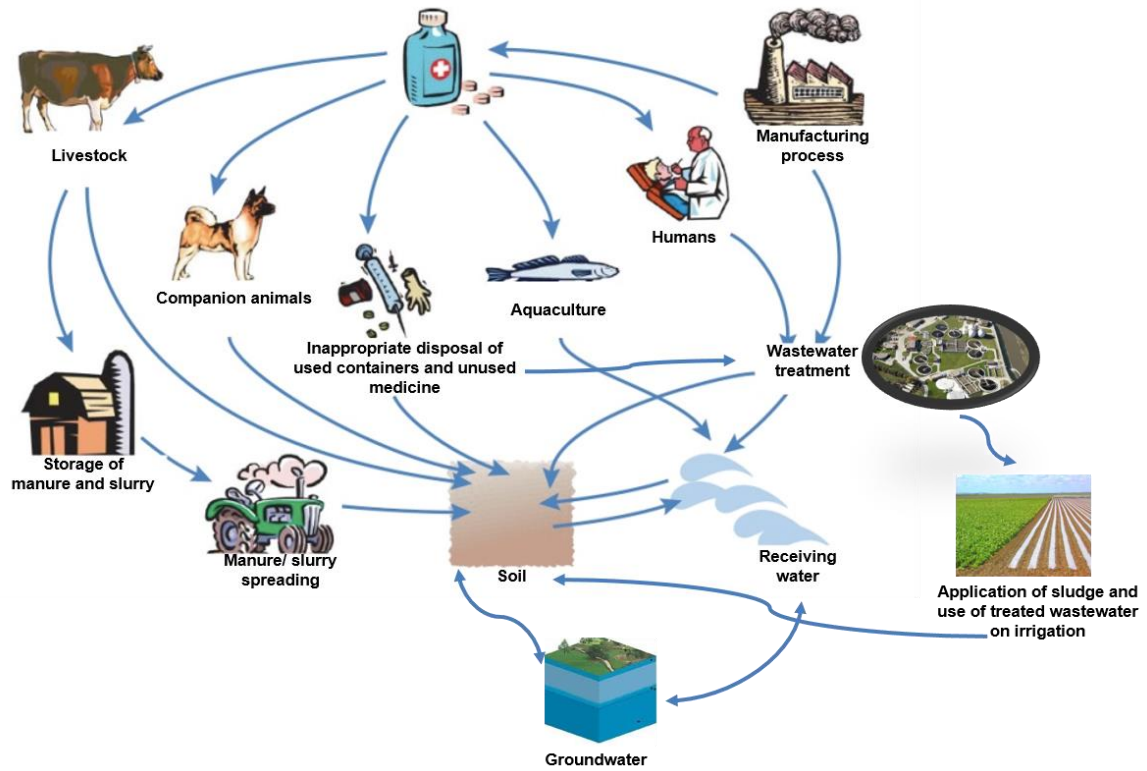
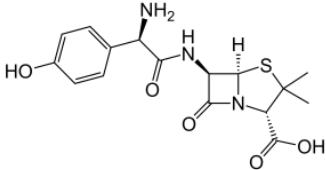
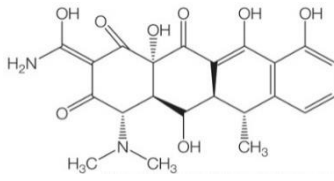
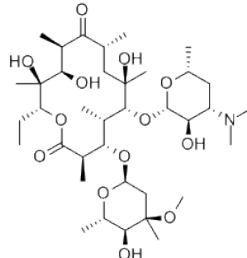
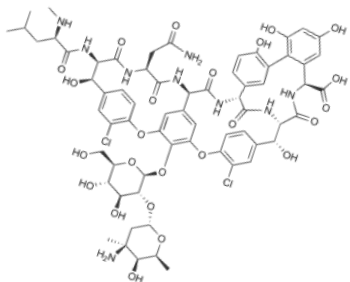
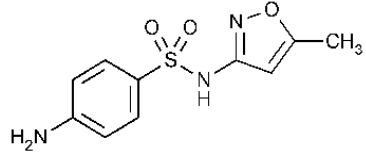
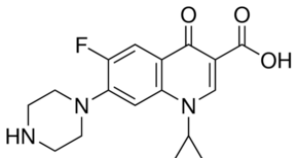


Figure 1- Routes of pharmaceuticals introduction into the environment (adapted from Silva (2014)).

1.1.1. Occurrence of antibiotics in the aquatic environment

Originally, the word *antibiotic* referred to any agent with biological activity against living organisms. Now, *antibiotic* refers to substances with antibacterial, anti-fungal or anti-parasitical activity (Kümmerer, 2009). In table 2, an overview of the most important classes of antibiotics is given.

Table 2- Important classes of antibiotic compounds (adapted from Kümmerer et al. (2009)).

Class	Example	Chemical structure
β-lactams	Amoxicillin	
Tetracyclines	Doxycycline	
Macrolides	Erythromycin A	
Glycopeptides	Vancomycin	
Sulfonamides	Sulfamethoxazole	
Qinolones	Ciprofloxacin	

In the 20th century, the discovery of antibiotics and their use in anti-infectious therapy constituted an unquestionable progress in medicine (Instituto Nacional de Saúde Doutor Ricardo Jorge, 2010). The antibiotics are the mostly used pharmaceuticals in human and veterinary medicine (Göbel et al., 2005), (Hirsch et al., 1999).

The most important classes of antibiotics for human medicine are β -lactams, sulfonamides (with or without trimethoprim (TMP)), macrolides and fluoroquinolones (table 3) (Göbel et al., 2004),(Hirsch et al., 1999). As already mentioned, antibiotics are extensively used in animal medicine and the main groups of pharmaceuticals used are tetracyclines, sulfonamides and fenicoles (table 3). According Food and Agriculture Organization of the United Nations (FAO), antibiotics authorized for use in aquaculture are tetracycline, fluoroquinolones, macrolides and sulfonamides potentiated with TMP or ormethoprim. In Norwegian aquaculture, from 2002 to 2005, an increase in the use of antibiotics in aquaculture was observed, which was accounted by newly-farmed fish species, especially Atlantic cod. However, for most countries specific data are missing (Kümmerer, 2009).

The bacteriostatic sulfonamide pharmaceuticals, which includes the SMX, are antibiotics extensively used and the wide use in factory farming without proper withdrawal periods has led to their accumulation in meat, eggs and milk as well as in fish (Hartig et al., 1999).

Table 3- Important antibiotics in human and animal medicine (adapted from Kemper et al. (2008)).

Class	Compounds	Primary usage
β-Lactams	Flucloxacillin	Humans
	Methicillin	Humans
	Phenoxymethylcillin	Humans
	Penicillin G	Humans
Fenicoles	Chloramphenicol	Cats, dogs
Fluoroquinolones	Ciprofloxacin	Humans
	Flumequin	Humans
	Ofloxacin	Humans
Macrolides	Erythromycin	Humans, cattle, chicken
	Roxithromycin	Humans
	Vancomycin	Humans
Sulfonamides	Sulfanilamide	Humans
	Sulfadimethoxine	Cattle, pigs, chicken
	Sulfadiazine	Cattle, sheep, chicken
	Sulfamethoxazole	Humans and animals
	Sulfapyridine	Pigs
	Sulfathiazole	Humans
Trimethoprim		In combination with sulfonamides
Tetracyclines	Chlortetracycline	Cattle, pigs
	Doxycycline	Humans, cats, dogs
	Oxytetracycline	Human, cattle, sheep, pigs
	Tetracycline	Humans, horse, sheep, pigs

The antibiotics are polar, non-volatile and defined as naturally, semi-synthetic and synthetic compounds with antimicrobial activity that can be applied parentally, orally or topically (Kemper, 2008), (Sajjad, 2014). The first antibiotics were of natural origin, but currently, antibiotics are obtained by chemical synthesis, such as the sulfonamides (e.g. SMX) or by chemical modification of compounds of natural origin, such as paclitaxel used in chemotherapy medication (Kümmerer, 2009), (De Souza, 2004).

Antibiotics are complex molecules that can be present in the environment in the neutral, cationic, anionic or zwitterion forms. Thus, the physicochemical and biological properties of these compounds vary with pH, in other words, properties such as solubility,

hydrophobic and hydrophilic character and partition coefficient, K_{ow} , of antibiotics depend essentially on pH (Sajjad, 2014).

It is documented in some studies that antibiotics are not completely metabolized in the body and thus are excreted into the environment unchanged or in the form of their metabolites via urine and feces (Carballa et al., 2004), (Gao et al., 2012), (Kemper, 2008). The rates of excretion are dependent on the substance, the dose ingested, the mode of application, the excreting species and time after administration (Bastos, 2012), (Bila and Dezotti, 2003), (Castiglioni et al., 2006), (Melo et al., 2009). For tetracyclines and sulfonamides it has been shown that rates of excretion vary in the range (40-90) % (Kemper, 2008). The disposal of expired or unused antibiotics is also a considerable source of these compounds in the environment (Gao et al., 2012). It is important to note that concentration limits of antibiotics in the environment are not regulated (Bengtsson-Palme and Larsson, 2016), (Kemper, 2008), (Milić et al., 2013).

Besides their use to prevent or treat diseases in humans, animals and plants, antibiotics are also used to promote the growth of animals in livestock and aquaculture operations (Gao et al., 2012), (Kemper, 2008), (Kümmerer, 2001). In 2001, it was reported that more than 70 % of veterinary antibiotics consumption in the USA was as growth promoters (Kümmerer, 2001). However, in 2006, growth promoters were banned in Europe and thus there was an actual decline in antibiotics used in veterinary medicine (Kemper, 2008). Aquacultures are an important source of antibiotics to the environment: (70-80) % of the antibiotics administered as pelleted feed medication are released into the aquatic environment via urinary and fecal excretion and in unused medicated food (Christensen et al., 2006).

Antibiotics have been detected in municipal sewage, hospital waste water, surface water, ground water and in soil, sediment and sludge samples (Gao et al., 2012) and the residual concentration of these compounds in the treated effluents depend on their removal during STP treatment (Göbel et al., 2004). So, several studies have been conducted to investigate the occurrence of antibiotics in STPs and surface waters, especially, since these compounds may promote bacterial resistance (Bastos, 2012).

Isidori et al. (2005) determined six antibiotics: erythromycin (ERY), oxytetracycline (OTC), SMX, ofloxacin (OFL), lincomycin (LCM) and clarithromycin (CAM) belonging to different classes of antibiotics in surface water samples from Germany and Italy. ERY was found in concentrations of 0.02 and 0.016 $\mu\text{g/L}$ in Germany and Italy, respectively. The concentrations achieved for OTC were 0.05 $\mu\text{g/L}$ (Germany) and 0.019 $\mu\text{g/L}$ (Italy). The

compounds OFL and SMX were found only in Germany with concentrations of 0.05 and 0.02 µg/L, respectively. CAM was detected in Germany and Italy with concentrations of 0.02 µg/L (Isidori et al., 2005).

In the study developed by Tamtam et al. (2008) the occurrence of seventeen antibiotics in the Seine River inner estuary was investigated. Quinolones, sulfonamides, nitroimidazoles and diaminopyrimidines were the four classes of antibiotics analyzed (from January to June 2006). All the seventeen compounds were detected at least once. In the specific case of SMX, it was observed that it was detected in every sample and showed the highest concentrations reaching 544 ng/L (Tamtam et al., 2008).

The presence of eleven antibiotics belonging to three classes was investigated in the Beibu Gulf, China (Zheng et al., 2012). ERY-H₂O, SMX and TMP were the most frequently detected, with mean concentrations in the range (0.51-6.30) ng/L. The concentrations of ERY-H₂O, SMX and sulfadimidine in the vicinity of aquaculture activities were larger, suggesting that a higher intensity of aquaculture activities could contribute to increasing the levels of antibiotics in the environment (Zheng et al., 2012).

In the research developed by Hirsch et al. (1999), eighteen antibiotics from the classes of macrolides, sulfonamides, penicillins and tetracyclines were analyzed. The investigated STP effluents and surface water samples showed frequent appearance of roxithromycin (ROX) and SMX with concentrations up to 6 µg/L. Neither tetracyclines nor penicillins could be detected at concentration levels above 50 and 20 ng/L, respectively (Hirsch et al., 1999).

The determination of thirteen sulfonamides was performed in primary and secondary effluents of STPs and in different surface waters (Hartig et al., 1999). In this study, the compounds SMX and sulfadiazine (SD) were detected with concentrations in the ranges (30-2000) and (10-100) ng/L, respectively (Hartig et al., 1999). As in the previous article, SMX was also detected in waste water samples from two STPs in Switzerland. SMX was detected in the primary effluent with a concentration ranging from (343-641) ng/L, in the secondary effluent with a concentration between (343-352) ng/L and in the tertiary effluent with a concentration of 352 ng/L (Göbel et al., 2004).

The occurrence of twenty-two antibiotics was investigated in eight STPs in Beijing, China (Gao et al., 2012). The antibiotics studied belonged to the fluoroquinolones, sulfonamides and macrolides classes and the most frequently detected antibiotics were OFL, norfloxacin (NOR), SD, SMX, ERY and ROX. The concentrations of fluoroquinolones OFL and NOR were in the range (0.15-1.2) and (0.0094-0.20) µg/L, respectively. For SD

and SMX, antibiotics belonging to the sulfonamides group, the concentration varied between (0.12-0.56) and (0.13-0.46) µg/L, respectively. The concentrations of ERY and ROX detected in effluent samples were in the ranges (0.051-0.30) and (0.054-0.36) µg/L, respectively.

The presence of twenty-eight antibiotics was investigated in South–East Queensland, Australia (Watkinson et al., 2009). In hospital effluents, antibiotics were found in concentrations in the range (0.01-14.5) µg/L, dominated by β-lactam, quinolone and sulfonamide groups. Antibiotics were also found in STPs influents, up to 64 µg/L, and effluents in the low ng/L range up to a maximum of 3.4 µg/L, with the macrolide, quinolone and sulfonamide antibiotics being the most prevalent. Similarly, antibiotics were detected in the low ng/L range, up to 2 µg/L in surface waters of six investigated rivers (Watkinson et al., 2009).

Among the different existent sulfonamides, SMX is one of the compounds most frequently detected in municipal sewage. However, concentrations of SMX in effluents from STPs vary widely, as these depend on the use of the antibiotic and the type of treatment used in the STPs (Sajjad, 2014). In the next table (table 4), the different concentrations of SMX in different aquatic matrixes are presented.

Table 4- Concentration of SMX in aquatic environment.

Localization	Concentration of SMX (ng/L)	Aquatic matrix	References
China	545-791	Effluents	Peng et al., 2006
Germany	30-85	Surface Water	Bila and Dezotti, 2003
Israel	90-150	Effluents	Avisar et al., 2009
Brazil	0.78-106	Surface water	Locatelli et al., 2011

In the body, SMX is metabolized and 50 % of the administered dose is excreted as the inactive human metabolite N4-acetylsulfamethoxazole (N-Ac-SMX) and only 10 % as the unchanged compound. There are few studies concerning the SMX metabolites: SMX and its metabolite N-Ac-SMX were detected in two urban STPs from Switzerland (Göbel et al., 2004). The maximum concentration determined for the metabolite was (943 ± 2.9) ng/L while for SMX the higher concentration was (641 ± 4.0) ng/L (Göbel et al., 2004). Although

the concentration was higher for SMX metabolite, it lacked relevant antibacterial activity (Brown, 2014). Also, Senta et al., (2013) detected the presence of SMX (323 ± 135) ng/L and N-Ac-SMX (214 ± 177) ng/L in a STP of Zagreb (Senta et al., 2013).

1.1.1.1. Bacterial resistance

The excessive and uncontrolled use of antibiotics in human and veterinary medicine causes two environmental problems: one is the contamination of water resources and the other is that some microorganisms can develop resistance to these pharmaceuticals (Heinemann et al., 2000), (Kemper, 2008). Bacteria previously susceptible to an antimicrobial compound can undergo changes in their genetic material, through mutation or through genetic transfer processes (such as transformation, transduction and conjugation), gaining pharmaceutical resistance. The evolution of antibacterial resistance in human and in animals is the result of the interaction between antibiotic exposure and the transmission of resistance within and between individuals (Heinemann et al., 2000). The resistance of bacteria is not developed only by direct therapeutic use of antibiotics, but also by indirect contact with them (Kemper, 2008).

The misuse of antibiotics by both practitioners and patients and the poor quality of pharmaceuticals marketed in developing countries and also, an increase of antimicrobials consumption in most developed countries, are factors related to bacterial resistance. For example, in children, it has been shown that at 200 days after birth more than 70 % of the infants had used at least one antibiotic (Guillemot, 1999). So, it is important to do an optimal antibiotic use and limit the diffusion of existing antibacterial resistance in the population and avoid the emergence of new strains of resistant bacteria (Fair and Tor, 2014) (Guillemot, 1999), (Heinemann et al., 2000), (Penesyan et al., 2015), (Zhang et al., 2015).

Combating bacterial resistance involves shortening the time to investigate new antibiotics, which currently exceeds a decade, and quickly find new therapeutic alternatives, since the antibiotics currently available are ineffective in combating the new strains of bacteria that arise all the days (ionline, 2015) or in another perspective to remove effectively the antibiotics from the environment, avoiding the development of more bacterial resistance. However, it is equally or even more important to make people aware of the proper use of antibiotics.

1.1.1.2. Sulfamethoxazole

1.1.1.2.1. Structure and physico-chemical properties

According to the International Union of Pure and Applied Chemistry (IUPAC), SMX is denominated 4-amino-N-(5-methyl-1,2-oxazol-3-yl)benzenesulfonamide, so $C_{10}H_{11}N_3O_3S$ is the molecular formula.

SMX is a representative antibacterial compound of the sulfonamide group and it is frequently used in human medicine to treat bronchitis and urinary infections and also in veterinary medicine, for prevention and treatment of infections, as well as growth promoter (Abellán et al., 2009). The bactericidal sulfonamide group is considered to be one of the first antimicrobial pharmaceuticals used and it was intensively manufactured since the 40s, revolutionizing the use of antibiotics in medicine. Sulfonamides have a bacteriostatic effect, inhibiting desoxyribonucleic acid (DNA) synthesis. The combination of the common antibacterial pharmaceutical TMP, a folic acid analogue, with SMX, inhibits two steps in the enzymatic pathway for folic acid synthesis, necessary for the synthesis of DNA and ribonucleic acid (RNA) precursors in bacteria, therefore necessary for the survival of bacteria.

The chemical structure of SMX and the chemical structure of the general sulfonamides are represented in figure 2 (Bastos, 2012). Table 5 summarizes the physicochemical properties of SMX.

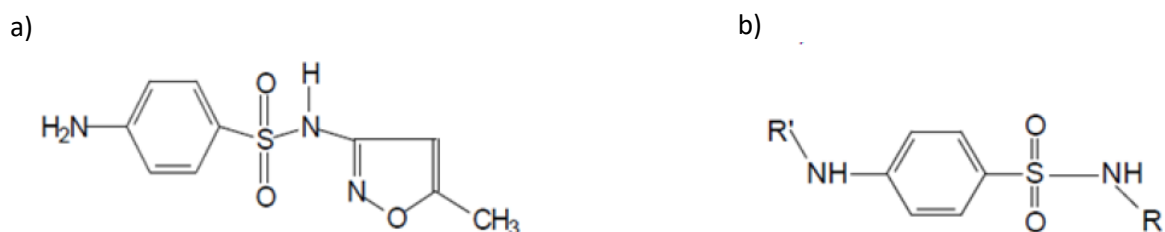


Figure 2- SMX chemical structure (a) and general chemical structure of sulfonamides (b).

Table 5- Physicochemical properties of SMX (adapted from Boreen et al., (2004), Sulfamethoxazole-Toxicology Data Network and Yalkowsky et al., (2010)).

Molecular weight (g/mol)	253.28
Water Solubility (mg/L at 37 °C)	610
Melting Point (°C)	167
Vapor pressure (mm Hg at 25 °C)	6.93×10^{-8}
Log K_{ow}	0.89
Dissociation constants	$pK_{a1}=1.6$ $pK_{a2}=5.7$
Bioconcentration Factor	3

If SMX is released onto soils, it is expected to have high mobility, since SMX have a log K_{ow} value lower than 10^4 , so it is a compound with low volatility and hydrophilic nature (Silva et al., 2012). The pK_{a1} and pK_{a2} of SMX indicate that this compound partially exists in the anionic form in the environment and anions generally do not adsorb strongly to soils containing organic carbon and clay. If released into water, SMX is not expected to adsorb to suspended solids and sediment based. So, in general, sulfonamides are not quickly biodegraded and can persist in soils. Bioconcentration is related to the ratio of the concentration of a particular chemical in a living organism to the chemical's concentration in the surrounding water. An estimated bioconcentration factor of 3 suggests that the potential of SMX bioconcentration in aquatic organisms is low (Sulfamethoxazole-Toxicology Data Network).

1.2. Removal processes for pharmaceuticals in STPs

In order to avoid the risks associated with the presence of pharmaceuticals in water, they should be eliminated before final release into the environment. In general, they can be eliminated by sorption (physical processes), biodegradation (biological processes) or photolysis and photocatalysis (oxidation processes).

The elimination of pharmaceuticals from waste water in STPs is dependent on the pharmaceuticals structural characteristics and physico-chemical properties, such as photosensitivity, biodegradability, lipophilicity and on the environmental conditions (Melo et al., 2009), (Radjenovic et al., 2007).

1.2.1. Physical processes

Sorption elimination involves the uptake of pharmaceuticals from the aqueous phase onto a solid phase (sorbent) and this allows the effluents to be purified. However, contaminants are not degraded or eliminated, only transferred to a new phase. Nevertheless, this approach proved to be an effective and economic purification method to be used as pre- or post-treatment process in STPs (Freire et al., 2000), (Jiuhui, 2008), (Melo et al., 2009). In STPs operating with an activated sludge system, sorption is the dominant process in the removal of lipophilic compounds, such as estrogens (Melo et al., 2009).

Also, adsorption of pharmaceuticals from STPs effluents, on activated carbons can be an efficient strategy to them. The work developed by Calisto et al., (2015) describes the single adsorption of seven pharmaceuticals (carbamazepine, oxazepam, SMX, piroxicam, cetirizine, venlafaxine and paroxetine) from water onto a commercially available activated carbon and a non-activated carbon, produced by pyrolysis of primary paper mill sludge (Calisto et al., 2015).

1.2.2. Biological processes

Biological processes are the most frequently used in the effluents treatment because they allow the treatment of large volumes of effluents, high rates of organic matter removal, the transformation of toxic organic compounds in carbon dioxide (CO₂) and water (H₂O) or methane (CH₄) and costs are relatively low (Freire et al., 2000), (Melo et al., 2009).

In general, degradation of organic compounds depends on their bioavailability and also on the ability of microbial organisms to transform and degrade them (Stumpe and Marschner, 2009). Biological processes may be aerobic or anaerobic. In aerobic processes, formation of CO₂ and H₂O happens, whereas in anaerobic we have the formation of CO₂ and CH₄ (Freire et al., 2000). However, some organic compounds are not degradable by the microorganisms and therefore are resistant to biological treatment. (Freire et al., 2000).

The enzymatic process, which belongs to biological processes, is a recent technology used in effluents biological treatment. Within this context, ligninolytic enzymes (lignin peroxidase and manganese peroxidase) have the capacity to degrade a large number of toxic and persistent substances (Freire et al., 2000).

1.2.3. Oxidation processes

The advanced oxidation processes (AOPs) are attractive technologies that have been extensively studied due to their potential as an alternative or an addition to conventional processes for treating waste water, destructing a wide range of organic substances resistant to conventional methods (Augugliaro et al., 2006), (Freire et al., 2000), (Lester et al., 2010).

The AOPs are defined as the chemical oxidation of target organic pollutants in water and these processes produce powerful transitory species, mainly hydroxyl radicals ($\cdot\text{OH}$), by the combination of oxidants (such as hydrogen peroxide (H_2O_2), chlorine (Cl_2), chlorine dioxide (ClO_2), permanganate (MnO_4^-) with ultraviolet (UV) radiation or by the combination between UV radiation and catalysts (Augugliaro et al., 2006), (Freire et al., 2000), (Lester et al., 2010), (Melo et al., 2009). AOPs have a high efficiency for organic matter oxidation, which can be converted to CO_2 , H_2O and innocuous mineral salts (Augugliaro et al., 2006). However, in most cases, the use of this type of treatment promotes the formation of a wide variety of by-products, which may be as toxic or even more toxic than the initial contaminant (Melo et al., 2009). UV radiation has been reported in the literature as being used in the degradation of pharmaceuticals compounds, but it can also produce subproducts that can be highly toxic and persistent in water (Bastos, 2012), so it is important to evaluate toxicity of subproducts formed. Heterogeneous photocatalysis is another effective method for the removal of some pharmaceuticals from the aquatic environment based on the chemical oxidation mediated by a semiconductor activated by UV radiation (Augugliaro et al., 2006). This method involves the use of catalysts, such as titanium dioxide (TiO_2), ferric oxide (Fe_2O_3) and silicon (Si). In general, TiO_2 is the photocatalyst mostly used due to its high stability over a wide pH range, water insolubility, photoactivity, low environmental impact, low toxicity and cost, when compared to other available semiconductors (Augugliaro et al., 2006), (Freire et al., 2000), (Melo et al., 2009). Although this method is efficient in the mineralization of several chemical species of environmental relevance, there are problems that hinder large-scale treatment, such as the difficulty of radiation penetration in the reaction medium and the separation of the catalysts from the sample. The work of Hu et al. (2007) examines direct photolysis of SMX by UVA light (UVA: $324 \leq \lambda \leq 400$ nm) and the

degradation of SMX in aqueous suspensions of nanophase TiO₂ irradiated with visible light ($\lambda > 400$ nm) and with UVA light. Experimental results demonstrated that no SMX degradation was observed in TiO₂ suspensions irradiated with visible light and direct photolysis of SMX by UVA was slow (less than 10 % degrading in 60 minutes). In comparison, 95 % SMX degradation was observed in UVA-irradiated TiO₂ suspensions over the same time. Rates of UVA–TiO₂ photocatalyzed SMX degradation were dependent on different variables, including initial SMX concentration, catalyst phase identity and concentration, electron acceptor identity and concentration, and the presence of non-target water constituents.

Photodegradation using sunlight is an interesting method for removing pharmaceuticals from the aquatic environments (Bastos, 2012), (Sajjad, 2014). In the aquatic environment, photodegradation can occur via two processes: direct and indirect photolysis, as can be seen in figure 3. These two processes are a primary pathway for abiotic transformation of the organic compounds in surface waters (Andreozzi et al., 2003). In the direct photolysis, light is absorbed directly by the chemical itself, leading to bond cleavage (Chen et al., 2013), (Liu and Liu, 2004). The direct photolysis was shown to be efficient for the removal of contaminants only when the absorption spectrum of the pollutant overlaps the emission spectrum of the UV lamp and the quantum yield (ϕ) of the photochemical process is reasonably large (Andreozzi et al., 2003), (Lester et al., 2010).

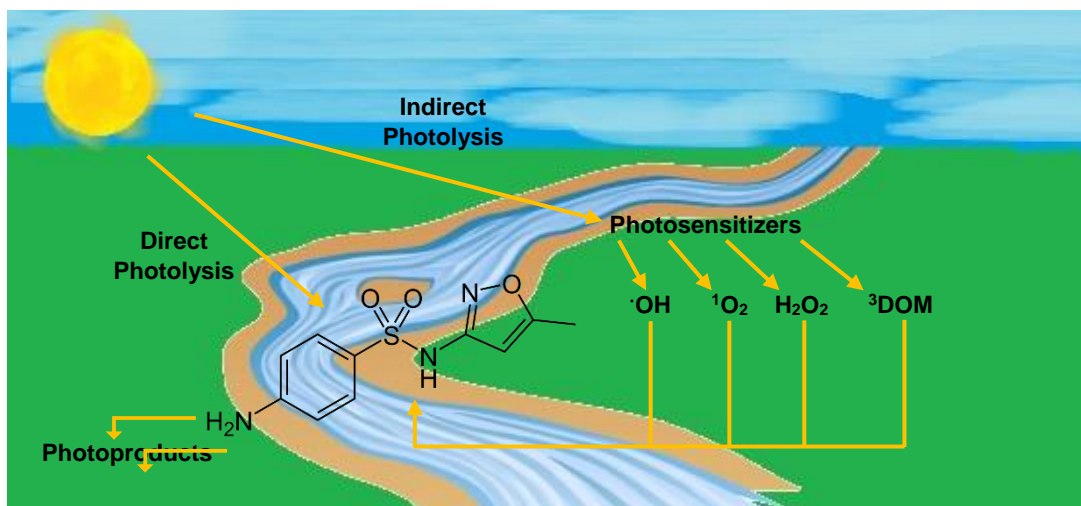


Figure 3- Direct and indirect photolysis occurring in the aquatic environment.

Andreozzi et al. (2003) evaluated the rate of degradation of six selected pharmaceuticals (carbamazepine, diclofenac, clofibric acid, OFL, SMX and propranolol)

submitting them to solar irradiation. Based on experimental results, the direct photolysis in distilled water for SMX, diclofenac, OFL and propranolol undergo fast degradation with a half-life time ($t_{1/2}$) of 2.4, 5.0, 10.6 and 16.8 days, respectively, whereas, under the same conditions, carbamazepine and clofibric acid presented a $t_{1/2}$ of around 100 days (Andreozzi et al., 2003). So, for some compounds, the direct photolysis is not an efficient process for their removal in water.

Indirect photolysis consists of light absorption by photosensitizers, which generate strong oxidant species, such as $\cdot\text{OH}$ or singlet oxygen ($^1\text{O}_2$). The most important natural photosensitizers are natural dissolved organic matter (DOM), nitrate and nitrite (Andreozzi et al., 2003), (Freire et al., 2000), (Lam et al., 2003), (Lester et al., 2010), (Lin and Reinhard, 2005), (Melo et al., 2009). For example, in the study above mentioned (Andreozzi et al., 2003), the influence of nitrate ions present in aqueous solutions was also studied and the results showed a reduction of $t_{1/2}$, thus an increase in the degradation rate (Andreozzi et al., 2003). DOM can act also as photosensitizer, however it has a dual role in photodegradation, acting not only as photosensitizer, but also as a filter of solar radiation. Total effect of the DOM presence depends on the balance between these opposite contributions, and for each target substance such effect may be different (Andreozzi et al., 2003), (Melo et al., 2009).

Some compounds may be photodegraded directly and indirectly in aqueous solution, as was proved in the case of estriol (E3) (Oliveira et al., 2016). Natural sunlight can degrade all estrogens in river water (Lin and Reinhard, 2005) and sea water (Zuo et al., 2006).

1.2.3.1. Photodegradation of SMX

SMX is not completely degraded in conventional STPs, thus affecting aquatic and terrestrial organisms. However, only few studies have been conducted to evaluate the effectiveness of photodegradation on the removal of antibiotics, including SMX, from drinking water and waste water effluents (Lester et al., 2010).

The photochemical transformation of SMX using a solar simulator was investigated by Trovó et al. (2009). Toxicity, persistence and route of degradation of SMX was evaluated in different water matrices: distilled water (pH = 4.8), distilled water + nitrate and sea water (pH = 8.1). In this study, differences in degradation rate in distilled water and sea water were verified, being the photodegradation in sea water matrix slower. It was also verified that indirect photolysis in the presence of nitrate in distilled water did not affect the SMX degradation rate. For the solution of SMX prepared in distilled water (pH = 4.8), during the first 45 minutes of irradiation a decay of 40 % of the initial concentration of SMX was

observed. The phototransformation rate slowed down markedly with time, probably because of the increase of pH from 4.8 to 6.4. Only after 30 hours of irradiation, 98 % of the initial concentration of SMX was removed. In the experiments using sea water (pH = 8.1) solutions, a slower kinetic was observed, where only a slight reduction in the SMX concentration (14 %) occurred after 7 hours. This was considered to be due to the fact that SMX photolysis is strongly affected by pH. They made the identification of nine products of photolysis in distilled water. In figure 4, the mechanism proposed by Trovó et al. (2009) for the degradation of SMX is represented. The cleavage of sulfonamide bond and rearrangement of the isoxazole ring represent the main pathways of degradation, which generate more abundant and persistent intermediates (C2, C3 and C8). On the aromatic rings C6, C9 and C1 hydroxylation reactions also occur. The addition of the hydroxyl radical to isoxazole ring formation occurs across C7, as well as with the C4, which is the only evidence of the opening of the isoxazole ring (Trovó et al., 2009).

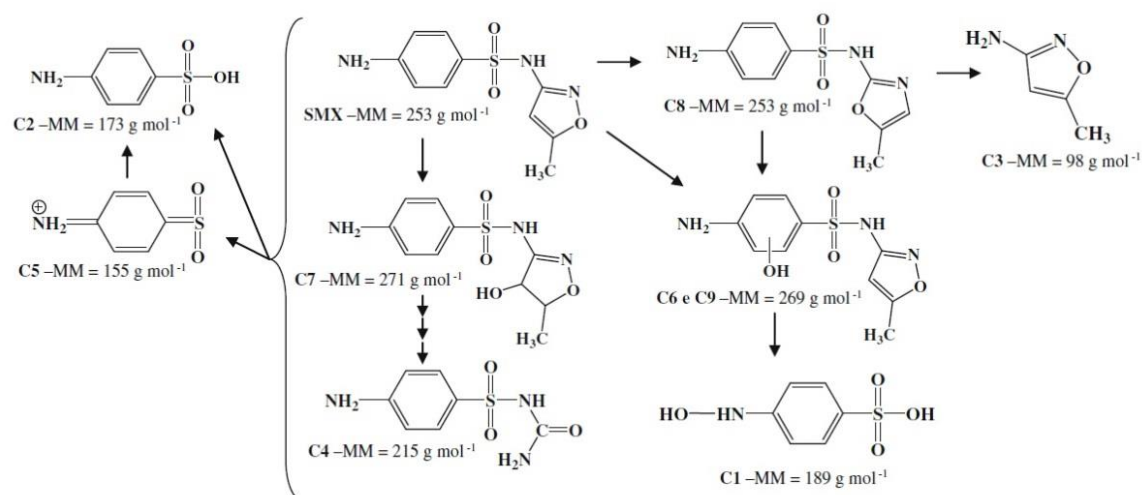


Figure 4- Degradation path of SMX by direct photolysis in distilled water (from Trovó et al. (2009)).

In the study developed by Bastos (2012), the direct photolysis of SMX in ultrapure water with UV radiation was carried out considering the variation of the concentration (10-50 mg/L) and of the pH (5-9). In the first 30 minutes of photolysis, the removal rate of SMX in the acid medium was higher than that observed in neutral medium. After 60 minutes of irradiation, SMX had the removal % of 99 in all experiments (Bastos, 2012).

1.2.3.2. Importance of photosensitizers

Photochemistry plays a crucial role in pharmaceuticals reduction in aquatic environments. Under solar irradiation, photochemical transformations involve direct and indirect reactions. As mentioned before, in indirect photodegradation the degradation of compounds can be induced by the presence of natural photoreactive substances, such as HS. All these constituents may generate strong oxidants, undergo photoreactions, and further oxidize and degrade environmental pollutants in natural water (Chen et al., 2013), (al Housari et al., 2010).

1.2.3.2.1. Humic substances

HS are heterogeneous mixtures of polydispersed organic materials, which result from biochemical and chemical reactions during the decay and transformation of plant and microbial remains, and therefore are formed in soils, sediments and natural waters. HS are main components of the natural organic matter in terrestrial (soil organic matter) and aquatic (DOM) systems.

In aqueous systems, like rivers, about 50 % of the dissolved organic materials are HS that affect pH and alkalinity. In terrestrial and aquatic systems, HS affect the chemistry, cycling and bioavailability of chemical elements, as well as transport and degradation of xenobiotic and natural organic chemicals. These substances also affect biological activity in aquatic ecosystems (IHSS, 2007), (Stevenson, 1994).

HS have a high-molecular-weight, with aromatic cores, substituted with functional groups and aliphatic cores (Aleksandrova et al., 2011). HS can be generally characterized as being rich in oxygen-containing functional groups, notably carboxylic group (COOH), but also phenolic and/or enolic hydroxyl group (OH), alcoholic OH and carbonyl group (C=O) of quinones (Stevenson, 1994). They can operationally be divided into three main fractions: humic acids (HA), fulvic acids (FA) and humin: HA are insoluble under acid conditions, but soluble at high pH values, FA are soluble in both alkali and acid conditions; humin is insoluble in all pH values.

Most of the data on HA, FA and humin refer to average properties and structure of a large ensemble of components of diverse structure and molecular weight. The precise properties and structure of a given HS sample depends on the water or soil source and the specific conditions of extraction (IHSS, 2007), (Stevenson, 1994).

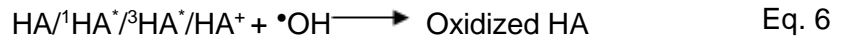
Photolysis of HS, under solar radiation, can lead to the formation of various reactive species, such as $^1\text{O}_2$, superoxide anion ($\text{O}_2^{\cdot-}$), hydroperoxyl radical (HO_2^{\cdot}), H_2O_2 and HS

triplet excited states ($^3\text{HS}^*$). Many photochemical reactions require molecular oxygen (O_2) in the initial step, since O_2 is a source of $\text{O}_2^{\cdot-}$ or $^1\text{O}_2$ in the presence of the photosensitizer and visible light (Bancirova, 2011). The mechanism of $^1\text{O}_2$ formation involves the energy transfer between $^3\text{HS}^*$ and the O_2 (Aguer et al., 1999), (Hessler et al., 1996).

However, the effect of HS on the pollutants photodegradation is complicated because it acts as photosensitizer, light filter and quencher of free radicals. As an example, the formation of some of these reactive species, during the irradiation of HA, is represented in the below mechanisms:



However, HA can also act as a light-filtering agent and/or a free radical quencher to inhibit degradation as shown in the next equation:



So, the overall effect of HA on the photodegradation of compounds depends on the competition between the opposing roles.

Chen et al. (2013) concluded that the HA photoactivated species ($^1\text{HA}^*$, $^3\text{HA}^*$, HA^+) are more efficient free radical quenchers than the parent HA. So, an increased free radical quenching efficiency and light screening effect led to an inhibition on the photodegradation of E3, which means that the HA had an impact in the indirect photodegradation of E3. In this study, it was found for the first time that the enhancement or inhibition role of HA in the photodegradation depended on the incident light intensity. HA accelerated the degradation as a photosensitizer under weak irradiation. In contrast, under the high incident light intensity, HA inhibited the photodegradation due to light screening and free radical quenching effects.

It was reported in different studies that the photodegradation of estrone (E1), 17 β -estradiol (E2) and E3 was enhanced in the presence of HS (Caupos et al., 2011), (Lin and Reinhard, 2005), (Oliveira et al., 2016), (Silva, 2014). However, under simulated light, the inhibition effect of HS on photodegradation of E1 was also reported (Atkinson et al., 2011). So, it was speculated that the differences in quality and type of DOM resulted in the different effects (Atkinson et al., 2011). In some studies were shown the distinct effects of HS on the photodegradation of pollutants under simulated sunlight (Chen et al., 2009), (Ge et al., 2009), (Yuan et al., 2009).

1.3. Objectives of the dissertation

The presence of SMX in the aquatic environment around the world was confirmed by the different studies presented. In addition, there is already some knowledge about the harmful effects of SMX, since it belongs to the group of antibiotics and therefore there is a risk of developing bacterial resistance. Consequently, the removal of this pharmaceutical from the aquatic environment is urgent.

So, the aims of this work are:

- 1) To study the SMX photodegradation behavior under simulated solar irradiation and thus to verify whether photodegradation may be an effective method for the removal of this antibiotic from effluents of STPs. The photodegradation rates of SMX will be followed by high performance liquid chromatography with fluorescence detection (HPLC-FLD).
- 2) To evaluate the effect of natural photosensitizers in the photodegradation, because it is known that these can influence the degradation rate of pharmaceuticals. So, the HA, FA and styrene divinylbenzene (XAD-4) fractions extracted from an estuarine water stream were chosen to evaluate indirect photodegradation caused by organic matter (OM) present in aquatic environments.
- 3) To understand the photodegradation behavior of SMX in the natural aquatic environment and due to the differences in the content and nature of DOM, salinity, samples from different origins (estuarine, fresh and waste waters samples) will be collected and used in this work. Several factors that might influence the

photodegradation kinetics of SMX will also be studied, such as pH, salinity and presence of inorganic compounds, such as calcium and magnesium, important constituents of sea water.

- 4) To evaluate the antibacterial activity before and after photodegradation to understand the consequences of this proposed method on combating bacterial resistance.

2. Materials and Methods

2.1. Chemicals

SMX – $C_{10}H_{11}N_3O_3S$ (purity > 98 %) used in these studies was provided by TCI (Europe). Ultrapure water, used in the preparation of solutions, was obtained from a Millipore system (Milli-Q plus 185).

Acetonitrile (HPLC grade) and acetic acid (p.a.) used for HPLC analysis, were obtained from VWR, Prolabo and Merck, respectively. Methanol (99.99 %) and nitric acid (>65 %) were purchased from Fisher Chemical and Sigma-Aldrich, respectively.

The pH solutions were adjusted using hydrochloric acid – HCl (NormaPur, 37 %) and sodium hydroxide – NaOH (ABSOLVE, 99.3 %) solutions.

The stock solution of phosphate buffer 0.1 M was prepared in ultrapure water from the mixture of 0.05 mol of sodium dihydrogen phosphate dihydrate – $NaH_2PO_4 \cdot 2H_2O$ (Fluka, Biochemika, ≥ 99.5 %) and 0.05 mol of di-sodium hydrogen phosphate dihydrate – $Na_2HPO_4 \cdot 2H_2O$ (Fluka, Biochemika, ≥ 99 %) for each litre of buffer.

The *Red Sea Salt* and sodium chloride – NaCl (99.3 %) were acquired from Red Sea Europe and ABSOLVE, respectively.

Calcium chloride dihydrate – $CaCl_2 \cdot 2H_2O$ (p.a.) and magnesium chloride hexahydrate – $MgCl_2 \cdot 6H_2O$ (p.a.) were provided from Merck and Riedel-de-Haën, respectively.

2.2. Instrumentation

Solar radiation simulator (Solarbox)

All samples were irradiated under simulated solar radiation using a Solarbox 1500 (Co.fo.me.gra, Italy). The irradiation device contained an arc xenon lamp (1500 W) and outdoor UV filters that limited the transmission of light with wavelengths below 290 nm. The irradiance of the lamp was set to 55 W/m^2 (290-400) nm and was kept constant during all the experiments. To monitor the irradiance level and temperature, a multimeter (Co.fo.me.gra, Italy), equipped with a UV (290-400) nm large band sensor and a black standard temperature sensor, was used. Through an air-cooled system, the device was

refrigerated. Furthermore, a parabolic reflection system guaranteed the uniformity of the irradiation inside the chamber.

HPLC-FLD

Quantitative analysis of SMX was achieved using a HPLC-FLD. This device consisted of a degasser DGU-20A5R, a column oven CTO-10AC, a pump LC-30AD and an autosampler SIL-30AC (all from Shimadzu). For the separation, a Kinetex XB-C18 column (2.6 μm , 100 mm x 4.60 mm) was used. Both the cell and column temperature were maintained at 25 °C and an injection of 20 μL was used. The mobile phase consisted of water (acidified with 1 % acetic acid):acetonitrile mixture (40:60, v/v) and the flow rate was maintained at 0.8 mL/min. Before use as mobile phase, water with 1 % of acetic acid and acetonitrile were filtered through a 0.2 μm polyamide membrane filters (Whatman). The detection of SMX was done by using a Prominence RF-20Axs fluorescence detector from Shimadzu with an excitation wavelength of 265 nm and an emission wavelength of 343 nm.

Conductivity, pH and salinity

Conductivity was measured using a Consort C861 multi-parameter analyser at 25 °C. Salinity and pH were measured using a MASTER REFRACTOMETER, from ATAGO and a pH/mV/°C meter pHenomenal® pH 1100L from VWR.

UV-Vis spectrophotometer and DOC

All UV-Visible (UV-Vis) spectra were obtained with a Shimadzu UV 2101 PC spectrometer using rectangular quartz cuvettes with an optical path length of 1 cm, between 200 and 800 nm.

Dissolved organic carbon (DOC) was measured using a Total Organic Carbon analyser, TOC-V_{CPH}, from Shimadzu, where samples were acidified with 2 % (v/v) of HCl 2 M, purged with nitrogen and covered with Parafilm M®, previously to the analysis.

Stock solution of potassium hydrogen phthalate ($\text{KHC}_8\text{H}_4\text{O}_4$) 1000 mg/L was prepared by dissolving 0.2125 g of $\text{KHC}_8\text{H}_4\text{O}_4$ in 100 mL of ultrapure water.

Calibration curve, used for quantification of DOC in different samples throughout the experimental work, were performed using standard solutions of $\text{KHC}_8\text{H}_4\text{O}_4$ in ultrapure water (0.0-10.0 mg/L), by dilution of proper amounts of the stock solution.

The coefficient of determination (R^2) and limit of detection (LOD) for the calibration curve obtained were 0.9984 and 0.613 mg/L, respectively. To confirm the stability of calibration curve, everyday a newly prepared standard solution [5.0 mg/L] of $\text{KHC}_8\text{H}_4\text{O}_4$ was prepared and analyzed before the samples analysis.

Atomic absorption spectrophotometer

To determine metals in environmental water samples by flame atomic absorption spectroscopy (air-acetylene) an atomic absorption spectrophotometer Perkin Elmer, Analyst 100 was used.

For this determination, water samples were filtered, using a membrane filter (0.2 μm , NL16 Whatman) and acidified with nitric acid to $\text{pH} \leq 2$ (adding 200 μL of nitric acid 65 % to 100 mL of sample). The samples were refrigerated until the analysis. Before determination of dissolved metals, the material used was previously washed with HNO_3 4 M followed by ultrapure water to prevent the contamination with metals ions.

To quantify the dissolved calcium, magnesium, sodium, potassium and iron by the flame atomic absorption method, calibration curves were made for each element. For calcium and magnesium determination, six standards were prepared by dilution of proper amounts of the stock solution 100 and 10 mg/L, respectively, in ultrapure water. Due to the possibility of complexation, for the calcium and magnesium determinations, 500 μL of lanthanum chloride (LaCl_2) 0.10 % were added to 50 mL of samples and standard solutions. Also, six standards were prepared by dilution of proper amounts of the stock solution 1000 mg/L in ultrapure water for sodium determination. For minimize the ionization of sodium, 400 μL of KCl 25 % were added to 50 mL of samples and standard solutions. For potassium and iron determination, four standards were prepared by dilution of proper amounts of the stock solution 400 and 100 mg/L, respectively, in ultrapure water.

Spectrofluorometer

All fluorescence spectra were acquired with a spectrofluorometer FluoroMax-4 (Horiba Jobin Yvon) and a quartz cell with an optical path length of 1 cm was used as

sample container. The excitation and emission wavelengths ranged from (200-540) nm and from (210-600) nm, respectively. Excitation and emission slits of 10 nm and an increment of 5 nm were chosen to acquire the spectra.

2.3. Humic substances

To study the effect of OM on SMX photodegradation, three fractions of HS were used to simulate dissolved organic matter (DOC) in the aquatic environment, since these substances are aquatic origin. These fractions, HA, FA and XAD-4, were extracted and isolated by Esteves (1995) from an estuarine stream that flows into the Aveiro lagoon, Portugal, during low tide at the bar entrance of Aveiro (Portugal) at 40°31'16"N and 8°46'34"W.

Different fractions of HS were previously (Esteves, 1995) extracted and isolated using a system of two resins in series - poly(methymetacrylate) (XAD-8) followed by XAD-4. After the isolation of HA and FA using the XAD-8 column, an additional step was applied to isolate the hydrophilic organic acids using the XAD-4 styrene resin, being the obtained substances called XAD-4 fraction (Esteves et al., 2009). The purified fractions of HS were subsequently characterized by elemental analysis by Esteves (1995).

In this work, UV-Vis spectrophotometry was used for HS fractions' characterization.

2.4. Environmental water samples

Surface and waste water samples were collected in cleaned amber glass bottles between October 2016 and February 2017 with the purpose of studying the SMX photodegradation in environmental aquatic matrices.

A surface estuarine water sample was collected from *Ria de Aveiro*, more precisely in the urban city center of Aveiro (*Fonte Nova, Ria de Aveiro, Aveiro, Portugal*). In this sampling site, water is typically known to have high contents of OM and salinity. *Ria de*

Aveiro is a shallow lagoon (about 1 m of depth) situated in the Northwest Atlantic coast of Portugal (40°38'N, 8°45'W) with 45 km length and 10 km width. The lagoon receives fresh water from two main rivers, the Antuã river with average flow of 5 m³/s and the Vouga river with 50 m³/s. In addition to the rivers mentioned above, *Ria de Aveiro* has a number of channels and among them two are more important, the *São Jacinto* and *Espinheiro* channels. This lagoon covers an area of 83 km² at high tide and 66 km² at low tide. *Ria de Aveiro* was affected by the increase of anthropogenic activities, namely building and land occupation, agricultural and industrial activities, leading to a significant change of the lagoon morphology, with the addition of anthropogenic nutrients and contaminants. Thus, there is a negative impact on the water circulation, as well as on the water quality of the lagoon. The main anthropogenic sources of pollution are domestic and industrial discharge flows (Lima, 2011).

Other surface water samples were tested: a fresh water from *Rio Novo do Príncipe* (Aveiro, Portugal), located in the rural and agricultural area of Aveiro and a fresh water from *Poço da Cruz* (Aveiro, Portugal), belonging to the *Mira* channel. Finally, a waste water sample was collected from the North Aveiro STP, after secondary treatment (corresponding to the final effluent, STPF). In Aveiro, there are two STPs (North and South of Aveiro) where domestic (South STP) and both domestic and industrial (North STP) effluents from 10 different locations are treated and discharged into the Atlantic Ocean, at a distance of 3.2 Km from the coast, at approximately 17 m depth. North STP is located in Cacia, Aveiro, and was projected to satisfy the effluents' treatment needs of Águeda, Aveiro (part of), Albergaria-a-Velha, Estarreja, Murtosa, Oliveira do Bairro and Ovar. It is dimensioned to serve a population of 272 000 inhabitants and an average daily flow of 48 705 m³ and performs the treatment of both domestic and industrial effluents (Lima, 2011).

All sampling sites are represented in figure 5.

After collection, all the samples were filtered through 0.22 µm nitrocellulose membrane filters (Millipore) avoiding bacteria activity and stored at 4 °C prior to use.

All water samples were characterized through UV-Vis spectrophotometry, atomic absorption spectrophotometry and measuring different parameters, such as DOC, salinity, pH and conductivity.

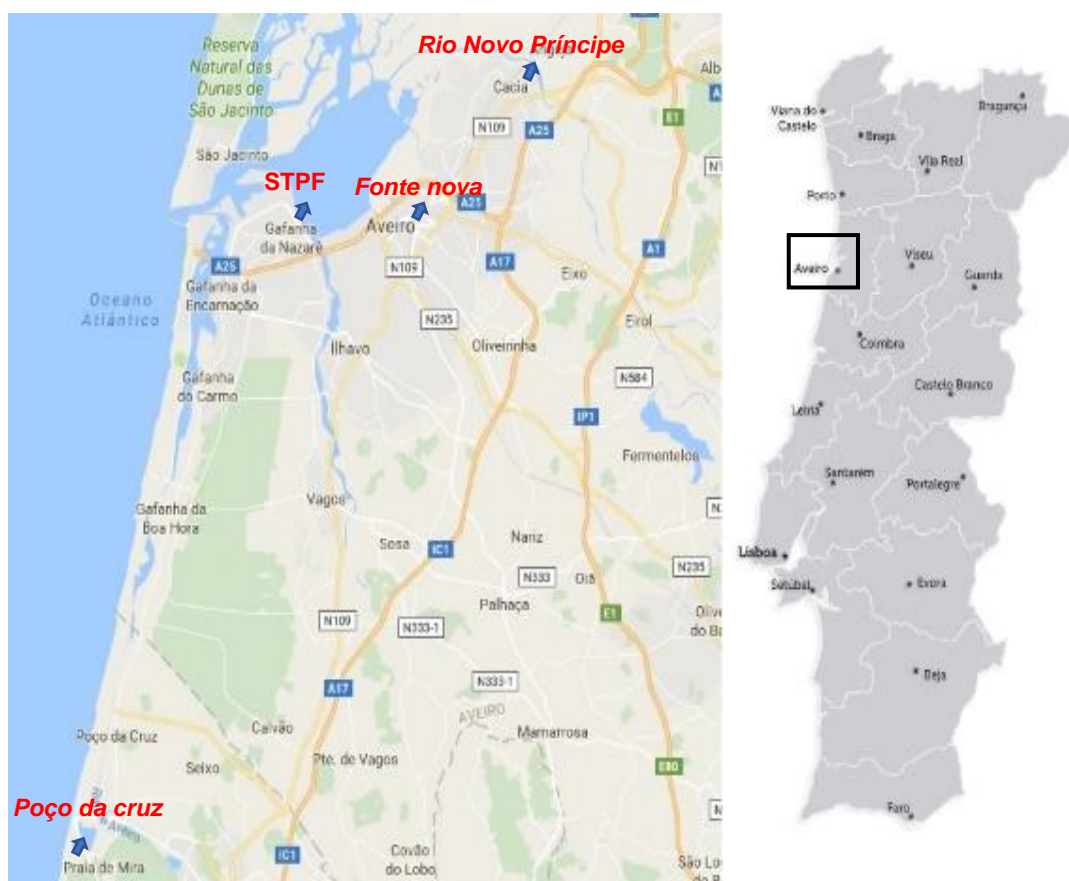


Figure 5- Location of the sampling points.

2.5. Photodegradation experiments

2.5.1. Solutions of SMX

SMX stock solution of 100 mg/L was prepared by dissolving 10 mg of SMX in a small quantity of methanol (less than 1 %) and stored at 4 °C in the dark.

The SMX calibration curve was obtained by preparation of standard solutions in ultrapure water, with concentrations 100, 50, 25, 10, 5 and 1 µg/L, by dilution of proper amounts of the stock solution.

For the evaluation of the antibacterial activity of SMX and its photoproducts, a 400 mg/L aqueous standard stock solution of SMX was prepared by dissolving SMX in a small volume of methanol (less than 1 %). Solutions were kept at 4 °C in the dark.

2.5.2. Photodegradation of SMX in batch mode

General procedure of SMX photodegradation

The SMX photodegradation studies were performed using quartz tubes (1.8 cm internal diameter and height of 20 cm) containing the compound solution. Thereafter, the tubes were placed on a suitable support to be maintained in suspension inside the irradiation chamber and subjected to irradiation making use of the Solarbox. For each set of experiments, four properly identified quartz tubes capped with Parafilm M[®] were introduced into the Solarbox: three of them were exposed to radiation and the other one was covered with aluminum foil to protect it from light (control). The controls were kept inside the Solarbox during the same time as the irradiated solutions. These controls will indicate the existence or not of any degradation by microbiological or thermal means, during the photodegradation experiments. Therefore, the decrease of SMX concentration in exposed solutions, as compared with controls, may be only ascribed to photo-induced degradation.

For kinetic studies, from each irradiated samples and controls, 1 mL aliquot was collected after 5, 10, 20, 30, 45, 60, 90, 120, 150 and 180 minutes; then every hour until 8 hours, after 10 hours of irradiation and then every 4 hours until no SMX was detected using HPLC-FLD.

The degradation percentage for each set of experiments was calculated in relation with the respective control. Experimental data was fitted to the pseudo first-order kinetic equation given below, using GraphPad Prism 5.:

$$C/C_0 = e^{-kt} \quad \text{Eq. 7}$$

where,

C – is the concentration of SMX exposed to light at different irradiation times ($\mu\text{g/L}$);

C_0 – is the concentration of SMX protected to light at different irradiation times ($\mu\text{g/L}$);

k – is the pseudo first-order degradation rate constant (h^{-1});

t – is time (h).

The determination quantum yield of photodegradation (ϕ) was performed by radiometry using the method described by Calisto et al. (2011), using the equations presented below:

$$\phi_{\lambda i} = \frac{\text{rate } \lambda i}{I_{\lambda i}^{abs}} \quad \text{Eq. 8}$$

where,

$\phi_{\lambda i}$ – is the quantum yield at the wavelength λi (mol/L·s or Ein/L·s);

$\text{rate } \lambda i$ – is the photodegradation rate of SMX induced by the absorption of radiation with wavelength λi (mol/L·s or Ein/L·s);

$I_{\lambda i}^{abs}$ – is the rate of light absorption at the wavelength λi (do not have units);

and

$$I_{\lambda i}^{abs} = I_{\lambda i}^0 \times (1 - 10^{-\varepsilon_{\lambda i} \times l \times C_0}) \quad \text{Eq. 9}$$

where,

$I_{\lambda i}^0$ – is the lamp emission intensity at the wavelength λi (W·m⁻²/nm);

$\varepsilon_{\lambda i}$ – is the molar absorptivity of the SMX at the wavelength λi (L/mol·m);

l – is the path length inside the photoreactor (m);

and

$$\phi_{\lambda i} = \frac{C_0 \times k_i}{I_{\lambda i}^0 \times (1 - 10^{-\varepsilon_{\lambda i} \times l \times C_0})} \quad \text{Eq. 10}$$

where,

k_i – is the pseudo first-order degradation rate constant at the wavelength λi (s⁻¹).

However, taking into account the experimental impossibility of determining the rate constant of a photodegradation process corresponding to the absorption of a single

wavelength, the photodegradation ϕ is often determined considering an overall average over the lamp emission wavelength range as given by equation 11:

$$\phi_{ave} = \frac{C_0 \times k}{\sum I_{\lambda_i}^0 \times (1 - 10^{-\epsilon_{\lambda_i} \times l \times C_0}) \times \Delta\lambda} \quad \text{Eq. 11}$$

where,

$\Delta\lambda$ – is the wavelength interval of acquisition of the spectral irradiance of the lamp (nm).

According to these equations, the units of the average quantum yield (ϕ_{ave}) should be mol/Ein. Taking into account that one Ein is equivalent to one mole of photons, the ϕ is a dimensionless quantity.

The SMX's photodegradation ϕ was calculated considering an overall average over the lamp emission wavelength range (290–800) nm and respective emission intensities, directly extracted from the lamp spectrum (as given by the manufacturer), for the irradiance level used during the experiments (55 W m⁻², 290–800 nm). The calculation of the ϕ was performed considering a diameter of the cylindrical photoreactor of 1.8 cm, a volume of irradiated solution of 20 mL and a solution exposure area of 36 cm².

Photodegradation of SMX in ultrapure water

For the direct photodegradation of SMX, a solution of 100 µg/L SMX, environmentally relevant concentration, in ultrapure water was prepared by dilution of the stock solution and transferred into quartz tubes (20 mL in each tube). The aliquots were collected at different times of irradiation, as described above, until a maximum of 3 hours of irradiation.

Photodegradation of SMX in environmental water samples

With the objective to study the SMX photodegradation when present in the aquatic environment, each one of the four environmental water samples collected was spiked with 100 µg/L of SMX. These solutions were distributed into quartz tubes and the aliquots in *Fonte Nova*, *Rio Novo do Príncipe*, *Poço da Cruz* and STPF samples, were collected as described previously until no SMX was detected.

Effect of HS on SMX photodegradation

To study the effect of HS on the SMX photodegradation, kinetic studies were performed using three fractions of HS (HA, FA and XAD-4). The SMX solutions of 100 µg/L were prepared in the presence of 20 mg/L of HA, FA or XAD-4 and subjected to irradiation until no SMX was detected.

Effect of pH on SMX photodegradation

Several experiments were performed to study the influence of pH in aqueous solutions on SMX photodegradation.

Firstly, a 100 µg/L of SMX solution prepared in a 0.001 M phosphate buffer with pH 5.00 and 7.30 adjusted with NaOH or HCl was irradiated until no SMX was detected using HPLC-FLD and aliquots were collected at different times following the order described above.

Secondly, an estuarine water sample spiked with 100 µg/L SMX with no pH adjustment (pH = 7.33) and with pH adjusted to 6.30 with HCl was also irradiated until no SMX was detected using HPLC-FLD.

At last, SMX solutions (100 µg/L) in absence and presence of each one of the three fractions of HS (HA, FA and XAD-4) at a concentration of 20 mg/L prepared in a 0.001 M phosphate buffer with pH 5.00 and 7.30 adjusted with NaOH or HCl were irradiated until no SMX was detected by HPLC-FLD.

Effect of sea salts on SMX photodegradation

The influence of sea salts on photodegradation behaviour was evaluated using 100 µg/L of SMX, dissolved in 0.001 M phosphate buffer with pH adjusted to 7.30 containing 21 ‰ of NaCl or 21 ‰ of sea salts (artificial sea water from *Red Sea Salts*). Both solutions were irradiated during 5 hours and analysed with HPLC-FLD. Results were compared with the ones obtained using an estuarine water sample spiked with 100 µg/L SMX and an ultrapure water with phosphate buffer at pH 7.30.

In order to obtain information on the possibility of inorganic compounds (such as calcium and magnesium) playing a role in the photodegradation of SMX, the following

experiment was conducted: 100 µg/L SMX solutions in 0.001 M phosphate buffer with pH adjusted to 7.30 with NaOH and containing 785 mg/L of magnesium or 261 mg/L of calcium were also irradiated during 5 hours and analysed with HPLC-FLD. These concentrations of magnesium and calcium were chosen because they are similar to the existing on *Red Sea Salts* mentioned previously.

To test the possible influence of ionic strength photodegradation, kinetics of the photodegradation of SMX was also performed using 21 ‰ of sea salts (artificial sea water from *Red Sea Salts*) and using 21 ‰ of NaCl spiked with 100 µg/L of SMX, dissolved in 0.001 M phosphate buffer with pH adjusted to 7.30 with NaOH and irradiated until a maximum of 18 hours. Results were compared with those obtained in previous sections using an estuarine water sample spiked with 100 µg/L SMX at pH 7.33 and an ultrapure water with phosphate buffer at pH 7.30.

2.5.3. Photodegradation of SMX in continuous flow mode

To study the SMX photodegradation in continuous flow mode, solutions of the compound kept in two reservoirs with 20 mL each were capped with Parafilm M[®] and covered with aluminum foil to protect them from light. The samples were pumped with a Longer Pump BT 100-1L, using a flow rate of 150.1 µL/min, through a narrow-bore (inner diameter: 0.8 mm and outer diameter: 1.6 mm), transparent tube of fluorinated ethylene propylene. Each one of the two tubes used had a total length of 2.80 m, however, just 1.50 m were placed in a flat plate inside the solarbox, while the rest of the tube was outside, to allow sample recirculation. It is important to refer that the reservoirs and part of the tubes that were outside the solarbox were all carefully covered with aluminum foil to protect them from light. One of the two plates were covered with aluminum foil to protect it from light (control). The scheme used to study the photodegradation in continuous flow mode is represented in figure 6. The control was kept inside the Solarbox during the same time as the irradiated flat plate containing the solution. During the photodegradation experiments, these controls were used to verify that there was not another type of degradation or adsorption to the inner walls of the tube besides photodegradation. So, the decrease of SMX concentration in exposed solutions may only be ascribed to photo-induced degradation.



Figure 6- Scheme of SMX photodegradation in continuous flow mode.

Residence time plays a significant role in the complete degradation of the target compound. So, to build the kinetic profile of SMX degradation, samples with 100 $\mu\text{g/L}$ were tested with different residence times, being varied by several consecutive cycles.

For the direct photodegradation of SMX, a solution of 100 $\mu\text{g/L}$ of SMX in ultrapure water was prepared by dilution of the stock solution and transferred to two reservoirs (5 mL in each). The aliquots were collected at different times of irradiation as described above until a maximum of 1 hour of irradiation.

With the objective to study the SMX photodegradation when present in the aquatic environment, each one of four environmental water samples collected was spiked with 100 $\mu\text{g/L}$ of SMX. These filtered solutions were distributed into reservoirs and the aliquots of *Fonte Nova*, *Rio Novo do Príncipe*, *Poço da Cruz* and STPF samples, were collected as described previously until a maximum of 5, 4, 4 and 5 hours of irradiation, respectively.

From each one of the irradiated samples and controls, 200 μL aliquot was collected after 3, 6, 9, 15, 21, 30, 45 and 60 minutes; then every 30 minutes until 3 hours and then every hour until no SMX was detected using HPLC-FLD.

The degradation percentage for each set of experiments was calculated in relation with the respective control and to perform the fittings of experimental data the same equation as in SMX photodegradation in batch mode was used.

2.5.4. Antibacterial activity

Before performing the antibacterial activity tests, SMX photodegradation experiments were done using five tubes placed inside the solarbox in the same way as referred in 2.5.2 section. All quartz tubes were capped with Parafilm M[®] and two of these tubes were covered with aluminum foil to protect them from light (controls).

For the direct photodegradation of SMX, a solution of 100 mg/L of SMX, concentration needed to detect bacterial growth, in ultrapure water was prepared by dilution of the stock solution and transferred to four quartz tubes (20 mL each).

With the aim of studying the antibacterial activity of SMX in aquatic environment during the photodegradation process, each one of three environmental water samples collected was spiked with 100 mg/L of SMX and these solutions were distributed into four quartz tubes.

Aliquots of the three replicates were collected after about 50 % of SMX photodegradation (t_1 – sample E), after more than 95 % of SMX photodegradation (t_2 – sample F) and when no SMX was detected (t_3 – sample G) by HPLC-FLD. All concentrations of SMX in ultrapure water and in environmental water samples at different times of irradiation used for antibacterial activity tests are on the table A1 (annex).

One of the dark controls (sample D) consisted in a SMX solution of 100 mg/L in the water matrix subjected to the irradiation and the aliquots were collected at zero time of irradiation to evaluate the antibacterial activity and t_1 , t_2 and t_3 of irradiation for analysis by HPLC-FLD to calculate the photodegradation rate and to evaluate the existence or not of any degradation by microbiological or thermal means, during the photodegradation experiments. The other control (sample C), with an expected SMX concentration corresponding to 50 % of degradation, was used to evaluate the existence of any loss of antibacterial activity due to thermal heat that samples might be subjected.

A 5 mL blank of the water matrix (no SMX added) was used to evaluate matrix effects on bioassays performance (sample A). Also, a 5 mL of a SMX standard with 50 % of the initial concentration not subjected to any irradiation (sample B) was used to compare its antibacterial activity with the one obtained with 50 mg/L SMX solution in the water matrix subjected to irradiation (containing any photoproducts formed during the irradiation).

The tests of antibacterial activity were performed using *Vibrio fischeri* ATCC 7744 incubated overnight in Nutrient Broth n.2 supplemented with 2 % of NaCl. This strain was chosen to represent bacteria present in environmental waters and because it is known to

play an important role in antibiotics' resistance dissemination (Cabral, 2010), (Chavez-dozal et al., 2013), (Backhaus and Grimme, 1999). Its detection is favoured since it emits luminescence (Hamada, 2008).

The strain was grown to optical density (OD) 0.9 at wavelength 600 nm and then was used in the bioassays in ultrapure water and in the different environmental water samples. All assays were performed in triplicate.

The cytotoxic effect was evaluated considering the bacterial growth at a wavelength of 600 nm and its luminescence at a wavelength of 420 nm using a Multiskan™ GO, Thermo Scientific, UK.

For the various samples tested, a growth control was performed, where the strain was grown in the water sample under study without SMX (control - sample A). Then, the % of viable cells was estimated at wavelength 420 nm using the following ratio:

$$\% \text{ of viable cells} = \left(\frac{O.D. \text{ in test}}{O.D. \text{ in sample A}} \right) \times 100 \quad \text{Eq. 12}$$

3. Results and Discussion

3.1. Calibration curve

The calibration curve was performed using six standard solutions of SMX with concentrations ranging from (1 to 100) µg/L and each standard was analysed in quadruplicate. These solutions were prepared by dilution of a 100 mg/L stock solution of SMX in ultrapure water and analysed by HPLC-FLD.

The equation used for SMX quantification and respective errors are presented below:

$$y = (1517 \pm 35) x + (4.4 \times 10^3 \pm 2.0 \times 10^3) \quad \text{Eq. 13}$$

where,

y – is the peak area obtained by HPLC-FLD;

x – is the concentration obtained at different times of irradiation.

The calibration curve allowed to obtain the value of R^2 of 0.9979 which confirms the good linear response in the studied range of concentrations.

The repeatability of retention time (t_r) and peak areas were measured through the relative standard deviation (RSD) and values below 5.0 % were obtained proving the good repeatability of the HPLC method. However, is also possible to calculate the LOD and the linearity (Lin) of response of the method using the equations described below (Esteves et al., 2004), (Lima, 2011), (Miller and Miller, 2010):

$$LOD_y = a + 3 S_{y/x} \quad \text{Eq. 14}$$

where,

a – is the intersection with the y-axis;

LOD_y – is the value of LOD in the y-axis;

$S_{y/x}$ – is the statistical parameter that estimates the random errors in the y axis;

and

$$S_{y/x} = \sqrt{\frac{\sum_i (y_i - \hat{y}_i)^2}{n-2}} \quad \text{Eq. 15}$$

where,

y_i – is the experimental values of y obtained for each calibration standard;

\hat{y}_i – is the calculated y -values by using the calibration curve equation (eq.13), corresponding to the individual x -values of standards;

n – is the number of standard solutions that were used for calibration;

and

$$LOD_x = \frac{3 S_{y/x}}{b} \quad \text{Eq. 16}$$

where,

b – is the slope of the calibration curve.

$$\text{Lin (\%)} = 100 - \text{RSD}_b \quad \text{Eq. 17}$$

where,

RSD_b – is the relative standard deviation of slope.

The value obtained for LOD on the y -axis was 53188 and the LOD for x -axis was 3.42 $\mu\text{g/L}$. Linearity obtained was 99.98 % suggesting that the method used is linear for the range of concentrations tested.

The results, obtained in the calibration procedure, allowed to determine the SMX concentration in the samples subjected to irradiation needed to determine the photodegradation rate.

3.2. Photodegradation of SMX in batch mode

3.2.1. Direct photodegradation kinetics of SMX

The study of direct photodegradation of SMX was performed in ultrapure water to investigate the rate of degradation in the absence of OM or salts.

So, the photodegradation of 100 µg/L of SMX prepared in ultrapure water was investigated irradiating the solution during 3 hours and results showed a decrease of SMX concentration with time (figure 7).

The experimental data were fitted by non-linear regression, according to the equation 7, referred in the section 2.5.2.

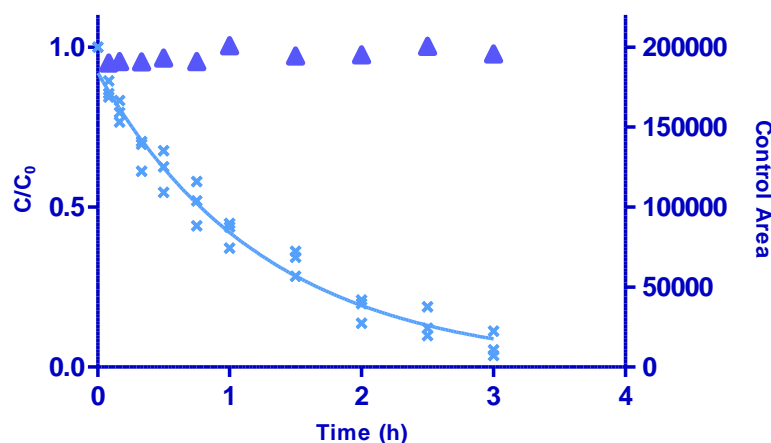


Figure 7- Kinetics of SMX photodegradation in ultrapure water - direct photodegradation (x) and control during the photodegradation experiment (▲).

To calculate the $t_{1/2}$ of SMX, the following equation was used:

$$t_{1/2} = \frac{\ln 2}{k} \quad \text{Eq. 18}$$

Photodegradation of SMX followed a pseudo first-order kinetic model with a rate constant of $(0.81 \pm 0.04) \text{ h}^{-1}$ and a $t_{1/2}$ of $(0.86 \pm 0.03) \text{ h}$. No degradation was observed in the tubes covered with aluminum foils (control tube), indicating that no degradation by microbiological or thermal means occurred. The same kinetic model was well adjusted for other studies of the photodegradation of E1 (Silva et al., 2016a), E2 (Silva et al., 2016b),

(Mazellier et al., 2008), (Liu and Liu, 2004), 17 α -ethinylestradiol (EE2) (Silva et al., 2016b), E3 (Oliveira et al., 2016) and also of psychiatric pharmaceuticals (Calisto et al., 2011).

The fast photodegradation of SMX in ultrapure water is in accordance with literature. For example, in the study performed by Trovo et al. (2009), experiments were conducted in a solar simulator equipped with a 1100 W xenon arc lamp and special filters restricting transmission of light below 290 nm and a rapid decay of 40 % of the initial concentration of SMX (10 mg/L) solution prepared in distilled water was observed during the first 45 minutes (Trovó et al., 2009). However, it is important to refer that the concentration of SMX used in the mentioned study was higher than that used in this work.

3.2.2. Photodegradation of SMX in the environmental water samples

3.2.2.1. Characterization of environmental water samples

In order to understand the results of SMX photodegradation in environmental water samples, the characterization of the samples collected was performed in terms of salinity levels, conductivity, DOC, pH, UV-Vis spectrophotometry and quantification of different dissolved elements by flame atomic absorption spectroscopy.

Salinity, conductivity, DOC and pH

Salinity, conductivity, DOC and pH values of the samples are presented in the table 6.

Salinity is the quantity of dissolved salt content of the water, being the salt compounds sodium chloride, magnesium sulfate, potassium nitrate and sodium bicarbonate. The sample of *Fonte Nova* has the highest value while fresh waters samples show a value of zero (table 6). It should also be noted that the STPF sample shows a low value of salinity comparing with the *Fonte Nova* sample (table 6). The values of salinity are in agreement with conductivity, with higher value for *Fonte Nova* sample and lower value for the two fresh waters samples (table 6).

Table 6- Salinity, conductivity, pH and DOC values of the samples tested and respective standard errors.

Sample	Salinity (‰)	Conductivity (mS/cm)	DOC [mg/L]	pH
<i>Fonte Nova</i>	20.8	24.000	5.5 ± 0.1	7.33
<i>Rio Novo Príncipe</i>	0.0	0.087	3.14 ± 0.07	7.20
<i>Poço da Cruz</i>	0.0	0.480	134.74 ± 0.08	8.11
STPF	2.0	2.820	26.45 ± 0.03	8.08

DOC analysis (table 6) indicates a greater content of organic carbon in the fresh water river *Poço da Cruz* sample [134.74 mg/L] comparing with the other samples, being the fresh water *Rio Novo Príncipe* sample [3.14 mg/L] the one with lower organic carbon content.

The pH measurements indicate that all environmental water samples are basic, with pH values higher than 7.

UV-Vis spectrophotometry

With respect to the UV-Vis spectrophotometry, larger absorbance values are most likely caused by higher chromophore content. The obtained results (figure 8) show the same trend for all water samples studied: decreasing of absorbance towards longer wavelengths.

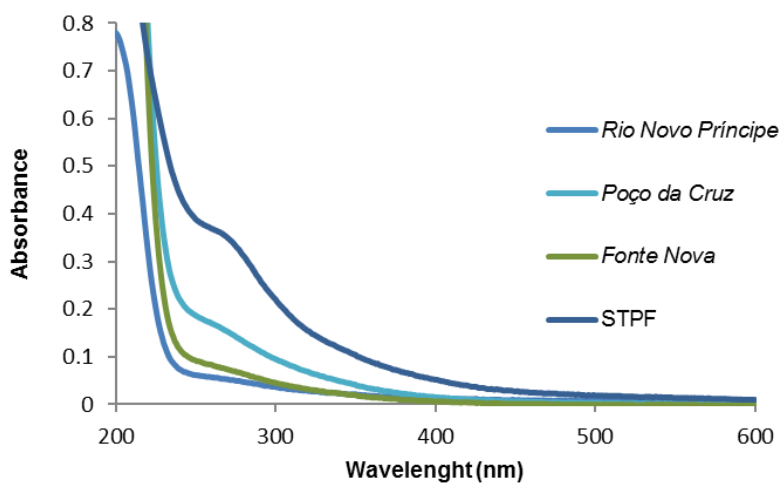


Figure 8- UV-Vis spectra of the environmental water samples analysed.

Through the investigated range of wavelength, the highest absorbance values were obtained for STPF sample, while the lowest values were for *Rio Novo Príncipe* sample.

To investigate the influence of the environmental water samples in SMX photodegradation, the absorbance values at 290 nm were measured in SMX (100 µg/L) solutions in ultrapure water and in STPF, *Rio Novo Príncipe*, *Poço da Cruz* and *Fonte Nova* water samples. Although SMX does not present a maximum of absorbance at 290 nm (figure 9), since radiation used in photodegradation studies are above 290 nm, the wavelength chosen to compare the absorbance values of SMX solutions in ultrapure water and in environmental samples was 290 nm. Results showed the increase of absorbance values in the order:

$$\text{Ultrapure water (0.011)} < \textit{Rio Novo Príncipe} (0.063) < \textit{Fonte Nova} (0.095) \\ < \textit{Poço da Cruz} (0.126) < \textit{STPF} (0.323)$$

due to the screen filter effect it could be expected a decrease of SMX photodegradation in this order.

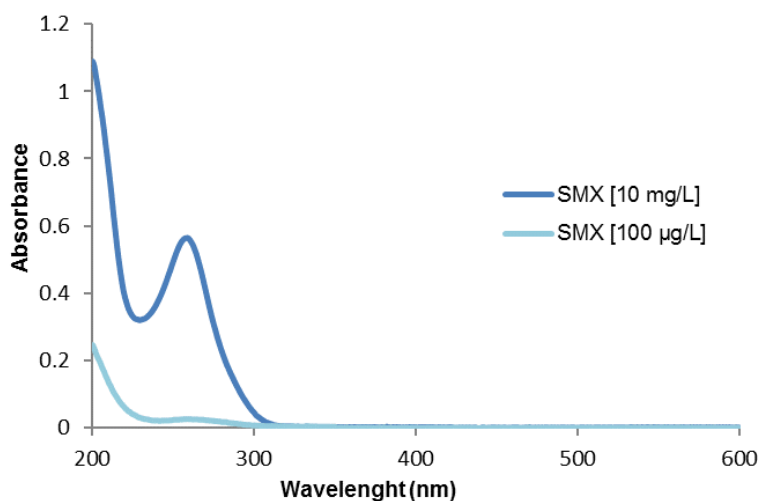


Figure 9- UV-Vis spectra of SMX [10 mg/L] and SMX [100 µg/L] in ultrapure water.

Atomic absorption spectrophotometry

To quantify the calcium, magnesium, sodium, potassium and iron using flame atomic absorption spectroscopy, calibration curves for each element were determined. Concentration range, R^2 and LOD obtained are summarized in the table 7.

Table 7- Concentration range used, calibration curve equation, R^2 and LOD obtained in determination of calcium, magnesium, sodium, potassium and iron by atomic absorption.

Element	Concentration range [mg/L]	Calibration curve equation	R^2	LOD [mg/L]
Calcium	1.0-6.0	$y = (0.0755 \pm 0.0005) x + (0.014 \pm 0.002)$	0.9998	0.0895
Magnesium	0.1-0.6	$y = (0.651 \pm 0.003) x + (0.007 \pm 0.001)$	0.9999	0.0059
Sodium	5-50	$y = (0.043 \pm 0.001) x - (0.03 \pm 0.03)$	0.9980	2.637
Potassium	2-16	$y = (0.0186 \pm 0.0006) x - (0.014 \pm 0.006)$	0.9967	1.142
Iron	0.5-5	$y = (0.0388 \pm 0.0005) x + (0.001 \pm 0.001)$	0.9997	0.136

The environmental water samples were diluted whenever necessary and results obtained are presented in table 8.

Table 8- Concentration of calcium, magnesium, sodium, potassium and iron determined in environmental samples and respective standard errors.

Sample	Calcium [mg/L]	Magnesium [mg/L]	Sodium [mg/L]	Potassium [mg/L]	Iron [mg/L]
<i>Fonte Nova</i>	277 ± 1	738 ± 1	5667 ± 1	291 ± 2	0.20 ± 0.04
<i>Poço da Cruz</i>	49.5 ± 0.2	8.31 ± 0.04	20.9 ± 0.5	7.63 ± 0.04	0.21 ± 0.02
<i>Rio Novo Príncipe</i>	4.47 ± 0.01	2.08 ± 0.02	9.34 ± 0.04	2.48 ± 0.03	0.053 ± 0.001
STPF	59.4 ± 0.4	46.8 ± 0.1	9.86 ± 0.01	40 ± 1	0.42 ± 0.05

It is possible to verify that *Fonte Nova* sample presented higher concentration for all dissolved elements, except iron, when compared with the other environmental water samples. This is in accordance with the higher salinity level measured in this sample

3.2.2.2. Photodegradation kinetics of SMX

In photodegradation experiments, the two fresh waters, a waste water and an estuarine water samples were spiked with SMX in order to obtain the same concentration used in the previous studies [100 µg/L] and were irradiated until no SMX was detected.

Experimental results were fitted by non-linear regression, according to the equation 7, in the same way that was made for kinetic of SMX photodegradation in ultrapure water.

The kinetic curves of SMX photodegradation in the different water samples tested are presented in figure 10. The kinetic curve of SMX in ultrapure water is also presented for comparison.

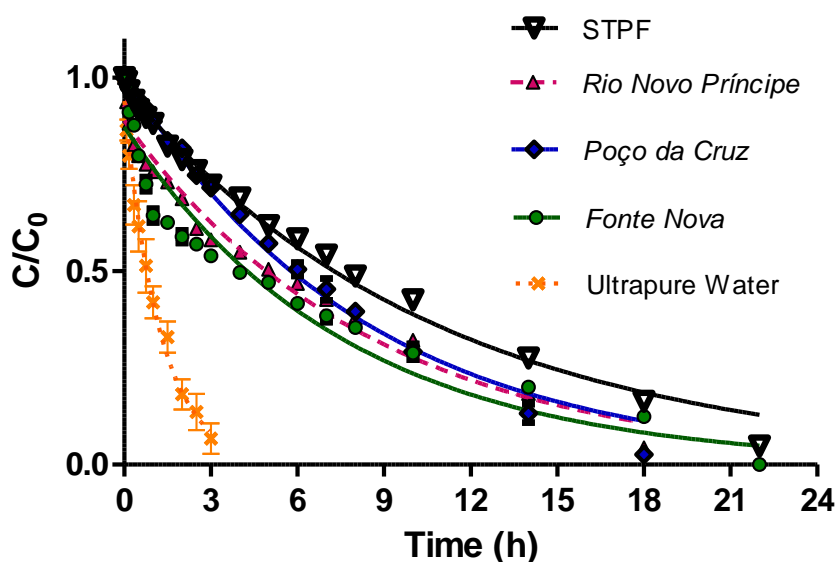


Figure 10- Kinetics of SMX photodegradation in ultrapure water and in environmental water samples. Shown error bars are standard deviations ($n = 3$) (note that, for most of the experimental points error bars are too small to be visible in the figure).

In these environmental water samples, there is an obvious decrease of the SMX photodegradation rate compared with the obtained in ultrapure water. On the other hand, after 14 hours of irradiation, the photodegradation of SMX in environmental water samples increased as follow: STPF - 72.46 % < Fonte Nova - 80.00 % < Rio Novo Príncipe - 81.65 % < Poço da Cruz - 86.77 %. However, in ultrapure water after only 3 hours of irradiation SMX was practically all degraded.

Results obtained are summarized in table 9 showing the different photodegradation behaviour of SMX in environmental water samples from different origins. These results showed that environmental water samples are less efficient to photodegradation of SMX, since the $t_{1/2}$ obtained in ultrapure water was lower than 1 hour, while in estuarine and riverine waters was around 6 hours and in STPF reached almost 8 hours (table 9).

Table 9- Data on apparent first-order rate constants, k_{meas} (h^{-1}), R^2 , $t_{1/2}$ (h), and $t_{1/2}$ (SSD) obtained in ultrapure water and in environmental water samples and respective standard errors.

Type of water	k_{meas} (h^{-1})	R^2	$t_{1/2}$ (h)	$t_{1/2}$ (SSD)
Ultrapure	0.81 ± 0.04	0.9900	0.86 ± 0.04	0.23 ± 0.01
Fonte Nova	0.13 ± 0.01	0.9397	5.3 ± 0.5	1.4 ± 0.1
Rio Novo do Príncipe	0.117 ± 0.007	0.9701	5.9 ± 0.4	1.56 ± 0.09
Poço da Cruz	0.122 ± 0.004	0.9916	5.7 ± 0.2	1.50 ± 0.05
STPF	0.092 ± 0.003	0.9907	7.54 ± 0.04	1.98 ± 0.07

For all environmental water samples, the first order rate constant of SMX photodegradation was much lower than the one obtained in ultrapure water. Also, it was in the STPF sample that the first order rate constant of SMX photodegradation was lower, $(0.092 \pm 0.003) \text{ h}^{-1}$, compared to the obtained in ultrapure water, $(0.81 \pm 0.04) \text{ h}^{-1}$. These results can indicate that the high capacity of STPF sample to absorb radiation originates a significant amount of light not available for SMX degradation (higher inner filter effect). These values are in accordance with the absorbance values determined for STPF which were higher than those for fresh and estuarine water samples.

It is important to highlight that $t_{1/2}$ is strictly related to the adopted experimental conditions and assuming that the lamp properly simulates sunlight, results can be converted into outdoor $t_{1/2}$, in summer sunny days (SSD) equivalents (table 9). Considering that the total energy reaching the ground on a cloudless summer day (45 °N latitude) is $7.5 \times 10^5 \text{ J/m}^2$, one summer sunny day (24 hours day/night cycle) corresponds to 3.8 hours of irradiation (Calisto et al., 2011). The conversion of the resulting $t_{1/2}$ (h) to $t_{1/2}$ (SSD) in environmental conditions, allows to observe enormous differences in the number of necessary SSD to reach the $t_{1/2}$ in ultrapure water and in environmental water samples. In ultrapure water, 0.23 SSD are needed to reach the $t_{1/2}$, while for natural environmental

samples the SSD varied between 1.4 and 1.98. This means that when SMX is present in natural environments its degradation rate becomes much slower, increasing its persistence, along with potential risks, such as increasing microbial resistance through the prolonged exposure of microorganisms to SMX. Thus, it is important to understand the main contributors for this decrease in the photodegradation rate.

The salinity of the samples used in this study ranged between 0, 2.0 and 20.8 for fresh waters, STPF and estuarine water samples, respectively (table 6). The highest salinity was measured on *Fonte Nova* sample. A decrease of OM content with increasing of salinity has been proven (Yang et al., 2015). Since lower OM content will result in a lower inner filter effect, this can explain the higher degradation rate observed in *Fonte Nova* sample in comparison with the observed in the other environmental samples. However, salinity also has been known to have an inhibitory effect on the photocatalytic degradation of sulfonamide antibiotics (Yang et al., 2015), which may explain why the first order rate constant of SMX photodegradation in *Fonte Nova* sample was much lower than the obtained in ultrapure water. Also, estuarine water contains various inorganic compounds that are high in Na⁺ and Cl⁻ ions and includes numerous other ions in minor concentrations (e.g., Ca²⁺, Mg²⁺, K⁺, I⁻, SO₄²⁻ and Br⁻) (Leal et al., 2015). In table 8, it is possible to verify that estuarine water presents higher concentration of sodium, calcium, magnesium and potassium when compared with the other samples tested. As mentioned before, indirect photolysis consists of light absorption by photosensitizers, which generate many photoreactants, such as ·OH or ¹O₂. It has also been referred that anions such as chlorides, carbonates, phosphates and sulphates have the ability to scavenge the ·OH (Umar and Aziz, 2013) that may contribute in the indirect photodegradation, since the addition of the ·OH to SMX isoxazole ring formation was mentioned by Trovó et al., 2009.

In this study, the pH of environmental water samples varied between 7.20 and 8.11 (table 6); these values are higher than that attributed to 100 µg/L SMX in ultrapure water (pH = 6.30). According to Dias et al. (2014), pH affects greatly the SMX speciation in solution and thus its UV-Vis spectrum. Since photodegradation rate constant depends upon the quantity of photons absorbed by each mole of SMX per unit of time and on the ϕ , it will also depend of the SMX speciation.

So, it is possible to conclude that salinity, the concentration of ions dissolved in environmental samples and pH have great influence in photodegradation rate of SMX, thus it is important to study their influence in more detail. In addition, the effect of

photosensitizers, such as HS, should also be evaluated as they can influence photodegradation.

3.2.3. Effect of HS on SMX photodegradation

3.2.3.1. Characterization of HS

To investigate the effect of HS on the SMX photodegradation, three fractions of HS were used: HA, FA and XAD-4 at a concentration of 20 mg/L. Each one of the HS fractions has different chemical and optical properties (Sierra et al., 2005) that can influence the degree of SMX photodegradation.

Elemental analysis

The purified fractions HA, FA and XAD-4 used in our photodegradation studies were characterized by Esteves et al. (1995) (table 10).

Table 10- Elemental analysis of HS fractions selected to study the effect of DOM on SMX photodegradation. Results are corrected for humidity at 60 °C and ashes at 750 °C (adapted from Esteves et al. (1995)).

Elemental analysis (%)					
	C	H	N	S	O
HA	54.8	4.0	3.6	1.8	32.4
FA	54.5	4.7	1.9	1.0	34.9
XAD-4	48.8	4.2	3.1	1.2	40.5

After analyzing the elemental analysis results (table 10) it can be seen that XAD-4 fraction has a lower carbon content than HA and FA; however, the oxygen content of XAD-4 is higher. This indicates greater content of oxygen functional groups on XAD-4 fraction than in the other two fractions used.

HSs are complex molecules, which consist of aromatic cores, substituted with functional groups and aliphatic cores (Aleksandrova et al., 2011) with different heat resistance. In the thermogravimetric analysis HA, with the higher carbon content, was found

to be the most thermo-resistant and only decomposes at temperatures higher than 300 °C, which suggests that this fraction have higher aromaticity and lower content of aliphatic chains and functional groups, comparing with FA and XAD-4 fractions (Esteves, 1995).

To further investigate the structural differences of the three fractions of HS used, UV-Vis spectrophotometry (figure 11) were performed.

UV-Vis spectrophotometry

The UV-Vis spectra of SMX [100 µg/L] in ultrapure water and in the presence of the three HS fractions were performed in the range (200 to 600) nm and show a continuous decrease of absorbance values from (200 to 600) nm for all HS isolates (figure 11).

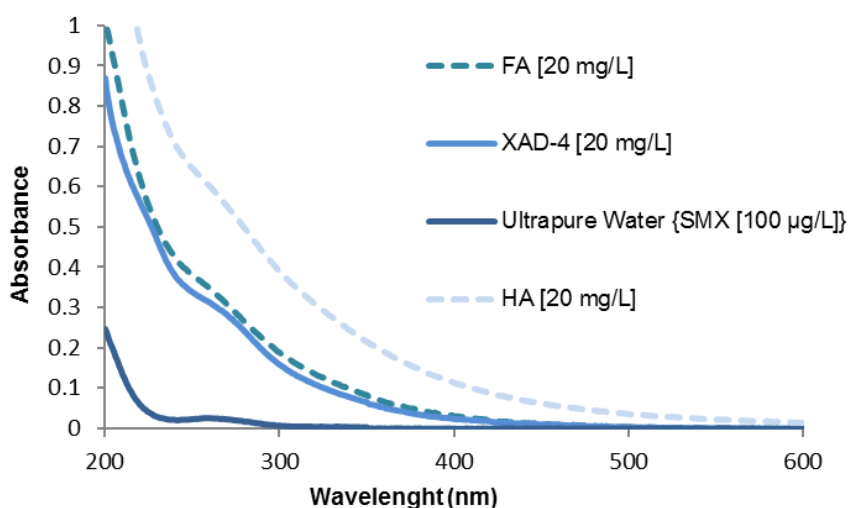


Figure 11- UV-Vis spectra of SMX in ultrapure water and in the three fractions of HS.

Through the observed range of absorbance, the highest values were obtained for HA, while the lowest were for XAD-4, which indicates the higher sensitivity of HA to absorb radiation. The same results were obtained previously in the study of HS from different origin by Esteves et al. (2009).

To study the effect of HS on the photodegradation of SMX, the absorbance values at 290 nm were measured in SMX solutions in absence of HS (ultrapure water) and in

presence of HS (HA, FA and XAD-4 at 20 mg/L). The results showed the increase of absorbance values in the order:

$$\text{Ultrapure water (0.011)} < \text{XAD - 4 (0.197)} < \text{FA (0.225)} < \text{HA (0.441)}$$

which can suggest that the rate of photodegradation of SMX in presence of HS could decrease in the same order due to the inner filter effect of HS.

3.2.3.2. Photodegradation kinetics of SMX

The studies of SMX photodegradation were performed in the presence of the three HS fractions (HA, FA and XAD-4), since the photodegradation of SMX can happen either as a direct phototransformation by absorption of light and/or be induced by the presence of HS. Photodegradation was performed using solutions containing 100 µg/L of SMX and 20 mg/L of HA, FA or XAD-4 which were irradiated during 4, 3 and 2.5 hours, respectively. Dark controls, obtained under the exact same conditions, were performed for all the irradiation experiments. Degradation in the dark due to thermal or hydrolytic processes was not observed.

The experimental results were fitted using a non-linear regression, according to the equation 7, as for SMX photodegradation kinetic in ultrapure water. The SMX photodegradation kinetic curves in presence of different HS fractions and kinetic curve in ultrapure water (for comparison) are presented in figure 12.

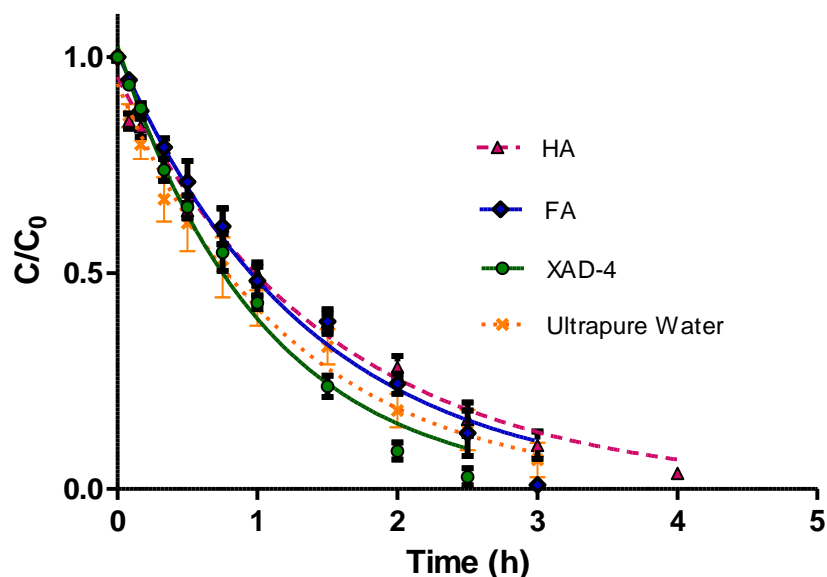


Figure 12- Kinetics of SMX photodegradation in absence and presence of three fractions of HS. Shown error bars are standard deviations (n=3) (note that, for most the experimental points, error bars are too small to be visible in the figure).

The obtained data for the variation of SMX concentration along irradiation time was fitted to a pseudo first-order kinetic model and shows a significant impact of each of HS fractions studied on the SMX photodegradation (figure 12).

Addition of HA [20 mg/L] caused an apparent decrease of the SMX photodegradation rate compared with the one obtained in ultrapure water. On the other hand, the addition of XAD-4 [20 mg/L] caused a slight acceleration of the SMX photodegradation rate.

For example, after 2 hours of irradiation, in ultrapure water, SMX was 81.83 % degraded. However, after the same time of irradiation, the results of SMX photodegradation were 71.78 %, 75.63 % and 91.19 % for HA, FA and XAD-4, respectively. These results showed that XAD-4 is the most efficient to photoinduce the SMX degradation, which is in accordance with the expected low inner effect for this fraction of HS. Each one of the HS fractions studied absorb the radiation due to the presence of chromophores' moieties (inner filter effect). Considering the UV-Vis spectra (figure 11), a low value of absorbance indicates the weak ability to absorb radiation, which causes that a significant amount of light can be available for SMX, resulting in an increase of its degradation. Therefore, if the generation of reactive species is not considered for the XAD-4 solution (since these moieties present

a weaker ability to absorb radiation), a higher SMX photodegradation will be expected in this solution, when compared with the FA and HA solutions. So, the strongest photoinductive properties were obtained for XAD-4, which resulted in a SMX $t_{1/2}$ of (0.73 ± 0.04) h compared to (0.86 ± 0.04) h in ultrapure water. The $t_{1/2}$ of SMX for the other HS was higher than the obtained in ultrapure water ($t_{1/2} = (0.94 \pm 0.06)$ h and $t_{1/2} = (1.05 \pm 0.05)$ h, for FA and HA fraction, respectively) (table 11).

In the absence of HS, a first order rate constant of (0.81 ± 0.04) h⁻¹ was obtained (table 11), which corresponds to the direct photodegradation of SMX. According to Caupos et al. (2011), the value of the rate constant in presence of HS can be calculated, considering that they do not have any photosensitizing properties, thus acting only as inner filter. The calculations of the initial fraction of light, absorbed by SMX alone and in presence of different HS fractions, were performed at 290 nm (at the higher absorbance of SMX in the spectral range of simulated sunlight), using the equation below:

$$\left(\frac{I_a}{I_0}\right)_{SMX/m} = \left(\frac{I_a}{I_0}\right)_m \times \frac{A_{SMX}}{A_m} \quad \text{Eq. 19}$$

where,

$\left(\frac{I_a}{I_0}\right)_{SMX/m}$ – is the fraction of light that was absorbed by SMX in presence of HS at 290 nm;

$\left(\frac{I_a}{I_0}\right)_m$ – is the fraction of light absorbed by the mixture (SMX + HS) at 290 nm;

A_{SMX} – is the value of absorbance of SMX at 290 nm (constant due to the constant value of the concentration);

A_m – is the absorbance value of the mixture (SMX + HS) at 290 nm.

Since the intensity of light absorbed depends on the absorbance value and the intensity of incident light, the ratio $\frac{I_a}{I_0}$ can be calculated, by using the following equation:

$$I_a = I_0(1 - 10^{-A}) \quad \text{Eq. 20}$$

In presence of HS, the radiation emitted by the lamp is mainly absorbed by HS fractions. As it was mentioned before, it is possible to calculate the first order rate constant of SMX degradation in the presence of HS acting only as an inner filter (k_{cal}), using the following equation:

$$k_{cal} = k_{SMX} \times \frac{\left(\frac{I_a}{I_0}\right)_{SMX/m}}{\left(\frac{I_a}{I_0}\right)_{SMX}} \quad \text{Eq. 21}$$

where,

$\left(\frac{I_a}{I_0}\right)_{SMX}$ – is the fraction of light absorbed by SMX alone (in ultrapure water);

k_{SMX} – is the first order rate constant of SMX direct photolysis (in absence of HS).

Combination of equations (19), (20) and (21) leads to calculate first order rate constant of SMX photodegradation in presence of HS fractions, as follows:

$$k_{cal} = k_{SMX} \times \frac{(1-10^{-A})_m}{(1-10^{-A})_{SMX}} \times \frac{A_{SMX}}{A_m} \quad \text{Eq. 22}$$

The contribution to photodegradation of each one of the three different isolates of HS was also studied and calculated using the next equation:

$$\text{contribution of HS [\%]} = \left(\frac{k_{meas} - k_{cal}}{k_{meas}} \right) \times 100 \quad \text{Eq. 23}$$

Table 11 shows the calculated and the measured rate constants in presence of HS, the contribution of HS, the $t_{1/2}$ obtained for SMX in ultrapure water and the three fractions of HS and the $t_{1/2}$ of SMX converted in SSD.

Table 11- K_{meas} (h^{-1}), R^2 , $t_{1/2}$ (h), $t_{1/2}$ (SSD), K_{cal} (h^{-1}) and contribution of three different HS isolates to degradation obtained and respective standard errors.

Type of water	k_{meas} (h^{-1})	R^2	$t_{1/2}$ (h)	$t_{1/2}$ (SSD)	K_{cal} (h^{-1})	HS Contribution (%)
Ultrapure	0.81 ± 0.04	0.9900	0.86 ± 0.04	0.23 ± 0.01	---	---
HA [20 mg/L]	0.66 ± 0.03	0.9894	1.05 ± 0.05	0.28 ± 0.01	0.51	23.1
FA [20 mg/L]	0.74 ± 0.04	0.9864	0.94 ± 0.06	0.25 ± 0.01	0.63	14.6
XAD-4 [20 mg/L]	0.96 ± 0.06	0.9881	0.73 ± 0.04	0.19 ± 0.01	0.65	32.0

The HS fractions can be promoted to a transient excited state in which they may react with oxygen present in solution, forming reactive species, or react directly with excited natural organic compounds, promoting an enhancement in the photodegradation rate. However, it is well known that OM, such as HS, can have two antagonist effects, the photosensitizing properties and the inner filter effect, that reduces the available energy to degrade pollutants in solution, resulting in a decrease of the photodegradation rate. The real effect of HS in photodegradation rate is obtained by the combination of these two effects (Andreozzi et al., 2003). The inner filter effect should be dominant for HA and FA fractions, because a decrease rate in the photodegradation rate was observed, with a first order rate constant of $(0.66 \pm 0.03) h^{-1}$ and $(0.74 \pm 0.04) h^{-1}$, respectively. Results suggest an inverse correlation between the HS aromaticity and their effect on photodegradation. HS characterization (table 10) indicated that HA must be the most hydrophobic fraction, more enriched in aromatic and/or chromophoric groups. On the other hand, results showed that XAD-4 fraction is the type of OM that seems to produce the higher number of reactive species, which can be explained by the greater content of oxygen functional groups, suggested by elemental analysis, where XAD-4 fraction presented a lower carbon content than HA and FA and a higher oxygen content (table 10).

The k_{calc} values for the photodegradation of SMX in presence of HS were $0.51 h^{-1}$, $0.63 h^{-1}$ and $0.65 h^{-1}$ for HA, FA and XAD-4, respectively. So, HA has the lowest value of K_{cal} , which indicates the high ability to act as inner filter. Consequently, a significant amount of light is not available for SMX, which results in a decrease of its photodegradation. The

fact that a decrease in SMX photodegradation rate was verified for HA and FA fractions, is due to the fact that the inner filter effect (that decreases the photodegradation rate of the target compound) is higher for these fractions, than their photosensitizing capacity (that increases the photodegradation rate of the target compound). This effect is more evident in the HA fraction with higher absorbance at 290 nm. The opposite is observed for the XAD-4 fraction.

The results show how important the presence of HS is on the photodegradation of SMX, as well as the type of HS fraction, that has also some effect on the SMX degradation rate. The highest contribution of XAD-4 (about 32 %), in the photodegradation of SMX, has been proven, which resulted in a lower $t_{1/2}$. It means that about 32 % of the overall SMX degradation is caused by photosensitized reactions. Lower contribution of HS, was obtained for HA and FA fractions, about 23 % and 15 %, respectively.

The conversion of the resulting $t_{1/2}$ (h) to $t_{1/2}$ (SSD) allows the determination of the $t_{1/2}$ of SMX in environmental conditions, being possible to observe the differences in the number of necessary SSD to reach the $t_{1/2}$ in presence or absence of HS fractions. In ultrapure water 0.23 SSD are needed to reach $t_{1/2}$, while when SMX is in presence of HS fractions the SSD varied between 0.19 and 0.28 SSD, being the lower value of SSD observed in presence of XAD-4.

Other authors reported an increase on photodegradation rate for estrogens due to photosensitizing reactions induced by the presence of this type of organic matter (Oliveira et al., 2016), (Silva et al., 2016a), (Silva et al., 2016b), while for other compounds, namely antibiotics, a decrease in the presence of this type of organic matter was observed (Leal et al., 2015). For less hydrophobic compounds the screening effect seems to be the reason for the delaying effect on photodegradation, while for hydrophobic compounds this decrease can also be attributed to hydrophobic association between the organic pollutant and the HS promoting the decay of excited state of pollutant (Leal et al., 2015).

3.2.4. Effect of pH on SMX photodegradation

3.2.4.1. Importance of pH

An important parameter in the photodegradation is the pH of the dispersion, which will influence the distribution of pollutant charges. Depending on the nature of the organic compound, an increase in the pH will have a positive or negative effect on its photodegradation rate.

SMX has two pK_a values (1.85 and 5.60) and the chemical structures change with pH according to figure 13.

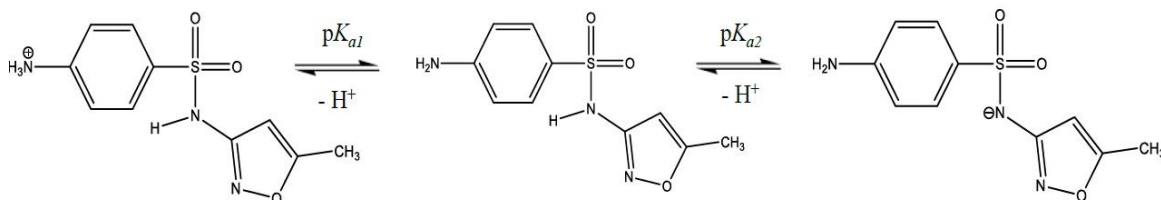


Figure 13- Variation of the chemical structure of SMX with pH.

According to the species distribution (figure 14), the molar ratio between SMX species depends on pH. At pH 1.0 around 88 % of SMX is in the protonated species, while at pH 4.0 almost 97 % is in the neutral form. At the pH of the environmental samples used in our study (higher than 7), more than 96.2 % of SMX is in the negative form.

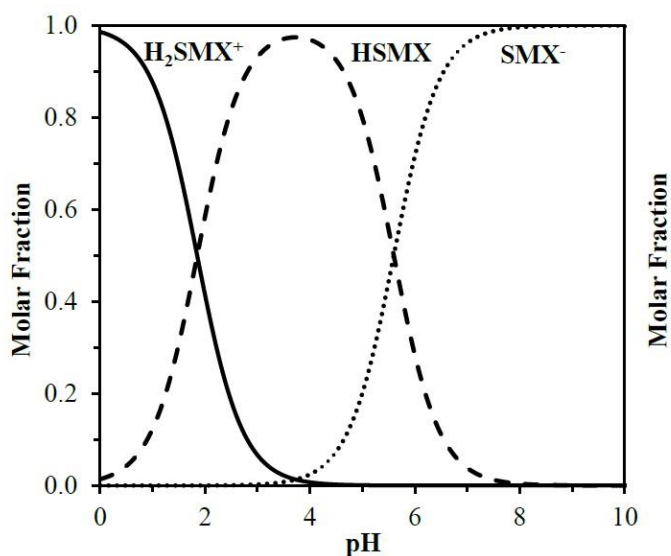


Figure 14- Speciation diagrams of SMX (adapted from Dias et al., (2014)).

UV-Vis spectrophotometry

To evaluate the influence of the speciation of SMX on photodegradation, since it depends on the light absorption, UV-Vis absorbance spectra of SMX at 10 mg/L in ultrapure water without pH adjustment (pH 6.30) and with pH adjusted to different values with NaOH 0.1 M or HCl 0.5 M (pH 4.97, 7.33 and 8.08) were obtained (figure 15).

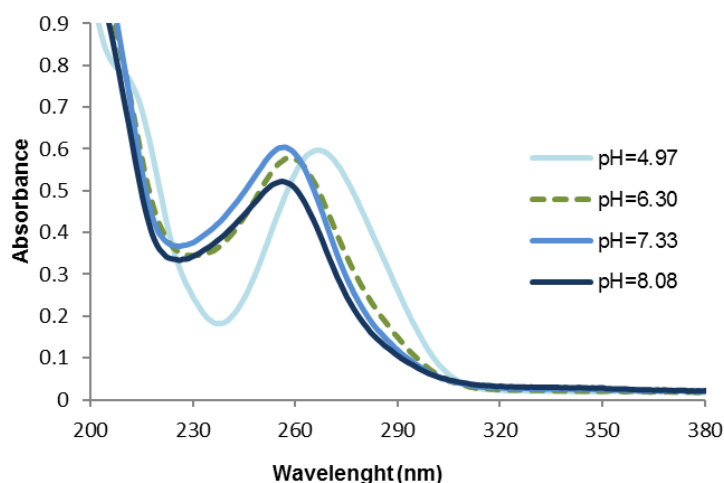


Figure 15- UV-Vis spectra of SMX [10 mg/L] in ultrapure water at different pH values.

These pH values were chosen, because the pH value of the HS tested previously was approximately 5, the pH 6.30 is the considered pH of ultrapure water and the pH 7.33 and 8.08 correspond to pH values measured for estuarine water and waste water samples, respectively. In all spectra presented in figure 15, a decrease in UV absorbance is observed especially above 270 nm. Comparing all the spectra, one can observe that the absorbance values shift to higher wavelengths at pH 4.97. For the other pH values analysed (6.30, 7.33 and 8.08) there are also differences, but they are not so remarkable.

However, if we compare absorbance at 290 nm (the lower wavelength used in the photodegradation experiments) for ultrapure water at the different pH values studied we can evaluate the possible influence of pH on SMX photodegradation in ultrapure water. The results showed the increase of absorbance values in the order:

$$pH\ 8.08\ (0.105) < pH\ 7.33\ (0.118) < pH\ 6.30\ (0.148) < pH\ 4.97\ (0.206)$$

Therefore, it could be expected that the rate of photodegradation of SMX increase in the same order. If we compare the absorbance at pH 6.30 and 7.33 it is possible to observe a decrease of 20 %, while between pH 6.30 and pH 8.0 there is a decrease of 30 %. This decrease can explain, at least partially, the lower photodegradation rate of SMX observed for the environmental water samples tested previously, when compared with the obtained in ultrapure water.

Also, comparing the absorbance at pH 6.30 and pH 4.97 it is possible to observe an increase of 40 %. HS tested are acidic compounds, so the influence of HS on SMX photodegradation rate mentioned previously may be influenced not only by the presence of the HS, but also by the pH decrease. To correctly evaluate the influence of HS in the SMX photodegradation rate, solutions containing 100 µg/L of SMX in the absence and presence of HA, FA, XAD-4 (20 mg/L), together with phosphate buffer (0.001 M) at pH 5.00 and 7.30 were irradiated for 1 hour. The results obtained are presented in figure 16, where the photodegradation rate (in percentage) is presented for each irradiated solution.

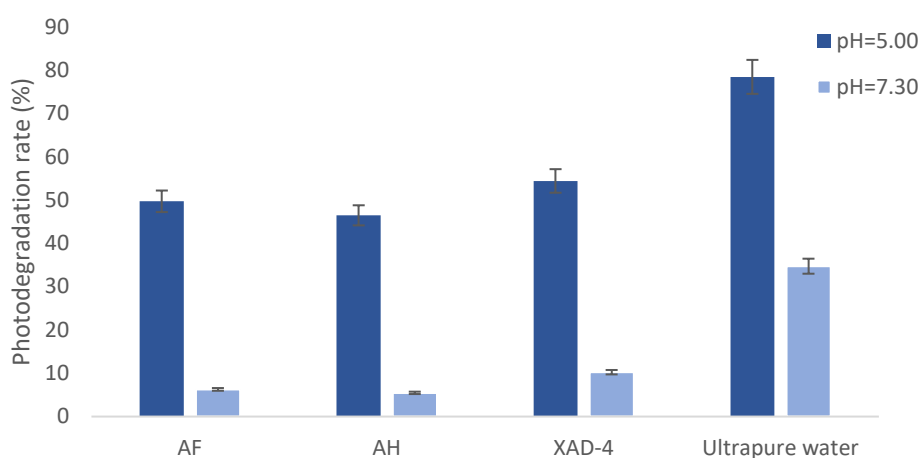


Figure 16- SMX photodegradation rate (%) in presence and absence of different HS fractions together with phosphate buffer (0.001 M) at pH 5.00 and 7.30 after 1 hour of irradiation. Shown error bars are standard deviations (n=3).

After analysing the results, it is possible to conclude that the photodegradation rate of SMX after 1 hour of irradiation in ultrapure water is much higher than the one obtained in all HS fractions for both pH values tested. Thus, the inner filter effect of HS is higher than their photosensitizing capacity, since the HS fractions absorb the radiation and, therefore, less radiation will be available for SMX photodegradation.

However, there is a similarity of the data obtained for the kinetics of SMX photodegradation (shown previously) in the presence of HS, for both pH. XAD-4 fraction was the most efficient in the photodegradation of SMX, whereas the least efficient was the HA. This can be explained by HA higher UV-Vis absorbance observed in figure 11, relatively to XAD-4 fraction.

Also, it is possible to verify that photodegradation of SMX is more efficient at pH 5.00 than pH 7.30 either in the absence or presence of the different HS fractions studied.

3.2.4.2. Photodegradation kinetics of SMX

3.2.4.2.1. In ultrapure water

The influence of pH in ultrapure water was studied adding 100 µg/L of SMX to phosphate buffer at pH 5.00 and 7.30 and irradiating during 1.5 and 10 hours, respectively. These results were compared with the kinetics of SMX photodegradation in ultrapure water at pH 6.30 without pH adjusted.

In figure 17, the kinetic curves of SMX photodegradation in ultrapure water at different pH values are presented.

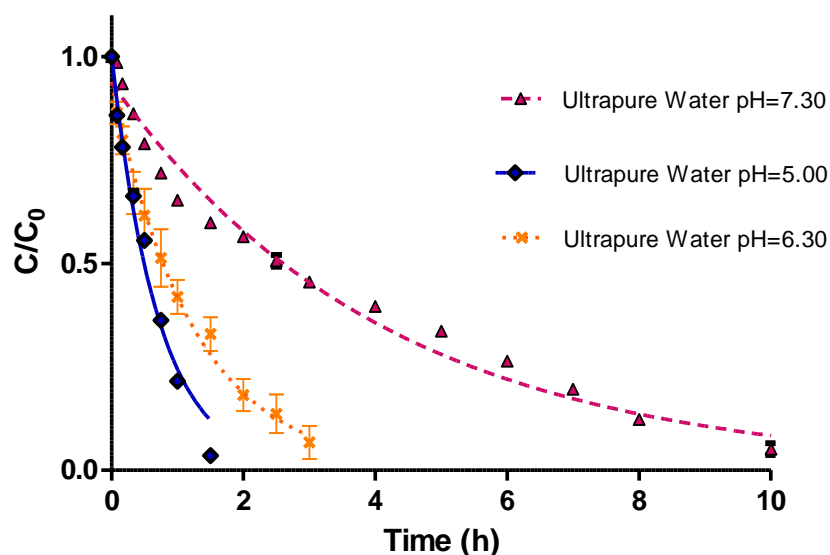


Figure 17- Kinetics of SMX photodegradation in ultrapure water with natural pH and with phosphate buffer at pH 5.00 and 7.30. Error bars in the graph are standard deviations (n=3) (note that, for most of the experimental points error bars are too small to be visible in the figure).

In table 12, K_{meas} (h^{-1}), R^2 , $t_{1/2}$ (h), $t_{1/2}$ (SSD) and ϕ_{ave} obtained for SMX photodegradation in ultrapure water at different pH are summarized.

Table 12- K_{meas} (h^{-1}), R^2 , $t_{1/2}$ (h), $t_{1/2}$ (SSD) and ϕ_{ave} obtained for SMX in ultrapure water at different pH values and respective standard errors.

Ultrapure water	k_{meas} (h^{-1})	R^2	$t_{1/2}$ (h)	$t_{1/2}$ (SSD)	ϕ_{ave}
pH = 5.00	1.4 ± 0.1	0.9812	0.49 ± 0.04	0.13 ± 0.01	1.72×10^{-7}
pH = 6.30	0.81 ± 0.04	0.9900	0.86 ± 0.04	0.23 ± 0.01	2.76×10^{-8}
pH = 7.30	0.24 ± 0.01	0.9767	2.9 ± 0.2	0.76 ± 0.05	2.42×10^{-8}

Considering the ultrapure water, at pH 5.00 a first order rate constant of $(1.4 \pm 0.1) h^{-1}$ was obtained, being this first order rate constant greater than that obtained for ultrapure water with other pH values.

By the analysis of figure 17 and table 12, it is possible to verify the high influence of the pH on SMX photodegradation, being pH 5.00 the most efficient, while pH 7.30 is the least efficient. For example, after 1 hour of irradiation, the photodegradation of SMX in ultrapure water at pH 7.30 was 34.71 %. However, after the same time of irradiation, photodegradation rate in ultrapure water at pH 6.30 and pH 5.00 was 58.07 % and 78.42 %, respectively. These results showed that ultrapure water at pH 5.00 is more efficient to induce the photodegradation of SMX than ultrapure water at pH 6.30 and 7.30, which resulted in a SMX $t_{1/2}$ of (0.49 ± 0.04) h for pH 5.00 compared to (0.86 ± 0.04) h and (2.9 ± 0.2) h obtained in ultrapure water at pH 6.30 and 7.30, respectively. The SSD varied between 0.13 and 0.76, being the highest values obtained for higher pH values.

Analysing the ϕ_{ave} (table 12), the highest value was obtained in ultrapure water at pH 5.00, while the lowest value corresponded to ultrapure water at pH 7.30, being in accordance with the expected, since the ϕ of a photodegradation process can be defined as the ratio between the photodegradation rate and the rate of light absorption. As can be seen in figure 15, there is a greater absorption of UV radiation in ultrapure water at pH 4.97 than at pH 6.30 and at pH 7.33, where the lowest absorption occurs, which is in agreement with the values obtained for the ϕ_{ave} .

So, it is possible to conclude that at pH 5.00 and 6.30 the photodegradation of SMX is more efficient than at pH 7.30, probably due to the fact that at pH 5.0 almost 97 % of SMX is in neutral form and, therefore, may not be complexed with other ions present in solution and thus photodegradation may be facilitated, while at pH 7.30 more than 96.2 % of SMX is in the negative form.

3.2.4.2.2. In estuarine water

To study the influence of pH on SMX photodegradation in environmental water samples, a sample from *Fonte Nova* was spiked with the same concentration of SMX [100 µg/L] used previously, adjusting the pH to 6.30 with HCl 0.5 M and irradiated during 8 hours. The results obtained were compared with the kinetics of SMX photodegradation in *Fonte Nova* sample at pH 7.33.

The kinetic curves of SMX photodegradation in the estuarine water sample at the two different pH values tested are presented in figure 18.

Apparent first order rate constants, R^2 , $t_{1/2}$ (h) and $t_{1/2}$ (SSD) obtained for SMX photodegradation in estuarine water at pH 6.30 and 7.33 are presented in table 13.

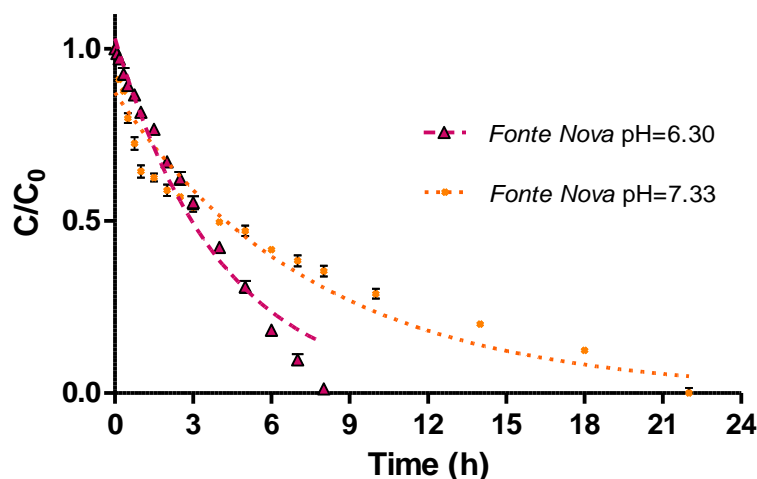


Figure 18- Kinetics of SMX photodegradation in estuarine water at pH 6.30 and 7.33. In the graph are also represented error bars with standard deviations (n=3) (note that, for most of the experimental points error bars are too small to be visible in the figure).

Table 13- k_{meas} (h^{-1}), R^2 , $t_{1/2}$ (h) and $t_{1/2}$ (SSD) obtained for estuarine water at different pH values and respective standard errors.

<i>Fonte Nova</i>	k_{meas} (h^{-1})	R^2	$t_{1/2}$ (h)	$t_{1/2}$ (SSD)
pH = 6.30	0.24 ± 0.02	0.9731	2.8 ± 0.2	0.74 ± 0.05
pH = 7.33	0.13 ± 0.01	0.9397	5.3 ± 0.5	1.4 ± 0.1

Once again, from the analysis of figure 18 and table 13, it is possible to verify that pH has a great influence on SMX photodegradation even when present in an estuarine water sample. Once present in the estuarine water sample at pH 7.33, SMX takes 22 hours to degrade almost completely, while in the estuarine water sample at pH 6.30 it only needs 8 hours. These results showed that environmental water sample from *Fonte Nova* at pH 6.30 is more efficient to induce the photodegradation of SMX than *Fonte Nova* at pH 7.33, which resulted in a SMX $t_{1/2}$ of about (2.8 ± 0.2) h compared to (5.3 ± 0.5) h obtained in *Fonte Nova* at pH 7.33. The SSD varied between about 0.74 and 1.4, evidencing once again the enormous influence of pH on photodegradation of SMX. For estuarine water sample at pH 6.30 a first order rate constant of (0.24 ± 0.02) h⁻¹ was obtained, being greater than that obtained for estuarine water at pH 7.33.

So, the great influence of pH either in ultrapure water or in the estuarine sample was proved. However, in environmental water samples there are other factors that can influence the photodegradation of SMX, because in estuarine water samples the first order rate constant is smaller than the one obtained in ultrapure water at the same pH. Thus, it is important to continue assessing other contributors to the decrease in the photodegradation rate.

3.2.5. Effect of sea salts on SMX photodegradation

3.2.5.1. Evaluation of inorganic salts on SMX photodegradation

Sea salts have been reported for influencing the photodegradation of some compounds in water samples, for example, OTC due to the occurrence of complexation (Leal et al., 2016). Since the estuarine sample presents high salinity levels it is important to evaluate the influence of sea salts on SMX photodegradation behaviour. As mentioned before, photodegradation in sea water samples, can be influenced by the presence of inorganic compounds, such as calcium and magnesium. In fact, these are two of the main constituents of sea water. Thus, the influence of calcium and magnesium on photodegradation of SMX was evaluated preparing two solutions, one with 261 mg/L of calcium and the other with 785 mg/L of magnesium. To both solutions 100 µg/L of SMX and phosphate buffer (0.001 M) were added and pH was adjusted to 7.30. These solutions were irradiated for 5 hours. Results of SMX photodegradation in those two solutions after 5 hours of irradiation were compared with those obtained in ultrapure water, in 21 ‰ of NaCl solution and in 21 ‰ of artificial sea salts solutions buffered with phosphate buffer (0.001 M) at pH 7.30 and in estuarine water at pH 7.33 (figure 19).

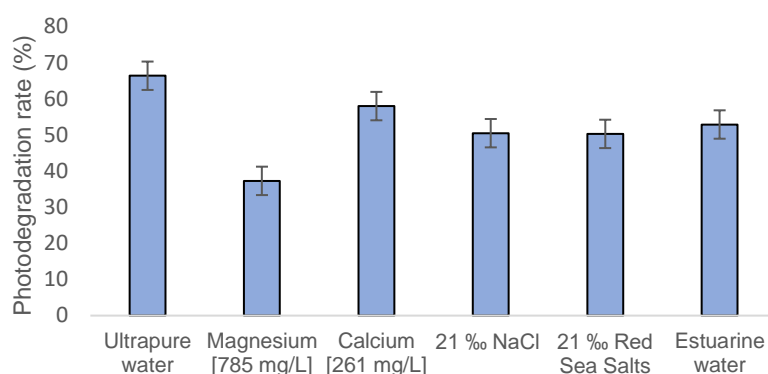


Figure 19- SMX photodegradation rate in ultrapure water in presence and absence of calcium, magnesium, sodium chloride and *red sea salts* with phosphate buffer at pH 7.30 and in estuarine water at pH 7.33 after 5 hours of irradiation. Shown error bars are standard deviations (n=3).

From the analysis of figure 19, it is possible to verify, that the addition of magnesium, calcium and sodium chloride decreased the photodegradation rate measured after 5 hours of irradiation comparing with the obtained in ultrapure water. The presence of magnesium is the one that most decreased the photodegradation rate, from $(66.4 \pm 0.3) \%$ to $(37.3 \pm 0.6) \%$. The effect of calcium is not so pronounced decreasing the photodegradation to $(58 \pm 1) \%$. The corrected 3D fluorescence spectra for SMX $100 \mu\text{g/L}$ in ultrapure water (figure 20 – (a)) exhibited a maximum at $\lambda_{\text{em}} \approx 350 \text{ nm}$ with $\lambda_{\text{exc}} \approx 260 \text{ nm}$. However, in presence of magnesium (figure 20 – (b)), there is a decrease of the fluorescence intensity of the SMX mentioned band and a new band appears at higher wavelengths, $\lambda_{\text{em}} = (440-480) \text{ nm}$ with $\lambda_{\text{exc}} = (375-410) \text{ nm}$, indicating the possible complexation between SMX and Mg^{2+} . In presence of Ca^{2+} (figure 20 – (c)) it is also possible to observe the fluorescence decrease of SMX band, although in this case no new fluorescence band is observed. The decrease of SMX fluorescence intensity in the presence of Mg^{2+} and Ca^{2+} can also be correlated with the decrease of UV-Vis absorbance at approximately 260 nm (figure 21).

In presence of 21 ‰ NaCl, it is possible to observe a decrease in SMX photodegradation rate to $(50.5 \pm 0.4) \%$. In this case, SMX fluorescence spectra (figure 20 – (d)) also presents a decrease in the SMX band at $\lambda_{\text{em}} \approx 350 \text{ nm}$ with $\lambda_{\text{exc}} \approx 260 \text{ nm}$, but besides the new band observed in the presence of magnesium, there is a second band observed at similar λ_{exc} of SMX in water but at higher $\lambda_{\text{em}} = (430-480) \text{ nm}$.

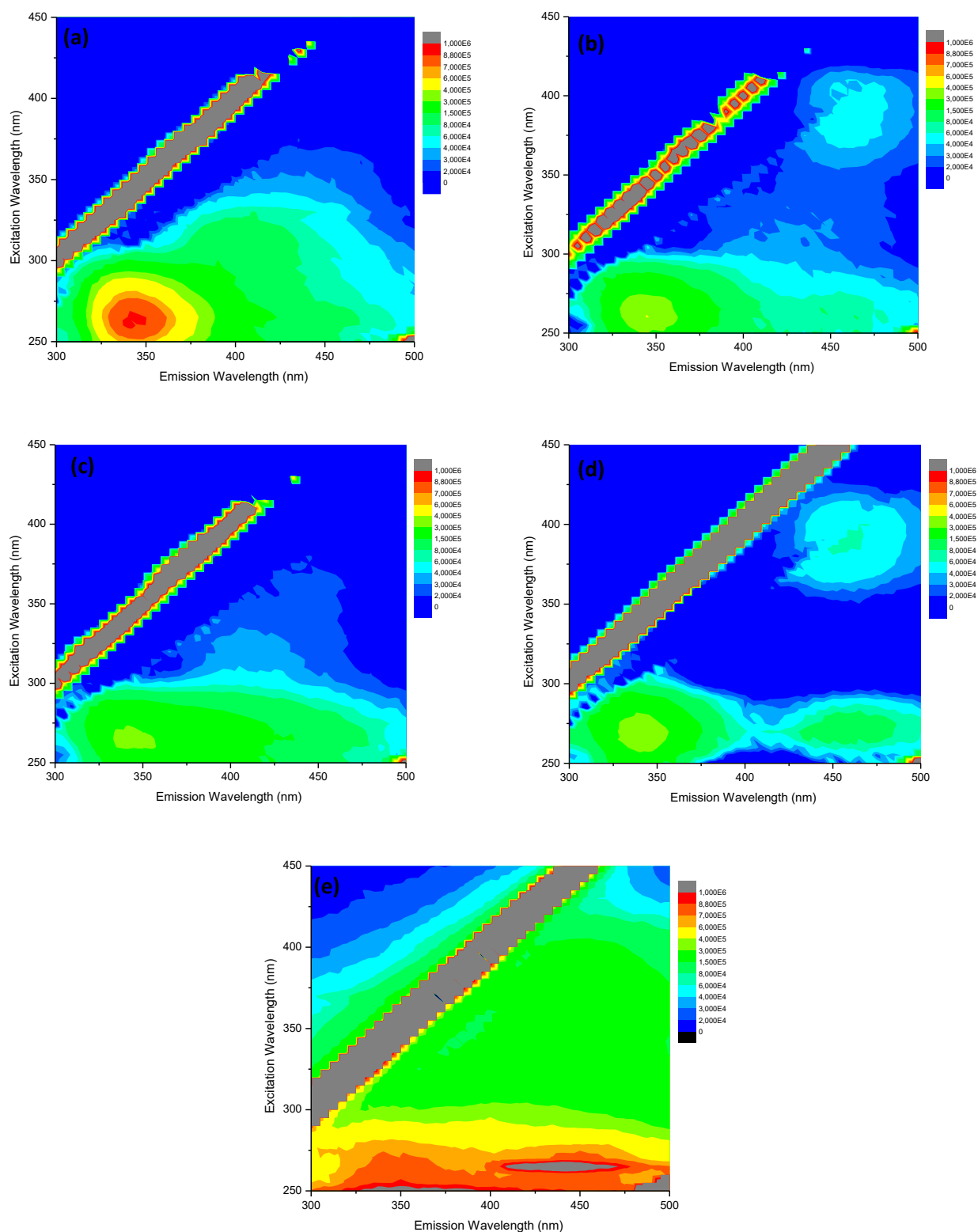


Figure 20- 3D fluorescence spectrum (contour map) of SMX 100 µg/L in ultrapure water at pH 7.30 with phosphate buffer (0.001M) in absence of salts (a) and in presence of 785 mg/L magnesium (b), 261 mg/L calcium (c), 21 g/L sodium chloride (d) and 21 g/L *Red Sea Salts* (e).

In presence of 21 ‰ *Red Sea Salts* the decrease in the photodegradation rate, (50.3 ± 0.5 %), is similar to the one observed in presence of 21 ‰ NaCl and in the estuarine environmental water sample, (53 ± 2 %). In what concerns the 3D fluorescence spectra there is an obvious increase of fluorescence intensity for low excitation wavelengths, (200-275) nm, and for emissions between (250-450) nm. The changes observed in the SMX 3D fluorescence spectra in presence of *Red Sea Salts* indicate that the salts present in this artificial sea salt sample induce changes in SMX either by complexation/interaction with inorganic compounds or by changes of ionic strength. Also, UV-Vis absorbance spectra (figure 21) presented lower absorbance for SMX in the presence of all inorganic salts tested, compared with SMX in ultrapure water.

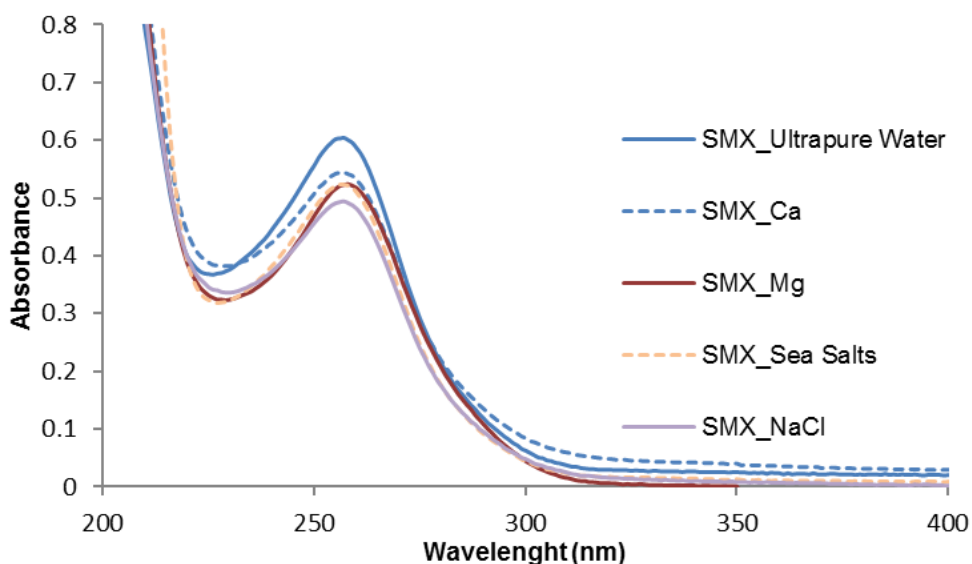


Figura 21- UV-Vis spectra of SMX 10 mg/L in ultrapure water at pH 7.30 with phosphate buffer (0.001 M) in absence of salts and in presence of 785 mg/L magnesium, 261 mg/L calcium, 21 ‰ sodium chloride and 21 ‰ *Red Sea Salts*.

Although individually calcium and, mainly, magnesium appear to have some influence on the photodegradation of SMX, when in a mixture with other compounds, it does not appear to have a considerable influence, since photodegradation of SMX after 5 hours of irradiation in 21 ‰ of *Red Sea Salts* is similar to the obtained in 21 ‰ NaCl and estuarine water sample.

3.2.5.2. Photodegradation kinetics of SMX

To further investigate the influence of sea salts on SMX photodegradation two solutions of 100 µg/L of SMX in 21 ‰ of NaCl solution and in 21 ‰ of artificial sea salts solution with phosphate buffer (0.001 M) at pH 7.30 were irradiated for 18 hours. The results were compared with the kinetics of 100 µg/L SMX photodegradation in *Fonte Nova* at pH 7.33 and in ultrapure water at pH 7.30 with phosphate buffer (0.001 M). As done previously, experimental results were fitted by non-linear regression and the obtained data for the variation of SMX concentration along irradiation time were fitted to a pseudo first-order kinetic model (figure 22). The results obtained show that salinity has a great influence on SMX photodegradation kinetics, since the addition of sodium chloride and synthetic sea salts leads to a significant decrease in the SMX photodegradation rate, when compared to the one obtained in ultrapure water at the same pH. It is also possible to conclude that kinetics with 21 ‰ of NaCl and 21 ‰ of sea salts are very similar to kinetics obtained with estuarine water sample. However, in the estuarine water sample 22 hours were necessary to degrade SMX almost completely, while in the NaCl and sea salts solutions prepared only 18 hours were needed. The difference observed may be attributed to screen filter due to the presence of organic matter in the environmental estuarine water sample.

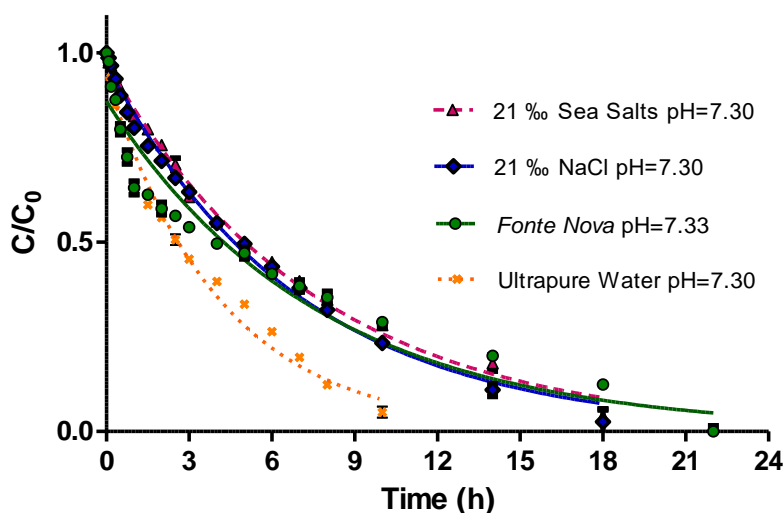


Figure 22- Kinetics of SMX photodegradation and curves of pseudo first-order decay fitted to the data by nonlinear regression when present in ultrapure water, in ultrapure water with sea salts and in a NaCl solution buffered with phosphate buffer at pH 7.30 and in estuarine water at pH=7.33. Shown error bars are standard deviations (n=3) (note that, for most of the experimental points error bars are too small to be visible in the figure).

Results of k_{meas} (h^{-1}), R^2 , $t_{1/2}$ (h), $t_{1/2}$ (SSD) and ϕ_{ave} obtained for SMX photodegradation in the different matrices used to evaluate the influence of sea salts in photodegradation behaviour of SMX are summarized in table 14.

Table 14- k_{meas} (h^{-1}), R^2 , $t_{1/2}$ (h), $t_{1/2}$ (SSD) and ϕ_{ave} obtained for ultrapure water, 21 ‰ sea salts, 21 ‰ NaCl buffered with phosphate buffer (0.001 M) at pH 7.30 and *Fonte Nova* sample at pH 7.33.

Type of water	k_{meas} (h^{-1})	R^2	$t_{1/2}$ (h)	$t_{1/2}$ (SSD)	ϕ_{ave}
Ultrapure pH = 7.30	0.24 ± 0.02	0.9767	2.9 ± 0.2	0.76 ± 0.05	2.42×10^{-8}
21 ‰ Sea Salts pH = 7.30	0.133 ± 0.004	0.9949	5.2 ± 0.1	1.37 ± 0.04	6.79×10^{-9}
21 ‰ NaCl pH = 7.30	0.143 ± 0.004	0.9938	4.8 ± 0.1	1.27 ± 0.04	1.23×10^{-8}
<i>Fonte Nova</i> pH = 7.33	0.13 ± 0.01	0.9397	5.3 ± 0.5	1.4 ± 0.1	---

For ultrapure water, a first order rate constant of $(0.24 \pm 0.02) h^{-1}$ was obtained, being higher than that obtained with 21 ‰ artificial sea salts, $(0.133 \pm 0.004) h^{-1}$, with 21 ‰ NaCl, $(0.143 \pm 0.004) h^{-1}$, and with estuarine water sample, $(0.13 \pm 0.01) h^{-1}$. These results showed that saline environmental water samples are less efficient to induce the photodegradation of SMX, which resulted in much longer SMX $t_{1/2}$ when compared to ultrapure water. The $t_{1/2}$ obtained in ultrapure water was $(2.9 \pm 0.2) h$, while in estuarine water, in a 21 ‰ artificial sea salts solution and in a 21 ‰ NaCl solution the $t_{1/2}$ obtained were (5.3 ± 0.5) , (5.2 ± 0.1) and $(4.8 \pm 0.1) h$, respectively. So, it is possible to conclude that besides the pH, salinity also has a high influence on SMX photodegradation.

The differences observed between SMX photodegradation kinetics in ultrapure water and in the presence of NaCl may be attributed to changes in the SMX structure influenced by the increase in the ionic strength, which is corroborated by the change in the 3D fluorescence spectra (figure 20 – (d)) that presents a decrease in the SMX band at $\lambda_{em} \approx 350$ nm with $\lambda_{exc} \approx 260$ nm, a new band at higher wavelengths, $\lambda_{em} = (440-480)$ nm with $\lambda_{exc} = (375-410)$ nm and a second band observed at similar λ_{exc} of SMX in water but at higher $\lambda_{em} = (430-480)$ nm. Also, it is known that chloride has the ability to scavenge the

hydroxyl radicals (Umar and Aziz, 2013) and thus, decrease the radicals concentration that induce SMX degradation.

The conversion of the $t_{1/2}$ (h) in $t_{1/2}$ in environmental conditions (SSD), allows to observe large differences in the number of necessary SSD to reach the $t_{1/2}$ between ultrapure water and the samples with inorganic salts. In ultrapure water (0.76 ± 0.05) SSD are needed to reach $t_{1/2}$, while when SMX is present in samples with high salinity the SSD varied between about 1.27 and 1.4 SSD. This means that when SMX is present in natural environments with high salinity levels its degradation rate becomes much slower, increasing the problems associated with the persistence of SMX in natural aquatic environments.

Similar to what was done in ultrapure water at different pH values, the ϕ was calculated for 21 ‰ artificial sea salts solution (6.79×10^{-9}) and 21 ‰ NaCl solution (1.23×10^{-8}) buffered at pH 7.30 and the values obtained were lower than those obtained in ultrapure water. These values are in line with the expected, since the photodegradation rate in these two solutions was lower than the obtained in ultrapure water (at all the pH values tested), being the lowest value of ϕ observed for the 21 ‰ *Red Sea Salts* solution.

Although the values obtained for the first order rate constant were very similar between samples with the same salinity, there is greater similarity between estuarine sample ($(0.13 \pm 0.01) \text{ h}^{-1}$) and the solution with 21 ‰ *Red Sea Salts* ($(0.133 \pm 0.004) \text{ h}^{-1}$). This may be due to the fact that in the sample of synthetic sea salts there are also ions, such as calcium and magnesium, characteristic of estuarine samples, that, as mentioned before, influence the SMX photodegradation rate.

3.3. Photodegradation of SMX in continuous flow mode

3.3.1. Photodegradation kinetics of SMX in ultrapure water and environmental water samples

In the photodegradation of SMX in continuous flow mode the concentration of SMX was used in batch mode. Thus, direct photodegradation of 100 µg/L SMX was performed in ultrapure water without pH adjusted irradiating the solution during 1 hour. Indirect photodegradation was performed in environmental water samples: *Fonte Nova*, *Rio Novo*

do *Príncipe*, *Poço da Cruz* and STPF and these samples were irradiated until no SMX was detected. Experimental results were fitted by non-linear regression, according to the equation 7, as in batch mode.

The kinetic curves of SMX photodegradation in ultrapure water and in the different water samples tested are presented in figure 23. The obtained data for the variation of SMX concentration along irradiation time were fitted to a pseudo first-order kinetic model.

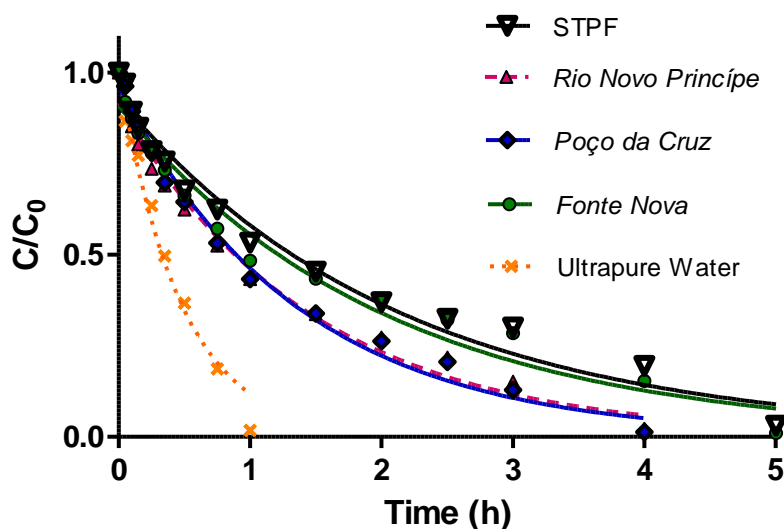


Figure 23- Kinetics of SMX photodegradation in continuous flow mode and curves of pseudo first-order decay fitted to the data by nonlinear regression when present in ultrapure water and in environmental samples.

In all samples studied, no degradation was observed in the tube covered with aluminum foils (control tube), indicating that no degradation by microbiological or thermal means occurred. So, the decrease of SMX concentration in these solutions can be only ascribed to photo-induced degradation.

For example, in ultrapure water, after 45 minutes of irradiation, SMX showed a photodegradation of 81.38 %, while in *Rio Novo do Príncipe* and *Fonte Nova* a photodegradation of 47.49 % and 42.81 %, respectively, was obtained.

The results presented in table 15 showed that environmental water samples are less efficient to photodegradation SMX than ultrapure water as already shown to occur. STPF sample was the one showing the lower efficiency to induce the photodegradation of SMX, which resulted in much longer SMX $t_{1/2}$ ((1.5 ± 0.1) h) when compared to ultrapure water ((0.32 ± 0.03) h). The conversion of the resulting $t_{1/2}$ in $t_{1/2}$ in environmental conditions allows

to observe differences in the number of necessary SSD to reach the $t_{1/2}$ between ultrapure water and environmental samples. In ultrapure water (0.085 ± 0.007) SSD were needed to reach $t_{1/2}$, while when SMX is present in natural environmental samples the SSD varied between (0.25 ± 0.01) and (0.39 ± 0.03) SSD.

Table 15- Photodegradation of SMX in flow mode - K_{meas} (h^{-1}), R^2 , $t_{1/2}$ (h) and $t_{1/2}$ (SSD) obtained in ultrapure water and in environmental water samples and respective standard errors.

Type of water	k_{meas} (h^{-1})	R^2	$t_{1/2}$ (h)	$t_{1/2}$ (SSD)
Ultrapure	2.1 ± 0.2	0.9812	0.32 ± 0.03	0.085 ± 0.007
Fonte Nova	0.49 ± 0.04	0.9698	1.4 ± 0.1	0.37 ± 0.03
Rio Novo Príncipe	0.69 ± 0.04	0.9841	1.01 ± 0.06	0.27 ± 0.02
Poço da Cruz	0.73 ± 0.03	0.9904	0.95 ± 0.05	0.25 ± 0.01
STPF	0.47 ± 0.03	0.9746	1.5 ± 0.1	0.39 ± 0.03

Analysing the data, and as expected, it is possible to conclude the same as in batch mode, that is, that the environmental water samples cause a great delay in the photodegradation of the SMX, due to the factors mentioned in the chapter 3.2.

However, the purpose of this study was not to prove the results obtained in chapter 3.2, but trying to obtain a method to photodegrade the samples in a more efficient way, since the tube in which the radiation is incident presents a smaller thickness. This objective was achieved, since the samples were photodegraded in a much shorter time, as can be verify in the figure 24. For example, in the case of the *Fonte Nova* sample, the SSD was reduced from 1.4 to 0.37. So, the main advantages of this method are related to the less irradiation time required, which leads to a lower lamp expenditure; also, the photodegradation in continuous mode is more easily applicable to reality, that is, it can be used as a tertiary system in STPs, since there is a defined effluent entrance and exit. The design of efficient processes for photodegradation of organic pollutants, in terms of energy and time, are needed for a sustainable approach. This was the first assessment of the potential of the continuous flow mode to be applied in an effluent tertiary treatment of waste water. Results are promising for the development of an economically viable green water

treatment technology, aiming at the photodegradation of organic pollutants under solar radiation.

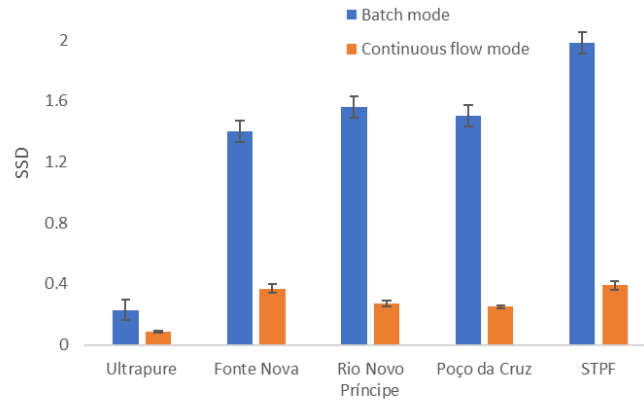


Figure 24- Comparison between SSD obtained in batch mode and continuous flow mode in ultrapure water and in environmental water samples in the same conditions.

3.4. Antibacterial activity

The bacterial growth was correlated with the luminescence of the bacteria, because considering only the bacterial growth it is not possible to know which cells are metabolically active. Thus, if the correlation is positive, luminescence converts in bacterial growth and demonstrates the viability of cells (metabolically active cells).

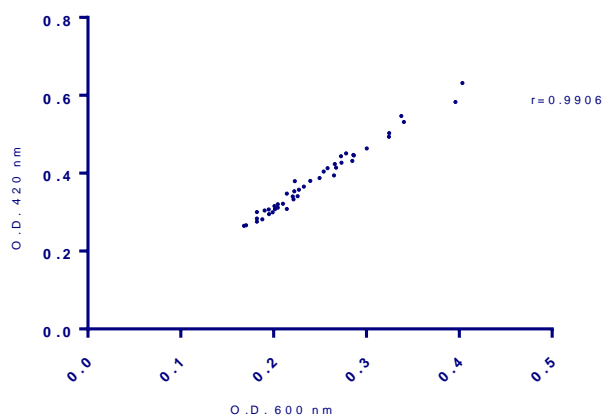


Figure 25- Correlation between luminescence at wavelength 420 nm and bacterial growth at wavelength 600 nm.

In figure 25, it is shown that the higher the luminescence the greater the bacterial growth, so data correlate positively. Therefore, luminescence data can be used for the interpretation of the cytotoxic effect of the samples under study. Thus, the following figures show the results obtained for the tests of antibacterial activity.

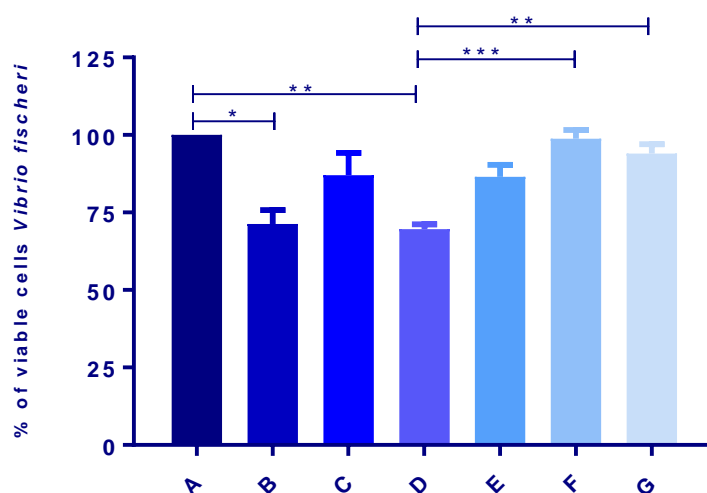


Figure 26- Percentage of viable cells *Vibrio fischeri* in A - ultrapure water (matrix) without SMX and without irradiation; B - control without irradiation (50 mg/L of SMX); C – control covered with aluminum at t_3 of irradiation (50 mg/L of SMX); D - control without irradiation (100 mg/L of SMX); E - sample at t_1 (50 mg/L of SMX); F - sample at t_2 (SMX concentration < 5 mg/L); G - sample at t_3 (no SMX detected). Statistical hypothesis test: * - p value = 0.05; ** - p value = 0.01; *** - p value = 0.001.

From the analysis of figure 26, a higher bacterial growth can be observed in sample A since no antibiotic was present, only ultrapure water. Thus, this bacterial growth corresponds to that of the culture medium where the bacteria *Vibrio fischeri* was grown. On the other hand, as would be expected, in sample D there was a greater inhibition of bacterial growth, indicating antimicrobial activity, since SMX was in its higher concentration tested.

It is also possible to see differences in terms of antibacterial activity between samples C and B; however, the antibacterial activity of B is less to the one of sample E although all of them present similar SMX concentrations (50 mg/L). This fact may suggest that temperature influences antibacterial activity, since sample C and E were exposed to the same temperature during the irradiation, whereas sample B was not irradiated and present a higher antibacterial activity.

As for samples F and G, similar bacterial activity was observed, which was higher than the presented by sample D, being these results statistically different (for

p value = 0.01). From the results obtained in ultrapure water, it can be concluded that the photodegradation of SMX leads to a loss of antibacterial activity and if the formation of photoproducts occurs these not exhibit higher antibacterial activity than SMX.

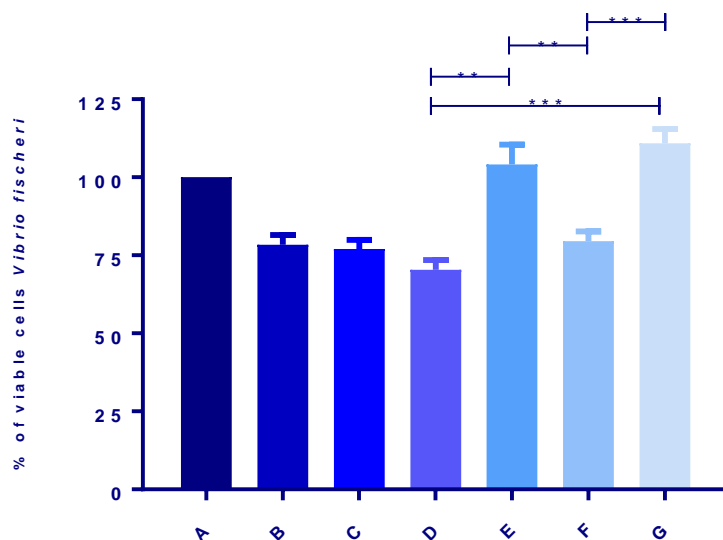


Figure 27- Percentage of viable cells *Vibrio fischeri* in A – *Poço da Cruz* (matrix) without SMX and without irradiation; B - control without irradiation (50 mg/L of SMX); C - control covered with aluminum at t_3 of irradiation (50 mg/L of SMX); D - control without irradiation (100 mg/L of SMX); E - sample at t_1 (50 mg/L of SMX); F - sample at t_2 (SMX concentration < 5 mg/L); G - sample at t_3 (no SMX detected). Statistical hypothesis test: **- ρ value = 0.01; ***- ρ value = 0.001.

From figure 27 it was possible to observe that sample A did not exhibit the highest bacterial growth. Although in sample A SMX was absent, the bacterial growth in *Poço da Cruz* matrix was lower than the obtained in the culture medium. So, the compounds present in the water matrix from *Poço da Cruz* have the ability to inhibit the bacterial growth, because also in samples E and G the bacterial growth is greater than in sample A, indicating that the photodegradation eliminates compounds of the own matrix.

As observed previously, sample D was the one in which the inhibition of bacterial growth was higher, indicating the antimicrobial activity of SMX. Samples A, B, C and D were not statistically different, although SMX concentration and irradiation times were different, which again indicates that the matrix had a great effect on bacterial growth, that might be even greater than SMX effect.

Sample E had higher bacterial activity than sample C, and although both had the same SMX concentration, sample E was subjected to irradiation. This suggests that, in

addition to the photodegradation of the compound, photodegradation of the matrix or some compound present in the matrix can occur, resulting in a higher bacterial activity in sample E.

Sample D and E were statistically different (for p value = 0.01), with a higher bacterial activity observed for sample E, indicating that photodegradation reduced the antibacterial activity of SMX. Sample E and F were also statistically different (for p value = 0.01), with higher SMX activity in sample F than in sample E. This suggests that photoproducts or photoproducts of the first photoproducts formed had higher antibacterial activity than SMX or the matrix compounds photodegradation may result in harmful compounds with antibacterial activity, which need more time of irradiation to photodegrade than SMX. However, in sample G the bacterial activity increased with respect to sample F (statistically different for p value = 0.001), indicating that whatever was formed in sample F disappeared at the end of the irradiation time. Once again it was proved that, for this particular case study, photodegradation was efficient to eliminate compounds that might increase the bacterial resistance.

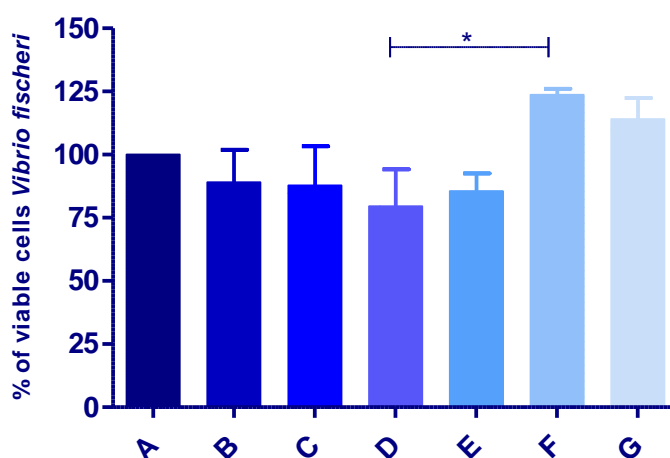


Figure 28- Percentage of viable cells *Vibrio fischeri* in A – *Fonte Nova* (matrix) without SMX and without irradiation; B - control without irradiation (50 mg/L of SMX); C - control covered with aluminum at t_3 of irradiation (50 mg/L of SMX); D - control without irradiation (100 mg/L of SMX); E - sample at t_1 (50 mg/L of SMX); F - sample at t_2 (SMX concentration < 5 mg/L); G - sample at t_3 (no SMX detected). Statistical hypothesis test: * - p value = 0.05.

Results of antibacterial activity obtained using an estuarine water sample are presented in figure 28. As observed for the riverine water sample, sample A did not exhibit the highest bacterial growth, indicating once again that the compounds present in the water

matrix have the ability to inhibit the bacterial growth. This fact is also proved, since in samples F and G the bacterial growth is greater than in sample A, so the photodegradation also eliminated compounds from the matrix, which inhibit the bacterial growth.

As before, in sample D was observed the higher inhibition of bacterial growth, indicating antimicrobial activity of SMX. Samples A, B, C, D and E were not statistically different, although SMX concentration and irradiation times were different, which again indicated that the matrix had a greater effect on bacterial growth than SMX. However, sample D and F were statistically different, with higher bacterial activity in sample F, indicating that photodegradation reduced the antibacterial activity of SMX.

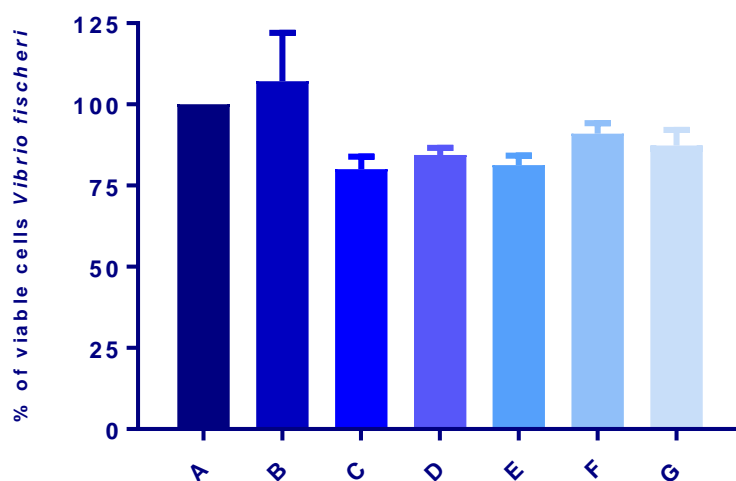


Figure 29- Percentage of viable cells *Vibrio fischeri* in A – STPF (matrix) without SMX and without irradiation; B - control without irradiation (50 mg/L of SMX); C – control covered with aluminum at t_3 of irradiation (50 mg/L of SMX); D - control without irradiation (100 mg/L of SMX); E - sample at t_1 (50 mg/L of SMX); F - sample at t_2 (SMX concentration < 5 mg/L); G - sample at t_3 (no SMX detected).

Finally, antibacterial tests were performed when SMX is in STPF sample (figure 29). All samples presented were not statistically different and bacterial growth in the sample STPF was much lower than that obtained in the culture medium, which did not allow to obtain many conclusions about the antibacterial activity of SMX in this water matrix. So, the compounds present in waste water matrix had a greater effect on bacterial growth than SMX, because it greatly inhibited bacterial growth. This effect may be due to the fact that the STPF effluent may have in its constitution other antibiotics or other compounds harmful to the bacteria *Vibrio fischeri* used in this study.

4. Conclusions

The occurrence of SMX in aquatic environments was already referred in several studies, and being an antibiotic, its removal or reduction in the environment is extremely important, mainly due to the problem of bacterial resistance.

Photodegradation can be used to improve the remediation processes of environments contaminated by SMX and other hazardous compounds from STPs in order to discharge effluents in the aquatic environment without its contamination.

Therefore, in this work, initially it was evaluated the SMX photodegradation in ultrapure water, using simulated solar radiation, in the presence of different HS fractions and in environmental water samples from different origins. From the results obtained, it was possible to conclude that SMX photodegradation in environmental water samples was much slower than in ultrapure water. In order to understand the reason for that photodegradation decrease several factors were evaluated, such as pH, salinity, as well as the presence of calcium, magnesium and ionic strength in the photodegradation rate of SMX.

This work brings together a set of results that allowed conclusions to be drawn:

- Direct photodegradation rate of SMX is pH dependent. The pH 5.00 is the most efficient among those tested, presenting a $t_{1/2}$ of (0.13 ± 0.01) SSD, while at pH 6.30 and 7.30 show a $t_{1/2}$ of (0.23 ± 0.01) and (0.76 ± 0.05) SSD, respectively. The quantum yield of SMX in ultrapure water at pH 5.00 (1.72×10^{-7}) was greater than the obtained in ultrapure water at pH 6.30 (2.76×10^{-8}) and at pH 7.30 (2.42×10^{-8}).
- The results obtained for HS fractions were affected by a variation of pH, because the natural pH of ultrapure water was higher than when HS were present. However, controlling the pH, it was possible to conclude that the presence of all HS was consistent with a decrease on the photodegradation rate of SMX either at pH 5.00 and 7.30 when compared with ultrapure water at the same pH. Thus, the inner filter effect was higher than the photosensitizing effect of HS, being more remarkable in the presence of HA.
- In the collected water samples, under the same conditions of irradiation, the photodegradation had a marked decrease when compared with SMX in ultrapure water ($t_{1/2}$ of 0.23 ± 0.01 SSD); the major decrease was observed in the STPF sample ($t_{1/2}$ of 1.98 ± 0.07 SSD). The *Fonte Nova*, *Rio Novo do Príncipe* and *Poço da Cruz* samples showed a $t_{1/2}$ of (1.4 ± 0.1) , (1.56 ± 0.09) and (1.50 ± 0.05) SSD, respectively. So, this work allowed to conclude that photodegradation might not prevent the

environmental accumulation of SMX, which was shown to be considerably resistant to photodegradation.

- The pH effect was studied in the estuarine water sample by comparing the pH value of this sample with the natural pH of ultrapure water. The $t_{1/2}$ in estuarine water at pH 6.30 (0.74 ± 0.05 SSD) was much lower than $t_{1/2}$ in estuarine water at pH 7.33 (1.4 ± 0.1 SSD). However, when comparing the value obtained for the $t_{1/2}$ at pH 6.30 in the estuarine sample with that obtained in the ultrapure water it was verified that the $t_{1/2}$ is higher in the estuarine sample and this can be explained by the higher absorbance of radiation by the estuarine sample matrix than the one observed in ultrapure water, leaving less radiation available for the SMX photodegradation (inner filter effect).
- pH is not sufficient to justify the slow photodegradation rate of SMX in environmental samples, thus, the influence of sea salts, namely calcium, magnesium and sodium chloride on photodegradation of SMX was also evaluated. It was possible to conclude that obtained results with the addition of 21 ‰ of NaCl (0.143 ± 0.004 h⁻¹) or 21 ‰ of sea salts (0.133 ± 0.004 h⁻¹) in ultrapure water at pH 7.30 were similar to the obtained in estuarine water sample at pH 7.33 (0.13 ± 0.01 h⁻¹). However, there is a greater similarity between estuarine sample (0.13 ± 0.01 h⁻¹) and the solution with 21 ‰ *Red Sea Salts* (0.133 ± 0.004 h⁻¹) and this may be due to the fact that in the sample of synthetic sea salts there are also ions, such as calcium and magnesium, characteristic of estuarine samples.

Concluding, it was proven that pH is extremely important on the photodegradation behaviour of SMX in all environmental samples tested, since they all have a pH higher than 7.0. However, for the estuarine sample, salinity also has an important influence, while for the fresh water samples DOC is a contributing factor for the decrease of the degradation rate of SMX due to its inner filter effect. For the STPF sample, photodegradation of SMX is influenced by all the three factors mentioned: pH, salinity and DOC.

Then, the SMX photodegradation in continuous flow mode was performed in ultrapure water and environmental samples. The photodegradation in this mode is much faster than the observed in batch mode, since the tube in which the radiation is incident presents a smaller thickness. Therefore, the radiation interacts easier with SMX in the sample and consequently, increases the photodegradation rate. In this way, this method of photodegradation becomes advantageous because it requires a lower exposure time to the radiation, and thus, a lower cost is associated to the lamp use. Also, the photodegradation

in continuous flow mode is a more efficient design for application to reality, and can be used as a sustainable approach for tertiary system in STPs.

Finally, bacterial resistance to SMX during and after photodegradation experiments was also evaluated either in ultrapure water or in the environmental water samples. It was concluded that photodegradation is an efficient method to combat the problem of bacterial resistance in water samples from different origins, since SMX was not detected by HPLC-FLD and the bacterial activity increased with SMX total photodegradation. Thus, the antibacterial effect of SMX is eliminated along with its photodegradation. However, with regard to the STPF sample tested, the same conclusions could not be obtained, since the STPF sample greatly inhibits bacterial growth and, therefore, it was not possible to obtain conclusions about the influence of SMX photodegradation on bacterial activity of the bacteria *Vibrio fischeri*.

5. Future Work

In order to complement the SMX photodegradation studies, the influence of synthetic photosensitizers should be tested, since the photodegradation of SMX in presence of natural photosensitizers and in environmental water samples is slower than in ultrapure water. Therefore, it is important to achieve a way to increase the photodegradation of SMX in environmental water samples in order to decrease the persistence of SMX in natural aquatic environment.

Since it is known that the formation of photodegradation products (that might be as or more toxic than the parent compound) may occur, the assessment of the SMX photoproducts formed, in ultrapure water and especially in environmental water samples by mass spectrometry, is essential. This study becomes even more important, since there are only few studies in literature related to the formation of SMX photoproducts in environmental water samples.

Besides the knowledge of the products formed and although the antibacterial activity of the products formed has been already evaluated in ultrapure and in environmental water samples, it is also important to do acute and chronic toxicity tests in these samples. Even though these studies are important for a correct assessment of the efficiency of the photodegradation process, the information in literature about the toxicity of SMX photodegradation products is scarce. Thus, it is crucial to increase the scientific community knowledge not only about the SMX photoproducts formed but also about their toxicity.

6. References

- Abellán, M.N., Giménez, J., Esplugas, S., 2009. Photocatalytic degradation of antibiotics: The case of sulfamethoxazole and trimethoprim. *Catalysis Today*, 144, pp. 131–136.
- Aguer, J., Richard, C., Andreux, F., 1999. Effect of light on humic substances: production of reactive species. *Analisis*, 27, pp. 387–390.
- al Housari, F., Vione, D., Chiron, S., Barbati, S., 2010. Reactive photoinduced species in estuarine waters. Characterization of hydroxyl radical, singlet oxygen and dissolved organic matter triplet state in natural oxidation processes. *Photochemistry Photobiology Science*, 9, pp. 78–86.
- Aleksandrova, O.N., Schulz, M., Matthies, M., 2011. A quantum statistical approach to remediation effect of humic substances. *Water, Air and Soil Pollution*, 221, pp. 203–214.
- Andreozzi, R., Marotta, R., Paxéus, N., 2003. Pharmaceuticals in STP effluents and their solar photodegradation in aquatic environment. *Chemosphere*, 50, pp. 1319–1330.
- Atkinson, S.K., Marlatt, V.L., Kimpe, L.E., Lean, D.R.S., Trudeau, V.L., Blais, J.M., 2011. Environmental factors affecting ultraviolet photodegradation rates and estrogenicity of estrone and ethinylestradiol in natural waters. *Archives of Environmental Contamination and Toxicology*, 60, pp. 1–7.
- Augugliaro, V., Litter, M., Palmisano, L., Soria, J., 2006. The combination of heterogeneous photocatalysis with chemical and physical operations: A tool for improving the photoprocess performance. *Journal of Photochemistry and Photobiology C: Photochemistry Review*, 7, pp. 127–144.
- Avisar, D., Lester, Y., Ronen, D., 2009. Sulfamethoxazole contamination of a deep phreatic aquifer. *Science of the Total Environment*, 407, pp. 4278–4282.
- Backhaus, T., Grimme, L.H., 1999. The toxicity of antibiotic agents to the luminescent bacterium *Vibrio fischeri*. *Chemosphere*, 38, pp. 3291–3301.
- Bancirova, M., 2011. Sodium azide as a specific quencher of singlet oxygen during chemiluminescent detection by luminol and Cypridina luciferin analogues. *Luminescence*, 26, pp. 685–688.
- Bastos, R.V., 2012. Estudo da degradação do antibiótico sulfametoxazol em solução aquosa por fotólise. (Master's Thesis), University of São Paulo.
- Bengtsson-Palme, J., Larsson, D.G.J., 2016. Concentrations of antibiotics predicted to

select for resistant bacteria: Proposed limits for environmental regulation. *Environment International*, 86, pp. 140–149.

Bila, D.M., Dezotti, M., 2003. Fármacos no meio ambiente. *Química Nova*, 26, pp. 523–530.

Boreen, A.L., Arnold, W.A., McNeill, K., 2004. Photochemical fate of sulfa drugs in then aquatic environment: Sulfa drugs containing five-membered heterocyclic groups. *Environmental Science & Technology*, 38, pp. 3933–3940.

Brown, G.R., 2014. Cotrimoxazole-optimal dosing in the critically ill. *Annals of Intensive Care*, 28, pp. 4–13.

Bu, Q., Wang, B., Huang, J., Deng, S., Yu, G., 2013. Pharmaceuticals and personal care products in the aquatic environment in China: A review. *Journal of Hazardous Materials*, 262, pp. 189–211.

Cabral, P.S.J., 2010. Water Microbiology. Bacterial Pathogens and Water. *International Journal of Environmental Research and Public Health*, 7, pp. 3657–3703.

Calisto, V., Domingues, M.R.M., Esteves, V.I., 2011. Photodegradation of psychiatric pharmaceuticals in aquatic environments - Kinetics and photodegradation products. *Water Research*, 45, pp. 6097–6106.

Calisto, V., Ferreira, C.I.A., Oliveira, J.A.B.P., Otero, M., Esteves, V.I., 2015. Adsorptive removal of pharmaceuticals from water by commercial and waste-based carbons. *Journal of Environmental Management*, 152, pp. 83–90.

Carballa, M., Omil, F., Lema, J.M., Llompарт, M., García-Jares, C., Rodríguez, I., Gómez, M., Ternes, T., 2004. Behavior of pharmaceuticals, cosmetics and hormones in a sewage treatment plant. *Water Research*, 38, pp. 2918–2926.

Castiglioni, S., Bagnati, R., Fanelli, R., Pomati, F., Calamari, D., Zuccato, E., 2006. Removal of pharmaceuticals in sewage treatment plants in Italy. *Environmental Science & Technology*, 40, pp. 357–363.

Caupos, E., Mazellier, P., Croue, J.P., 2011. Photodegradation of estrone enhanced by dissolved organic matter under simulated sunlight. *Water Research*, 45, pp. 3341–3350.

Chavez-doal, A., Gorman, C., Erken, M., Steinberg, P.D., Mcdougald, D., Nishiguchi, K., 2013. Predation Response of *Vibrio fischeri* Biofilms to Bacterivorous Protists. *Journal*

Applied and Environmental Microbiology, 79, pp. 553–558.

Chen, Y., Hu, C., Hu, X., 2009. Indirect Photodegradation of Amine Drugs in Aqueous Solution under Simulated Sunlight. *Environmental Science & Technology*, 43, pp. 2760–2765.

Chen, Y., Zhang, K., Zuo, Y., 2013. Direct and indirect photodegradation of estriol in the presence of humic acid, nitrate and iron complexes in water solutions. *Science of the Total Environment*, 463–464, pp. 802–809.

Christensen, A.M., Ingerslev, F., Baun, A., 2006. Ecotoxicity of mixtures of antibiotics used in aquacultures. *Environmental Toxicology and Chemistry*, 25, pp. 2208–2215.

De Souza, M.V.N., 2004. Novos produtos naturais capazes de atuar na estabilização de microtúbulos, um importante alvo no combate ao câncer. *Química Nova*, 27, pp. 308–312.

Dias, N.I., Souza, S.B., Pereira, H.O.S.J., Moreira, C.F., Dezotti, M., Boaventura, A.R.R., Vilar, J.P.V., 2014. Enhancement of the photo-Fenton reaction at near neutral pH through the use of ferroxalate complexes: A case study on trimethoprim and sulfamethoxazole antibiotics removal from aqueous solutions. *Chemical Engineering Journal*, 247, pp. 302–313.

Esteves, V.I., 1995. Extração e caracterização de substâncias húmicas de diferentes ambientes aquáticos (Doctoral Dissertation), University of Aveiro.

Esteves, V.I., Lima, S.S.F., Lima, D.L.D., Duarte, A.C., 2004. Using capillary electrophoresis for the determination of organic acids in Port wine. *Analytica Chimica Acta*, 513, pp. 163–167.

Esteves, V.I., Otero, M., Duarte, A.C., 2009. Comparative characterization of humic substances from the open ocean, estuarine water and fresh water. *Organic Geochemistry*, 40, pp. 942–950.

Fair, R.J., Tor, Y., 2014. Antibiotics and Bacterial Resistance in the 21st Century. *Perspectives in Medicinal Chemistry*, 6, pp. 25–64.

Fent, K., Weston, A.A., Caminada, D., 2006. Ecotoxicology of human pharmaceuticals. *Aquatic Toxicology*, 76, pp. 122–159.

Freire, R.S., Pelegrini, R., Kubota, L.T., Durán, N., Peralta-Zamora, P., 2000. Novas tendências para o tratamento de resíduos industriais contendo espécies organocloradas.

Química Nova, 23, pp. 504–511.

Gao, L., Shi, Y., Li, W., Niu, H., Liu, J., Cai, Y., 2012. Occurrence of antibiotics in eight sewage treatment plants in Beijing, China. *Chemosphere*, 86, pp. 665–671.

Ge, L., Chen, J., Qiao, X., Lin, J., 2009. Light-Source-Dependent Effects of Main Water Constituents on Photodegradation of Phenicol Antibiotics: Mechanism and Kinetics. *Environmental Science & Technology*, 43, pp. 3101–3107.

Göbel, A., McArdell, C.S., Suter, M.J.F., Giger, W., 2004. Trace determination of macrolide and sulfonamide antimicrobials, a human sulfonamide metabolite, and trimethoprim in wastewater using liquid chromatography coupled to electrospray tandem mass spectrometry. *Analytical Chemistry*, 76, pp. 4756–4764.

Göbel, A., Thomsen, A., McArdell, C.S., Joss, A., Giger, W., 2005. Occurrence and sorption behavior of sulfonamides, macrolides, and trimethoprim in activated sludge treatment. *Environmental Science & Technology*, 39, pp. 3981–3989.

Guillemot, D., 1999. Antibiotic use in humans and bacterial resistance. *Current Opinion Microbiology*, 2, pp. 494–498.

Hamada, N., 2008. Ensaios de toxicidade empregados na avaliação de efeitos no sistema de tratamento de esgotos e efluentes, e seu entorno, utilizando organismos aquáticos (Master's dissertation), University of São Paulo.

Hartig, C., Storm, T., Jekel, M., 1999. Detection and identification of sulphonamide drugs in municipal wastewater by liquid chromatography coupled with electrospray ionisation tandem mass spectrometry. *Journal of Chromatography A*, 854, pp. 163–173.

Heinemann, J.A., Ankenbauer, R.G., Amábile-Cuevas, C.F., 2000. Do antibiotics maintain antibiotic resistance? *Drug Discovery Today*, 5, pp. 195–204.

Hessler, D.P., Frimmel, F.H., Oliveros, E., Braun, A.M., 1996. Quenching of singlet oxygen ($^1\Delta_g$) by humic substances. *Journal of Photochemistry and Photobiology B*, 36, pp. 55–60.

Hirsch, R., Ternes, T., Haberer, K., Kratz, K.L., 1999. Occurrence of antibiotics in the aquatic environment. *Science of the Total Environment*, 225, pp. 109–118.

International Humic Substances Society, 2007. What are Humic Substances?. Available at: <http://www.humicsubstances.org/whatarehs.html> (accessed in 13th November 2016).

Instituto Nacional de Saúde Doutor Ricardo Jorge, 2010. Resistência Aos Antimicrobianos.

Available at:
<http://www.insa.pt/sites/INSA/Portugues/AreasCientificas/DoencasInfecciosas/AreasTrabalho/Resistencia/Paginas/inicial.aspx> (accessed in 18th November 2016).

Isidori, M., Lavorgna, M., Nardelli, A., Pascarella, L., Parrella, A., 2005. Toxic and genotoxic evaluation of six antibiotics on non-target organisms. *Science of the Total Environment*, 346, pp. 87–98.

Jiuhui, Q.U., 2008. Research progress of novel adsorption processes in water purification: a review. *Journal of Environmental Sciences*, 20, pp. 1–13.

Jornal online, 2015. Uso excessivo de antibióticos. Available at:
<http://online.sapo.pt/481002> (accessed in 5th October 2016).

Katsumata, C.P., Silva, M.P., Batista, A.P.S., Teixeira, A.C.S.C., 2014. Tratamento de água contaminada com fármacos por meio de fotólise UV e UV/H₂O₂. *XX Brazilian Congress of Chemical Engineering*, 1, pp. 1–8.

Kemper, N., 2008. Veterinary antibiotics in the aquatic and terrestrial environment. *Ecological Indicators*, 8, pp. 1–13.

Kümmerer, K., 2009. Antibiotics in the aquatic environment - A review - Part I. *Chemosphere*, 75, pp. 417–434.

Kümmerer, K., 2001. Drugs in the environment: Emission of drugs, diagnostic aids and disinfectants into wastewater by hospitals in relation to other sources - A review. *Chemosphere*, 45, pp. 957–969.

Lam, M.W., Tantuco, K., Mabury, S.A., 2003. PhotoFate: A new approach in accounting for the contribution of indirect photolysis of pesticides and pharmaceuticals in surface waters. *Environmental Science & Technology*, 37, pp. 899–907.

Leal, J.F., Esteves, V.I., Santos, E.B.H., 2016. Use of sunlight to degrade oxytetracycline in marine aquaculture's waters. *Environmental Pollution*, 213, pp. 932–939.

Leal, J.F., Esteves, V.I., Santos, E.B.H., 2015. Does light-screening by humic substances completely explain their retardation effect on contaminants photo-degradation? *Journal of Environmental Chemical Engineering*, 3, pp. 3015–3019.

Lester, Y., Avisar, D., Mamane, H., 2010. Photodegradation of the antibiotic sulphamethoxazole in water with UV/H₂O₂ advanced oxidation process. *Environmental*

Technology, 31, pp. 175–183.

Lima, D.L.D., 2011. Métodos Analíticos: Destino Ambiental de Poluentes Orgânicos. (Doctoral Dissertation), University of Aveiro.

Lin, A.Y.C., Reinhard, M., 2005. Photodegradation of Common Environmental Pharmaceuticals and Estrogens in River Water. *Environmental Toxicology and Chemistry*, 24, pp. 1303–1309.

Liu, B., Liu, X., 2004. Direct photolysis of estrogens in aqueous solutions. *Science of the Total Environment*, 320, pp. 269–274.

Locatelli, M.A.F., Sodr , F.F., Jardim, W.F., 2011. Determination of antibiotics in Brazilian surface waters using liquid chromatography-electrospray tandem mass spectrometry. *Archives of Environmental Contamination and Toxicology*, 60, pp. 385–393.

Mazellier, P., M it , L., De Laat, J., 2008. Photodegradation of the steroid hormones 17 β -estradiol (E2) and 17 α -ethinylestradiol (EE2) in dilute aqueous solution. *Chemosphere*, 73, pp. 1216–1223.

Melo, S.A.S., Trov , A.G., Bautitz, I.R., Nogueira, R.F.P., 2009. Degrada o de f rmacos residuais por processos oxidativos avan ados. *Qu mica Nova*, 32, pp. 188–197.

Mili , N., Milanovi , M., Leti , N.G., Sekuli , M.T., Radoni , J., Mihajlovi , I., Miloradov, M.V., 2013. Occurrence of antibiotics as emerging contaminant substances in aquatic environment. *International Journal of Environmental Health Research*, 23, pp. 296–310.

Miller, J.N., Miller, J.C., 2010. Statistics and Chemometrics for Analytical Chemistry, Technometrics. 6th ed., Pearson Prentice Hall, Harlow England.

Oliveira, C., Lima, D.L.D., Silva, C.P., Otero, M., Esteves, V.I., 2016. Photodegradation behaviour of estriol: An insight on natural aquatic organic matter influence. *Chemosphere*, 159, pp. 545–551.

Penesyanyan, A., Gillings, M., Paulsen, I.T., 2015. Antibiotic discovery: Combatting bacterial resistance in cells and in biofilm communities. *Molecules*, 20, pp. 5286–5298.

Peng, X., Wang, Z., Kuang, W., Tan, J., Li, K., 2006. A preliminary study on the occurrence and behavior of sulfonamides, ofloxacin and chloramphenicol antimicrobials in wastewaters of two sewage treatment plants in Guangzhou, China. *Science of the Total Environment*, 371, pp. 314–322.

- Radjenovic, J., Petrovic, M., Barceló, D., 2007. Analysis of pharmaceuticals in wastewater and removal using a membrane bioreactor. *Analytical and Bioanalytical Chemistry*, 387, pp. 1365–1377.
- Sajjad, H., 2014. Comparação entre diferentes processos de degradação do antibiótico sulfametoxazol. (Doctoral Dissertation), University of São Paulo.
- Senta, I., Terzic, S., Ahel, M., 2013. Occurrence and fate of dissolved and particulate antimicrobials in municipal wastewater treatment. *Water Research*, 47, pp. 705–714.
- Sierra, M.M.D., Giovanela, M., Parlanti, E., Soriano-Sierra, E.J., 2005. Fluorescence fingerprint of fulvic and humic acids from varied origins as viewed by single-scan and excitation/emission matrix techniques. *Chemosphere*, 58, pp. 715–733.
- Silva, C.P., 2014. Ocorrência e destino de estrogénios e antibióticos no ambiente, avaliados por metodologias analíticas de baixo custo. (Doctoral Dissertation), University of Aveiro.
- Silva, C.P., Lima, D.L.D., Groth, M.B., Otero, M., Esteves, V.I., 2016a. Effect of natural aquatic humic substances on the photodegradation of estrone. *Chemosphere*, 145, pp. 249–255.
- Silva, C.P., Lima, D.L.D., Otero, M., Esteves, V.I., 2016b. Photosensitized Degradation of 17 β -estradiol and 17 α -ethinylestradiol: Role of Humic Substances Fractions. *Journal of Environmental Quality*, 45, pp. 693–700.
- Silva, C.P., Otero, M., Esteves, V., 2012. Processes for the elimination of estrogenic steroid hormones from water: A review. *Environmental Pollution*, 165, pp. 38–58.
- Stevenson, F.J., 1994. Humus Chemistry: Genesis, Composition, Reactions. 2th ed., John Wiley & Sons, New York.
- Stumpe, B., Marschner, B., 2009. Factors controlling the biodegradation of 17 β -estradiol, estrone and 17 α -ethinylestradiol in different natural soils. *Chemosphere*, 74, pp. 556–562.
- Sulfamethoxazole-Toxicology Data Netw. Available at: <https://toxnet.nlm.nih.gov/cgi-bin/sis/search2/f?./temp/~BBkDzd:3> (accessed in 10th October 2016).
- Tamtam, F., Mercier, F., Le Bot, B., Eurin, J., Tuc Dinh, Q., Clément, M., Chevreuil, M., 2008. Occurrence and fate of antibiotics in the Seine River in various hydrological conditions. *Science of the Total Environment*, 393, pp. 84–95.
- Trovó, A.G., Nogueira, R.F.P., Agüera, A., Sirtori, C., Fernández-Alba, A.R., 2009.

Photodegradation of sulfamethoxazole in various aqueous media: Persistence, toxicity and photoproducts assessment. *Chemosphere*, 77, pp. 1292–1298.

Umar, M., Aziz, H.A., 2013. Photocatalytic Degradation of Organic Pollutants in Water. *Organic Pollutants - Monitoring Risk and Treatment*, chapter 8, pp. 195–207.

Watkinson, A.J., Murby, E.J., Kolpin, D.W., Costanzo, S.D., 2009. The occurrence of antibiotics in an urban watershed: From wastewater to drinking water. *Science of the Total Environment*, 407, pp. 2711–2723.

Yalkowsky, S.H., He, Y., Jain, P., 2010. Handbook of aqueous solubility data. 2th ed., CRC Press, Boca Raton.

Yang, C.C., Huang, C.L., Cheng, T.C., Lai, H.T., 2015. Inhibitory effect of salinity on the photocatalytic degradation of three sulfonamide antibiotics. *International Biodeterioration and Biodegradation*, 102, pp. 116–125.

Yuan, F., Hu, C., Hu, X., Qu, J., Yang, M., 2009. Degradation of selected pharmaceuticals in aqueous solution with UV and UV/H₂O₂. *Water Research*, 43, pp. 1766–1774.

Zhang, Q.Q., Ying, G.G., Pan, C.G., Liu, Y.S., Zhao, J.L., 2015. Comprehensive evaluation of antibiotics emission and fate in the river basins of China: Source analysis, multimedia modeling, and linkage to bacterial resistance. *Environmental Science & Technology*, 49, pp. 6772–6782.

Zheng, Q., Zhang, R., Wang, Y., Pan, X., Tang, J., Zhang, G., 2012. Occurrence and distribution of antibiotics in the Beibu Gulf, China: Impacts of river discharge and aquaculture activities. *Marine Environmental Research*, 78, pp. 26–33.

Zuo, Y., Zhang, K., Deng, Y., 2006. Occurrence and photochemical degradation of 17 β -ethinylestradiol in Acushnet River Estuary. *Chemosphere*, 63, pp. 1583–1590.

7. Annex

Table A1- Concentration of SMX (mg/L) in ultrapure water and in different environmental water samples used for antibacterial activity tests.

Identification	Ultrapure water		<i>Fonte Nova</i>		<i>Poço da Cruz</i>		STPF	
	Time of irradiation (h)	Concentration of SMX (mg/L) analysed by HPLC-FLD	Time of irradiation (h)	Concentration of SMX (mg/L) analysed by HPLC-FLD	Time of irradiation (h)	Concentration of SMX (mg/L) analysed by HPLC-FLD	Time of irradiation (h)	Concentration of SMX (mg/L) analysed by HPLC-FLD
A	0	0	0	0	0	0	0	0
B	0	50.92	0	50.95	0	50.36	0	50.49
C	133	50.25	275	50.81	251	50.12	253	50.08
D	0	100.91	0	100.73	0	100.78	0	100.98
E1	2	50.94	27	46.29	20	49.36	22.5	45.25
E2	2	47.44	27	44.66	20	51.65	22.5	46.34
E3	2	50.70	27	45.45	20	54.30	22.5	47.02
F1	38	0.49	137	1.26	103	1.99	111	3.08
F2	38	<LOD	137	0.89	103	2.19	111	3.22
F3	38	0.46	137	1.47	103	2.20	111	3.27
G1	133	<LOD	275	<LOD	251	<LOD	253	<LOD
G2	133	<LOD	275	<LOD	251	<LOD	253	<LOD
G3	133	<LOD	275	<LOD	251	<LOD	253	<LOD

